

Root development of maize (*Zea mays*) in water-deficient and nitrogen-limited soil

Yutong Jiang

Department of Natural Resource Sciences

Faculty of Agricultural and Environmental Sciences

McGill University, Montreal

May 2024

A thesis submitted to McGill University in partial fulfillment of
the requirements for the degree of Doctor of Philosophy

© Yutong Jiang, 2024

TABLE OF CONTENTS

TABLE OF CONTENTS	II
LIST OF TABLES	VII
LIST OF FIGURES	VIII
LIST OF APPENDICES	XIII
ABSTRACT	1
RÉSUMÉ	3
ACKNOWLEDGEMENT	5
CONTRIBUTION TO ORIGINAL KNOWLEDGE.....	7
PREFACE AND CONTRIBUTION OF AUTHORS	9
GENERAL INTRODUCTION.....	11
CHAPTER 1	13
Literature review.....	13
1.1 Root types	14
1.1.1 Axial roots	14
1.1.2 Lateral roots	15
1.2 The anatomy of maize root tissue	17
1.3 Root plasticity in the soil environment.....	21

1.3.1 Roots respond to soil water limitation	21
1.3.2 Roots respond to low nitrogen concentration	25
1.3.3 Roots respond to phosphorous, potassium, and micronutrient availability	28
1.4 Water uptake	30
1.4.1 Water uptake by maize roots	30
1.4.2 Root hydraulic conductance under water deficit	31
1.5 N uptake by roots	32
1.5.1 N movement from soil to the root surface	32
1.5.2 NO ₃ ⁻ uptake by roots	34
1.6 Conclusions and future directions.....	36
FORWARD TO CHAPTER 2.....	38
CHAPTER 2	39
Distinctive plasticity of maize (<i>Zea mays</i>) root types to variable nitrate concentrations.....	39
2.1 Abstract.....	40
2.2 Introduction.....	41
2.3 Materials and methods	41
2.4 Results.....	44
2.5 Discussion.....	46
2.6 References.....	49
FORWARD TO CHAPTER 3.....	52

CHAPTER 3	53
Plasticity of maize (<i>Zea mays</i>) roots depends on water content in nitrogen fertilized soil	53
3.1 Abstract	54
3.2 Introduction.....	55
3.3 Materials and methods	56
3.3.1 Soil.....	56
3.3.2 Growth chamber experiment.....	57
3.3.3 Field study.....	59
3.3.4 Plant and soil sampling	60
3.3.5 Plant and soil analyses	60
3.3.6 Xylem measurements.....	61
3.3.7 Maize transpiration calculation.....	62
3.3.8 Statistical analyses	63
3.4 Results.....	63
3.4.1 Root development in pot-grown maize responds to N fertilization in well-watered soil	63
3.4.2 Root hydraulic conductance associated with crown roots in pot-grown maize.....	64
3.4.3 Root development in field-grown maize generally does not respond to N fertilization	67
3.4.4 Root hydraulic conductance associated with crown roots in field-grown maize.....	69
3.5 Discussion.....	71
3.5.1 Root plasticity to N fertilizer inputs under well-watered condition	71

3.5.2 Roots were insensitive to N fertilizer inputs under dry soil.....	73
3.6 Conclusions.....	74
3.7 References.....	75
FORWARD TO CHAPTER 4.....	79
CHAPTER 4	80
Water-conducting roots responsible for nitrogen uptake in maize (<i>Zea mays</i>)	80
4.1 Abstract	81
4.2 Introduction.....	82
4.3 Materials and methods	84
4.3.1 Soil and maize.....	84
4.3.2 Split-root pot design.....	84
4.3.3 Experimental treatments	85
4.3.4 Plant sampling and analysis.....	86
4.3.5 Soil sampling and analysis.....	89
4.3.6 Nitrogen calculations	90
4.3.7 Statistical analyses	91
4.4 Results.....	91
4.4.1 Root morphology of primary, seminal and crown roots	91
4.4.2 Hydraulic conductance of crown roots declined in dry soil	93
4.4.3 Crown roots responsible for N uptake, with help from embryonic roots in dry soil ...	97
4.4.4 Nitrification was uniform among the root types	100

4.5 Discussion.....	102
4.6 Conclusions.....	106
4.7 References.....	107
GENERAL DISCUSSION	111
GENERAL CONCLUSIONS.....	121
REFERENCES	123
APPENDICES	139

LIST OF TABLES

Chapter 1

Table 1. 1 Genes and their functions in maize root development..... 20

Chapter 3

Table 3. 1 Soil moisture, soil mineral N concentration, maize properties at V6 stage in a growth chamber experiment..... 66

Chapter 4

Table 4. 1 Xylem number, xylem area, and calculated hydraulic conductance, determined from three segments (tip: 0–20 mm from root tip, mid: 40–60 mm from root tip, base: 0–20 mm from the base of the stem) of a representative thin-sectioned axial root for each type (primary, seminal and crown, 1st and 2nd whorls) of maize grown to the V3 or V6 stages in a split-root system. The split-root system was kept at a constant water potential (-5kPa or -30kPa). Values are the mean \pm standard error, n= 4. Different letters in the same column indicate significant differences among the same region of each root type within the same growth stage. Asterisks (*) indicate significant differences among water potential treatments of each root type within the same growth stage... 94

Table 4. 2 Percentage of ¹⁵N from added ¹⁵NO₃-N in maize shoot, roots, and soil after 0, 24 and 48 h of exposure to ¹⁵N enrichment. Maize was grown in split-root system with a constant water potential (-5kPa or -30kPa). At V3 and V6 stages, one of the chambers, either the inner or outer, received an injection of ¹⁵N-KNO₃ solution (18.4% atom ¹⁵N excess), while the other chamber received ¹⁴N-KNO₃ solution, ensuring exposure of only one root type (either the embryonic seminal and primary roots, or the crown roots) to ¹⁵N-KNO₃ solution. Data are the mean \pm standard errors; n = 4..... 98

LIST OF FIGURES

Chapter 1

Fig. 1. 1 (a) Maize root types, taken from Viana, G., Scharwies, J.D., Dinneney, J.R. 2022. Deconstructing the root system of grasses through an exploration of development, anatomy and function. *Plant Cell Environ.* **45**: 602–619. Doi: <https://doi.org/10.1111/pce.14270>. (b) emergence of the maize embryonic roots, (c) the longitudinal anatomy of maize roots, image from Jen Dixon, (d) cross-sectional anatomy, taken from Lynch, J.P., Strock, C.F., Schneider, H.M., et al. 2021. Root anatomy and soil resource capture. *Plant Soil* **466**: 21–63. doi: <https://doi.org/10.1007/s11104-021-05010-y>..... 19

Fig. 1. 2 (a) Hydropatterning of maize roots revealed by microscale computed tomography (bars = 5 cm), taken from Bao, Y., Aggarwal, P., Robbins, N.E., et al. 2014. Plant roots use a patterning mechanism to position lateral root branches toward available water. *Pro. Natl. Acad. Sci.* **111**: 9319–9324. doi: <https://doi.org/10.1073/pnas.1400966111>. (b) Plasticity of maize lateral roots to heterogenous NO_3^- concentration, revised from Yu, P., Hochholdinger, F., Li, C. 2019. Plasticity of lateral root branching in maize. *Front. Plant Sci.* **10**: 363. <https://doi.org/10.3389/fpls.2019.00363>. 25

Chapter 2

Fig. 2. 1 Shoot biomass (a) and plant N content (b) at harvest, plus the chlorophyll content (c) after 27 days of maize planting. Maize was harvested at the V3 stage, after roots were exposed to variable NO_3^- concentrations (mean value of measured NO_3^- concentration from 15 to 29 days) in perlite-filled pots for 30 days. Error bars are standard error of the mean (n=15)..... 45

Fig. 2. 2 Length of primary axial root (a), seminal axial roots (b) crown axial roots (c), length of primary lateral roots (d), seminal lateral roots (e) and crown lateral roots (f), and surface area of primary lateral roots (h), seminal lateral roots (i) and crown lateral roots (j) at V3 stage after roots were exposed to variable NO_3^- concentrations (mean value of measured NO_3^- concentration from 15 to 29 days) in perlite-filled pots for 30 ddays. Error bars are standard error of the mean (n=15) 46

Chapter 3

Fig. 3. 1 Root morphological traits, including (A) Lateral root length, (B) axial root length, (C) lateral root surface area, (D) axial root surface area, (E) number of crown roots (1st whorl), (F) number of crown root (2nd whorl) from maize (V6 stage) in a growth chamber environment. Bars noted by a different letter are significantly different ($p < 0.05$). Maize was grown in pots with two levels of N fertilizer (equivalent to 85 and 170 kg N ha⁻¹) and watered to a constant water potential of -15 or -5 kPa. NS, not significant ($p > 0.05$). Error bars represent standard error of means, n = 20..... 65

Fig. 3. 2 (A) The N uptake of maize (V6 stage) grown in pots with two levels of N fertilizer (equivalent to 85 and 170 kg N ha⁻¹) and watered to a constant water potential of -15 or -5 kPa. Boxplots show the minimum, median and maximum values, and bars with different letters were significantly different ($p < 0.05$). NS, not significant ($p > 0.05$). (B) The N uptake was related to the root hydraulic conductance of maize, where r is the Pearson correlation coefficient for n=20 observations for water potential of -15 or -5 kPa. The procedure for measuring root hydraulic conductance is explained in Table S4. 67

Fig. 3. 3 Rainfall and temperature (A), and soil water potential and cumulative transpiration (B) of two field growing seasons at Sainte-Anne-de-Bellevue, Québec, Canada. Data was collected at the

V1 to V7 stages of maize growth in 2021 and 2022. Maize was seeded on June 7, 2021, and May 12, 2022. Soil water potential in the root-associated soil at the V1, V3, V5 and V7 growth stages was averaged among N fertilization treatments (0, 72, 96 or 120 kg N ha⁻¹ during the growing season), and reported as mean ± standard error (n = 48 in 2021, and n = 64 in 2022)..... 68

Fig. 3. 4 Root morphological traits, including lateral root length and surface area (A), axial root length and surface area (B), number of 1st whorl and 2nd whorl crown roots (C) of field-grown maize from the V1 to V7 growth stages during the 2021 and 2022 seasons at Sainte-Anne-de-Bellevue, Québec, Canada. The fertilizer treatment delivered about 40% of the target N rate banded as ammonium sulfate at planting (0, 32, 40 or 50 kg N ha⁻¹) and the remaining 60% side-dressed as calcium ammonium nitrate at the V6 stage, supplying 0, 72, 96 or 120 kg N ha⁻¹ during the growing season. Data points are the mean with standard error bars, n= 16. Asterisk (*) indicates significant difference ($p < 0.05$) compared to control plot received 0 kg ha⁻¹..... 69

Fig. 3. 5 Root hydraulic conductance (A) and the N uptake (B) at the V1, V3, V5, and V7 stages of maize growth in a field at Sainte-Anne-de-Bellevue, Québec, Canada. The fertilizer treatment delivered about 40% of the target N rate banded as ammonium sulfate at planting (0, 32, 40 or 50 kg N ha⁻¹) and the remaining 60% side-dressed as calcium ammonium nitrate at the V6 stage, supplying 0, 72, 96 or 120 kg N ha⁻¹ during the growing season. Data points are the mean with standard error bars. Asterisk (*) indicates significant difference ($p < 0.05$) compared to control plot received 0 kg ha⁻¹. The relationship between maize N uptake and root hydraulic conductance (C) was fitted to best-fit lines (with 95% confidence intervals) when r , the Pearson correlation coefficient, was significant ($p < 0.05$). The procedure for measuring root hydraulic conductance is explained in Table S6..... 70

Chapter 4

Fig. 4. 1 Root morphological traits, including axial root length (a, b), lateral root length (c, d), lateral root surface area (e, f) of maize grown in the split-root system to the V3 or V6 stages. Maize was grown in pots kept at a constant water potential (-5kPa or -30kPa). Data was pooled among N tracer treatments, and plants with the same water potential were pooled together (n = 20). Different letters over the bars represent significantly differences (p < 0.05, Tukey's honestly significant test). NS, not significant (p > 0.05). 92

Fig. 4. 2 Measured hydraulic conductance of maize grown in the split-root system until the V3 (a) and V6 stages (b). Maize was grown in pots kept at a constant water potential (-5kPa or -30kPa). Hydraulic conductance was determined with the root exudation method, with one primary, seminal, 1st whorl crown root, and 2nd whorl crown root collected from each of the 12 individual plants grown under one water potential for analysis (n = 12). Error bars represent standard error of means. Different letters over the bars represent significantly differences (p < 0.05, Tukey's honestly significant test). NS, not significant (p > 0.05)..... 96

Fig. 4. 3 Nitrogen uptake by embryonic roots and crown roots of maize grown in the split-root system until V3 (a) and V6 stages (b). Maize was grown in pots kept at a constant water potential (-5kPa or -30kPa). Nitrogen uptake rate was calculated from the ¹⁵N enrichment in maize shoot after 0h, 24h, and 48h ¹⁵N enrichment periods. At V3 and V6 stages, one of the chambers, either the inner or outer, received an injection of ¹⁵N-KNO₃ solution (18.4% atom ¹⁵N excess), while the other chamber received ¹⁴N-KNO₃ solution, ensuring exposure of only one root type (either embryonic or crown roots) to ¹⁵N-KNO₃ solution. Boxplots show minimum, median, maximum. The dots show outliers. Different letters over the bars indicate significantly different (p < 0.05, Tukey's honestly significant test). NS, not significant (p > 0.05). 100

Fig. 4. 4 Gross nitrification arounds embryonic roots and crown roots of maize grown in the split-root system until (a) V3 and (b) V6 stages. Maize was grown in pots kept at a constant water potential (-5kPa or -30kPa). Gross nitrification rate was calculated from the ^{15}N isotope dilution after 0h, 24h, and 48h ^{15}N enrichment periods. At V3 and V6 stages, one of the chambers, either the inner or outer, received an injection of ^{15}N - KNO_3 solution (18.4% atom ^{15}N excess), while the other chamber received ^{14}N - KNO_3 solution, ensuring exposure of only one root type (either embryonic or crown roots) to ^{15}N - KNO_3 solution. Boxplots show minimum, median, maximum. The dots show outliers. Different letters over the bars indicate significantly different ($p < 0.05$, Tukey's honestly significant test). NS, not significant ($p > 0.05$). 101

LIST OF APPENDICES

Chapter 2

Table S2. 1 Measured NO_3^- concentration in leachate, representing maize root exposure to NO_3^- in perlite-filled pots receiving modified Hoagland solution containing 0 to 8 mM NO_3^- , 15 to 29 d after planting maize seeds. The NO_3^- concentration extracted from perlite with 2 M KCl solution at maize harvest (30 d after seeding) is reported. LOD is the limit of detection. Data are the mean \pm standard error of the mean (n=15) 139

Table S2. 2 Root dry mass, tips and number of roots of primary, seminal and crown roots, after maize roots were exposed to variable NO_3^- concentrations (mean value of measured NO_3^- concentration from 15 to 29 d) in perlite-filled pots for 30 d. Data are mean \pm standard error . 140

Fig. S2. 1 Comparison of the maize root length measured by ruler versus WinRhizo software (Regent Instruments, Quebec, Canada). The error bars are standard error (n = 10) 141

Chapter 3

Table S3. 1 Goodness-of-fit statistics for shoot biomass of field-grown maize, estimated by the Root Zone Water Quality Model, in response to variable N fertilizer rates. The field experiment was in Sainte-Anne-de-Bellevue, Québec, Canada. Root mean square error (RMSE), relative root mean square error (RRMSE), and coefficient of determination (R^2) were calculated with equations S1 to S4, below. n = number of observations. 142

Table S3. 2 Biostimulant treatments had no effect ($p>0.05$, n.s.: not significant) on the growth and nitrogen (N) uptake of maize (V6 stage), which varied according to the N fertilizer \times soil water treatments ($p<0.001$, ***), but not the 3-way interaction ($p>0.05$, n.s.) in a growth chamber environment. Values are the mean \pm standard error, n= 5..... 144

Table S3. 3 Xylem number and area, measured from three segments (tip: 0–20 mm from root tip, mid: 40–60 mm from root tip, base: 0–20 mm from the base of the stem) of a representative thin-sectioned axial root for each type (primary, seminal and crown, 1st and 2nd whorls) of maize (V6 stage) in a growth chamber environment. Maize was grown in pots with two levels of N fertilizer (equivalent to 85 and 170 kg N ha⁻¹) and watered to a constant soil water potential of -15 and -5 kPa. Values are the mean ± standard error, n= 4..... 145

Table S3. 4 Root hydraulic conductance, estimated for segments (tip: 0–20 mm from root tip, mid: 40–60 mm from root tip, base: 0–20 mm from the base of the stem) of a representative thin-sectioned axial root for each type (primary, seminal and crown, 1st and 2nd whorls) of maize (V6 stage) in a growth chamber environment. Maize was grown in pots with two levels of N fertilizer (equivalent to 85 and 170 kg N ha⁻¹) and watered to a constant soil water potential of -15 and -5 kPa. Values are the mean ± standard error, n= 4..... 147

Table S3. 5 Xylem area measured from three segments (tip: 0–20 mm from root tip, mid: 40–60 mm from root tip, base: 0–20 mm from the base of the stem) of a representative thin-sectioned axial root for each type (primary, seminal and crown, 1st and 2nd whorls) of maize (V1 to V7 stage) in a simulated-field condition. Maize was grown in pots with two levels of N fertilizer (equivalent to 0 and 50 kg N ha⁻¹) before seeding and moistened to the average soil water content from the 2021 and 2022 field seasons. Pots received 50 kg N ha⁻¹ treatment before seeding, with additional N fertilizer applied at a rate of 70 kg N ha⁻¹ at the V6 stage. Some data was missing because roots did not produce enough root length for anatomical measurements. Values are the mean ± standard error, n= 4..... 148

Table S3. 6 Root hydraulic conductance, estimated for segments (tip: 0–20 mm from root tip, mid: 40–60 mm from root tip, base: 0–20 mm from the base of the stem) of a representative thin-

sectioned axial root for each type (primary, seminal and crown, 1st and 2nd whorls) of maize (V6 stage) in a simulated-field condition. Maize was grown in pots with two levels of N fertilizer (equivalent to 0 and 50 kg N ha⁻¹) before seeding and moistened to the average soil water content from the 2021 and 2022 field seasons. Pots received 50 kg N ha⁻¹ treatment before seeding, with additional N fertilizer applied at a rate of 70 kg N ha⁻¹ at the V6 stage. The pots received 50 kg N ha⁻¹ treatment before seeding were supplied with N fertilizer at the rate of 70 kg N ha⁻¹ at V6 stage. Some data was missing because roots did not produce enough root length for anatomical measurements. Values are the mean ± standard error, n= 4. 151

Table S3. 7 Maize yield of two field growing seasons at Sainte-Anne-de-Bellevue, Québec, Canada. Data was collected at the V1 to V7 stages of maize growth in 2021 and 2022. The fertilizer treatment delivered about 40% of the target N rate banded as ammonium sulfate at planting (0, 32, 40 or 50 kg N ha⁻¹) and the remaining 60% side-dressed as calcium ammonium nitrate at the V6 stage, supplying 0, 72, 96 or 120 kg N ha⁻¹ during the growing season. 154

Fig. S3. 1 Water retention curve of the soil used in the growth and field experiment. Soil was collected from the maize growing field in Sainte-Anne-de-Bellevue, Québec, Canada. Soil at this location is a sandy-loam Humic Gleysol of the St. Amable series containing 620 g sand kg⁻¹, 60 g clay kg⁻¹, and 48 g organic C kg⁻¹, with pH 6.3, field capacity of 23% and an average bulk density of 1110 kg m⁻³. Data points are the mean with standard error bars, n= 3. 155

Fig. S3. 2 Maize shoot biomass and N concentration (V1 to V7 stage) and soil mineral N concentration in plots receiving variable N fertilizer rates located in Sainte-Anne-de-Bellevue, Québec, Canada. Maize plants and root-associated soil were collected at V1, V3, V5, and V7 stages in 2021 and 2022. The control plot received 0 kg ha⁻¹ (2022 only) while fertilized plots had about 40% of the target N rate (30, 40 and 50 kg N ha⁻¹) banded as ammonium sulfate at planting and

the remaining 60% side-dressed as calcium ammonium nitrate at the V6 stage, supplying 72, 96 and 120 kg N ha⁻¹ during the growing period. Data points are the mean with standard error bars, n= 16. Asterisk (*) indicates significant difference ($p < 0.05$) compared to control plot received 0 kg ha⁻¹..... 156

Fig. S3. 3 Lateral root plasticity of three types – primary, seminal and crown – from maize (V1 to V7 stage) collected in 2022 from plots receiving variable N fertilizer rates located in Sainte-Anne-de-Bellevue, Québec, Canada. The control plot received 0 kg ha⁻¹ while fertilized plots had about 40% of the target N rate (30, 40 and 50 kg N ha⁻¹) banded as ammonium sulfate at planting and the remaining 60% side-dressed as calcium ammonium nitrate at the V6 stage, supplying 72, 96 and 120 kg N ha⁻¹ during the growing period. Data points are the mean with standard error bars, n= 16. 157

Fig. S3. 4 Stomatal conductance of maize (V3 to V5 stage) in a growth chamber environment. Maize was grown in pots with two levels of N fertilizer (equivalent to 85 and 170 kg N ha⁻¹) and watered to a constant soil water potential of -15 and -5 kPa. Error bars represent standard error of means, n = 20. 158

Fig. S3. 5 Anatomical structure of (A) axial root types – primary, seminal, crown (1st whorl), crown (2nd whorl) – of field-grown maize roots and (B) lateral roots. The scale bar = 100 µm, except for the base of second whorl crown root with a scale bar = 200 µm..... 159

Chapter 4

Fig. S4. 1 Schematic illustration of the split-root system. Maize seeds were pre-germinated for about 10 d before transplanting to the split-root pots designed to segregate the embryonic root system (primary and seminal roots) from the crown roots. An inner chamber (PVC pipe with 5 cm diameter, 25 cm height) was placed in the middle of the outer chamber (PVC pipe with 10 cm

diameter, 30 cm height). The bottom of split-root pots was covered with the aluminum foil to prevent water and soluble nutrient losses. 160

Fig. S4. 2 Soil water potential in the inner and outer pots of the split-root system. Tensiometers were inserted into the inner and outer chambers to monitor the soil water potential of the pots. The plants were watered to achieve the target soil water potential (-5kPa or -30kPa) every 2 days, from the first day after transplanting the maize seedling to the split-root system until the V6 stage. Data represents the mean and standard error, n = 4..... 161

Fig. S4. 3 Shoot biomass (a, b) and root length (c, d) were the same for maize planted in split-root pots and control pots (PVC pipe with 10 cm diameter, 30 cm height, without an inner chamber). Maize was grown in pots watered to a constant water potential (-5kPa or -30kPa) and was destructively sampled at the V3 and V6 stages. Values are the mean ± standard error, n = 4.... 162

Fig. S4. 4 The ¹⁵N enrichment (atom% excess) of maize shoot, crown root, seminal root, and primary root after 0, 24 and 48 h of exposure to ¹⁵N enrichment in the split-root system, and the V3 and V6 stages. Maize was grown in pots kept at a constant water potential (-5kPa or -30kPa). At V3 and V6 stages, one of the chambers, either the inner or outer, received an injection of ¹⁵N-KNO₃ solution (18.4% atom ¹⁵N excess), while the other chamber received ¹⁴N-KNO₃ solution, ensuring exposure of only one root type (either embryonic or crown roots) to ¹⁵N-KNO₃ solution. Points with error bars represent the mean and standard error, connected with the best-fit line, n = 4. Some data points and lines are missing due to the death of primary and seminal roots by the V6 stage. 163

Fig. S4. 5 Soil mineral N (NO₃⁻ and NH₄⁺) in the inner chamber and outer chamber of the split-root system after 0, 24 and 48 h exposure to ¹⁵N enrichment at the V3 and V6 stages. The inner and outer chambers were kept at a constant water potential (-5kPa or -30kPa). At V3 and V6 stages,

one of the chambers, either the inner or outer, received an injection of $^{15}\text{N-KNO}_3$ solution (18.4% atom ^{15}N excess), while the other chamber received $^{14}\text{N-KNO}_3$ solution, ensuring exposure of only one root type (either embryonic or crown roots) to $^{15}\text{N-KNO}_3$ solution. Data was pooled among each chamber type (inner or outer) with the same water potential, regardless of received KNO_3 solution type ($^{14}\text{N-KNO}_3$ or $^{15}\text{N-KNO}_3$). Data points represent the mean and standard error, $n = 12$.

..... 164

Fig. S4. 6 The relationship between maize N uptake rate and root hydraulic conductance of embryonic and crown roots. The relationship was described with best-fit lines (with 95% confidence intervals) when r , the Pearson correlation coefficient, was significant ($p < 0.05$). Maize was grown in pots kept at a constant water potential (-5kPa or -30kPa). Data collected from V3 and V6 growth stage were pooled, $n = 16$ for each root type. 165

Fig. S4. 7 Stele area, cortex thickness, stele/cortex ratio of maize grown in the split-root system until V3 and V6 stages. Maize was grown in pots watered to a constant water potential (-5kPa or -30kPa). One primary, seminal, 1st whorl crown root, and 2nd whorl crown root collected from each of the 4 individual plants ($n = 4$). Error bars represent standard error of means. Different letters over the bars represent significantly different ($p < 0.05$, Tukey's honestly significant test). NS, not significant ($p > 0.05$)..... 166

Fig. S4. 8 Stomatal conductance of maize grown in the split-root system V6 stages. Maize was grown in pots watered to a constant water potential (-5kPa or -30kPa). The stomatal conductance was measured at the mid-blade of the newest fully formed leaf when maize reached V2, V4, and V6 stages. Error bars represent standard error of means ($n = 12$). Asterisks (*) indicate the significant difference between the water potential treatments ($p < 0.05$)..... 167

Fig. S4. 9 Soil pH in the inner chamber and outer chamber of the split-root system after 0, 24 and 48 h exposure to ¹⁵N enrichment at the (a) V3 and (b) V6 stages. The inner and outer chambers were kept at a constant water potential (-5kPa or -30kPa). At V3 and V6 stages, one of the chambers, either the inner or outer, received an injection of ¹⁵N-KNO₃ solution (18.4% atom ¹⁵N excess), while the other chamber received ¹⁴N-KNO₃ solution, ensuring exposure of only one root type (either embryonic or crown roots) to ¹⁵N-KNO₃ solution. Data points represent the mean and standard error, n = 4. Different letters represent significantly different (p < 0.05, Tukey's honestly significant test)..... 168

ABSTRACT

Maize is a staple food crop of global importance. Optimal yield and quality in the maize crop depend on the nitrogen (N) uptake, which is supplied primarily by nitrate (NO_3^-) in soil. Since transpiration controls the amount of soil water containing NO_3^- that reaches the root surface, water scarcity could limit the NO_3^- uptake by maize. My Ph.D. research evaluated the plasticity of the maize root system, as an adaptive strategy that could sustain N uptake in water-deficient and N-limited conditions. Specific objectives were: (1) to investigate the morphological plasticity of maize root types exposed to variable NO_3^- concentrations, (2) to identify the morphological and anatomical plasticity of maize roots affecting their hydraulic conductance in response to N fertilizer rates and soil water contents, and (3) to quantify the NO_3^- uptake rates in embryonic and crown roots across a soil water gradient. There was a root-specific growth response of maize roots exposed in porous media with variable NO_3^- concentrations (0, 1, 2, 3.9 and 7.8 mM NO_3^-) up to the vegetative 3-leaf (V3) growth stage. Higher NO_3^- concentration induced positive quadratic growth in laterals of the seminal and crown root types, with no change in the growth of all axial roots and laterals of primary roots. Maize lateral roots were longer, with greater surface area and more crown roots formed in moister conditions with higher rates of N fertilizer addition than with lower rates. For example, pot-grown maize had 23% longer lateral roots, a 16% increase in lateral root surface area, and 15% more crown roots when grown in well-watered soil ($\psi_{\text{soil}} = -5$ kPa) received high N treatment (equivalent to 170 kg N ha⁻¹) than low N treatment (equivalent to 85 kg N ha⁻¹). Water, NO_3^- and other solutes flowed primarily through the crown roots, which had more xylem vessels with a larger surface area and were responsible for more of the root hydraulic conductance than other root types in pot-grown and field-grown maize. Maize N uptake was not

related to root hydraulic conductance in drier soils, but tended to increase when N fertilizer was applied to wetter soils, in both pot and field environments. Maize N uptake differed among root types, based on ^{15}N -labeled KNO_3 tracking in a split-root system. By the V3 growth stage, crown roots produced 176% and 143% greater xylem area than primary and seminal roots, resulting in over 300% greater root hydraulic conductance and 2-fold greater N uptake of crown roots under the wet soil ($\psi_{\text{soil}} = -5$ kPa). However, under the dry soil ($\psi_{\text{soil}} = -30$ kPa), seminal and crown roots had similar root hydraulic conductance and N uptake, suggesting that soil water availability impacts NO_3^- uptake dynamics. Acknowledging these plastic responses of maize roots and their association with N uptake is important for prioritizing root-based traits in maize breeding programs and soil water management, particularly in environments with water-deficient and N-limited environments.

RÉSUMÉ

Le maïs est une culture vivrière d'importance mondiale. Le rendement optimal et la qualité de la culture du maïs dépendent de l'absorption de l'azote (N), qui est fourni principalement par le nitrate (NO_3^-) dans le sol. Comme la transpiration contrôle la quantité d'eau du sol contenant du NO_3^- qui atteint la surface des racines, le manque d'eau pourrait limiter l'absorption de NO_3^- par le maïs. Ma recherche de doctorat a évalué la plasticité du système racinaire du maïs, en tant que stratégie adaptative qui pourrait soutenir l'absorption d'azote dans des conditions de manque d'eau et de limitation de l'azote. Les objectifs spécifiques étaient les suivants: (1) étudier la plasticité morphologique des types de racines de maïs exposés à diverses concentrations de NO_3^- , (2) identifier la plasticité morphologique et anatomique des racines de maïs affectant leur conductance hydraulique en réponse aux taux d'engrais N et aux teneurs en eau du sol, et (3) quantifier les taux d'absorption de NO_3^- dans les racines séminales et les racines coronaires à travers un gradient d'eau du sol. Les racines de maïs exposées dans un milieu poreux avec des concentrations variables de NO_3^- (0, 1, 2, 3,9 et 7,8 mM NO_3^-) jusqu'au stade végétatif de 3 feuilles (V3) ont eu une réponse de croissance spécifique à la racine. Une concentration plus élevée de NO_3^- a induit une croissance quadratique positive des racines latérales des types de racines séminales et de racines coronaires, sans changement dans la croissance de toutes les racines axiales et des racines latérales des racines primaires. Les racines latérales du maïs étaient plus longues, avec une plus grande surface et davantage de racines coronaires se sont formées dans des conditions humides avec des taux d'ajout d'engrais N plus élevés qu'avec des taux plus faibles. Par exemple, le maïs cultivé en pot avait des racines latérales 23 % plus longues, une augmentation de 16 % de la surface des racines latérales et 15 % de racines coronaires en plus lorsqu'il était cultivé dans un sol bien arrosé ($\psi_{\text{soil}} = -5$ kPa)

avec 170 kg N ha⁻¹ plutôt qu'avec 85 kg N ha⁻¹. L'eau, le NO₃⁻ et d'autres solutés ont circulé principalement à travers les racines coronaires, qui avaient plus de vaisseaux du xylème avec une plus grande surface et étaient responsables d'une plus grande partie de la conductance hydraulique de la racine que d'autres types de racines dans le maïs cultivé en pot et en plein champ. L'absorption d'azote par le maïs n'était pas liée à la conductance hydraulique des racines dans les sols plus secs, mais avait tendance à augmenter lorsque des engrais azotés étaient appliqués sur des sols plus humides, à la fois dans les environnements en pot et en plein champ. L'absorption d'azote par le maïs diffère selon les types de racines, d'après le suivi du KNO₃ marqué à l'azote 15 dans un système de racines divisées. Au stade de croissance V3, les racines de la couronne produisaient une surface de xylème supérieure de 176 % et 143 % à celle des racines primaires et séminales, ce qui se traduisait par une conductance hydraulique des racines supérieure de plus de 300 % et une absorption de l'azote deux fois plus importante par les racines coronaires dans un sol humide ($\psi_{\text{soil}} = -5$ kPa). Cependant, dans un sol sec ($\psi_{\text{soil}} = -30$ kPa), les racines séminales et les racines coronaires avaient une conductance hydraulique et une absorption d'azote similaires, ce qui suggère que la disponibilité de l'eau dans le sol a un impact sur la dynamique de l'absorption de NO₃⁻. La reconnaissance de ces réponses plastiques des racines de maïs et de leur association avec l'absorption d'azote est importante pour donner la priorité aux caractéristiques des racines dans les programmes de sélection du maïs et la gestion de l'eau du sol, en particulier dans les environnements où l'eau est déficiente et l'azote limité.

ACKNOWLEDGEMENT

First, I sincerely thank my supervisor, Dr. Joann Whalen, for her supervision, support, and patience throughout my academic journey. Her mentorship has been instrumental in shaping my academic growth and the development of my independence and strong personality. I am grateful for her invaluable suggestions and comments to my proposals, presentations, posters, and manuscripts.

I would like to thank my committee members and comprehensive examiners, Dr. Brian T. Driscoll, Dr. Cynthia Kallenbach, Dr. Valerie Gravel, and Dr. Abdolhamid Akbarzadeh, for their suggestions and comments. Many thanks to Dr. Geoffrey Sunahara for providing me with constructive comments on my experimental designs, proposals, and oral presentations. I am grateful for Mohammed Antar, Michael Ruppert, Marc Samoisette, and Serge Lussier's technical support in the field. I would also like to thank Sarah-Ann Persechino and Michael Rourke Gossage-Bleho for their assistance in the greenhouse, and Dr. Youssef Chebli for the professional guidance on microscopy. I am grateful for the technical support provided by William Boyd Dumais, Hicham Benslim, and Khosro Mousavi in preparing the experimental materials. Special thanks to Aurelie Stil from the University of Montreal for generously allowing me to use the equipment for my experiment.

To the members of the SERG group at McGill University, both current and past - Lijun, Elias, Noura, Liz, Aidan, Krisztina, Fang, Lucy, and Fatima, thank you all for your help in the field – I am deeply grateful for your support in the field, constructive feedback on my work, and the mental support that kept me going. Special thanks to Chih-Yu for his invaluable guidance and mentorship in developing my research questions and experimental design.

I want to thank my dear friends in Montreal – Qian, Zhiwei, Yuhang, Shuting, Tiffany, Jiaxin, Shimin, Ruixue, Wei, Zhijia, Zhengyuan – who have become not just friends but more like family. You guys literally brighten my life, bringing so much joy and happiness to the cold and dark winter. Finally, heartfelt thanks to my beloved family for their endless support and encouragement. This journey would not have been possible without their love, patience, and unwavering support.

CONTRIBUTION TO ORIGINAL KNOWLEDGE

The research conducted in this thesis provides 3 distinct contributions to knowledge:

(1) My original idea is to quantify the plasticity of maize root types to NO_3^- concentration in a porous environment. My approach of growing maize in the perlite media is original because it offers a solid support that mimics a porous soil environment, in contrast to the vast majority of studies that studied maize root growth in liquid hydroponic system. Moreover, I devised a method to control and monitor the NO_3^- concentration in the perlite environment for several weeks. Based on the distinctive plasticity of three maize root types, I proposed a mechanistic explanation for why crown and seminal lateral roots respond to NO_3^- exposure, while the axial roots are insensitive to the NO_3^- concentration in perlite media.

(2) My results showed that maize growth is primarily constrained by water, and then by the NO_3^- supply, in pot and field environments. It appears that maize root showed plasticity to N fertilizer inputs in well-watered soil, but not in dry soil conditions. While the root hydraulic conductance was not related to N uptake in a drier soil, there was a positive association between root hydraulic conductance and N uptake in wetter soil.

(3) I present a first report that tracks ^{15}N - NO_3^- uptake by the embryonic roots and crown roots across a soil water gradient. The segregation of embryotic and crown roots was achieved in a soil-based split-root experiment with split-injection of stable isotope ^{15}N . Crown roots were responsible for most of the NO_3^- uptake during vegetative growth (up to the V3 stage) in a wetter soil (-5 kPa), owing to their higher root hydraulic conductance. However, NO_3^- uptake was achieved by both embryonic roots and crown roots in drier soil (-30 kPa) at the V3 growth stage. Embryonic roots

of maize have the adsorptive surface area to sustain NO_3^- uptake in water-deficient soils, when there is not enough water to deliver NO_3^- and other solutes to the surface of crown roots.

PREFACE AND CONTRIBUTION OF AUTHORS

This thesis consists of four chapters, headed by a general introduction that states the overall objectives. A statement of the contributions to knowledge is provided, according to the guidelines of the Graduate and Postdoctoral Studies Office, McGill University. Chapter 1 is a literature review that summarizes the plastic response of maize roots to the environment stimuli in the agricultural soils and how maize roots absorb NO_3^- and water. Chapters 2 to 4 are my original research on maize roots in greenhouse and field experiments, which are written as scientific manuscripts. Connecting paragraphs are provided to show the connections between each chapter, according to the guidelines of the Graduate and Postdoctoral Studies Office, McGill University.

The candidate is the first author on all manuscripts. Co-authors include Dr. Joann K. Whalen and Dr. Chih-Yu Hung. The candidate reviewed the literature, formulated the research ideas, developed the experimental design, performed the experiments, collected data, conducted the statistical analysis, interpreted the findings, and wrote all the manuscripts. Dr. Whalen provided financial support, advice about the experimental design and data interpretations, and review the manuscripts. Dr. Chih-Yu Hung participated in experimental design, data interpretation and revised the manuscript of Chapter 2. The thesis research was funded by China Scholarship Council (CSC), Mitacs Accelerate Program and NSERC Discovery Grant.

The manuscript-based chapters are presented in the following order:

Chapter 2. Jiang, Y., Hung CY., Whalen, J.K., 2023. Distinctive plasticity of maize (*Zea mays*) root types to variable nitrate concentration. Canadian Journal of Plant Science. <https://doi.org/10.1139/cjps-2022-0246>

Chapter 3. Jiang, Y., Whalen, J.K., Plasticity of maize (*Zea mays*) roots depends on water content in nitrogen fertilized soil (In preparation for Plant Growth Regulation)

Chapter 4. Jiang, Y., Whalen, J.K., Water-conducting roots responsible for nitrogen uptake in maize (*Zea mays*) (In preparation for Plant and Soil)

GENERAL INTRODUCTION

Maize (*Zea mays*) is the third most produced staple crop in the world, with the annual yield $>1.2 \times 10^9$ Mt per year. Maize is a multi-functional crop that provides grain for human consumption, as well as stover for biofuel production and animal feeding (FAO, 2022). Climate change is creating water-deficits that could reduce maize production by 15 – 20% annually (Lobell and Schlenker, 2011). Moreover, soil water deficit limits nitrogen (N) uptake by maize roots that rely on transpiration-driven water fluxes to acquire nitrate (NO_3^-), the predominant plant-available N form in soil. As soil water content declines, closure of stomates in maize leaves reduces transpiration, which in turn limits NO_3^- uptake, potentially limiting the yield and quality of this N-demanding crop.

Maize roots absorb water and N from soil throughout the growing season, with around 25% of the water and 50% of N uptake obtained during the vegetative stage (Bender et al., 2013; Ordóñez et al., 2020). Embryonic primary and seminal roots, along with their lateral roots, are responsible for water and nutrient uptake in the first 14 d of seedling growth (up to V2; Ahmed et al., 2016). Subsequently, shoot-borne crown roots emerge and dominate the water uptake (Ahmed et al., 2018). Each root type may adjust their morphological and anatomical traits in response to water-deficits and N limitation.

The differential growth of lateral roots connected to the embryonic and crown root types alters the root hydraulic conductance, which directly affects the mass flow of water and NO_3^- from soil to the adsorptive root surface. Crown roots, for instance, have 60% more xylem elements and a 5-fold higher hydraulic conductance than primary and seminal roots, so they are responsible for most of the water and N uptake in the root system (Tai et al., 2016). The higher conductance of

crown roots results in 10^3 times more water uptake rate (Ahmed et al., 2018) and two-fold higher N uptake rate (Liu et al., 2020) in the crown roots than the embryonic roots. However, as soil dries, the hydraulic conductance of crown axial root will decrease significantly due to the inability of the large crown roots (average diameter 1 – 4 mm) to access water occluded in micropores $<10 \mu\text{m}$ (Yang et al., 2019). In water-deficient soils, embryonic roots are expected to be more important for water and N uptake during early vegetative growth. Thin seminal roots (average diameter 0.9 – 1.5 mm) and laterals (average diameter <0.5 mm) can grow into soil pores containing capillary water, NO_3^- and other solutes (Cahn et al., 1989; Zhan and Lynch, 2015). So far, we lack quantitative evidence of the NO_3^- uptake by diverse root types when maize is grown in water-sufficient versus water-deficient soil.

The global objective of thesis is to evaluate the plasticity of the maize root system, as an adaptive strategy that could sustain N uptake in water-deficient and N-limited conditions. The objectives include: (1) to investigate the morphological plasticity of maize root types exposed to variable NO_3^- concentrations, (2) to identify the morphological and anatomical plasticity of maize roots affecting their hydraulic conductance in response to N fertilizer rates and soil water contents, and (3) to quantify the NO_3^- uptake rates in embryonic and crown roots across a soil water gradient.

CHAPTER 1

Literature review

Maize (*Zea mays*) is the third most staple crop, along with wheat and rice. Being produced by more than 1.2×10^9 Mt per year, maize accounts for 94% of human cereal consumption, along with wheat and rice, and it is widely used in biofuel and animal feed sectors (FAO, 2022). Nevertheless, maize production faces the challenges of water-deficit. The unpredictable climate changes alter rainfall pattern, potentially reducing maize production by 15 – 20% per year (Lobell and Schlenker, 2011). Furthermore, soil water-deficit may limit the accessibility of nitrogen (N) to maize roots and compromise the yield potential because the uptake of mobile nitrate (NO_3^-) relies on mass flow (Plett et al., 2020).

Maize relies upon a complex root system to acquire water and nutrients from the soil. Over long-term evolution, modern maize has developed less adaptable root systems compared to its wild ancestor, teosinte, possibly due to the selective breeding for specific environments (Chen et al., 2022). For example, maize shows less variability in lateral root branches, aerenchyma, and number of xylems, than teosinte under edaphic stress (Mano et al., 2006; Burton et al., 2013). However, maize may be exposed to water-deficit and N-limited conditions during its lifespan, and a plastic root system that adjusts morphological and anatomical traits in response to soil water and nitrogen (N) levels can optimize resource uptake. Maize is genetically programmed to grow multiple axial root types – primary, seminal, crown, and brace roots - during its lifespan (Fig. 1. 1a). Multiple root types have evolved distinct morphological and anatomical plasticity in response to the environment. Root plasticity depends on the functions of each root type, including anchoring above-ground biomass in the soil and absorbing soil water and mineral nutrients to meet its growth

needs, which vary during its lifespan. Consequently, information about the plasticity of different root types supports a trait-based breeding approach to optimize the root system development for efficient N uptake, particularly when there is limited water and N deficiency in soil.

The objectives of this review are to 1) describe the structure and function of different maize root types, 2) show how roots respond to soil abiotic environments, including water and nutrient limitations, and 3) illustrate how roots absorb water and N uptake, especially when there is a water-deficit. Knowledge gained from this review helps understand how maize plasticity aids water and N uptake from water-limited and N-deficient soils.

1.1 Root types

1.1.1 Axial roots

Maize has embryonic (primary and seminal roots) and post-embryonic (crown and brace roots) roots in its root system. Primary roots emerge first from the basal pole of the embryo. The primary root penetrates the endosperm and seed coat, protected by a sheath known as the coleorhiza, within 2–4 d after planting the seeds in moist soil (Fig 1. 1b). Responsible for absorbing water and anchoring the seedling, the primary axial root grows to ~30 cm long and 1.7–3 mm in diameter (Tuberosa et al., 2002). Seminal roots, the second root type produced in the maize life cycle, emerge from the scutellar node (Fig. 1. 1b) around 7–10 d after seed germination. The initiation of seminal roots is controlled by genes *rtcs* (*rootless concerning crown and seminal roots*) and *rum1* (*rootless with undetectable meristems 1*, Table 1), which enable the seminal roots to penetrate the differentiated scutellar node tissue without a coleorhiza. Up to 13 seminal axial roots are produced, with a length of 10–65 cm and a diameter of 0.9–1.5 mm, depending on the maize genotype (Hund et al., 2004; Tai et al., 2016). In the first 14 d after germination, approximately half of the total root system of the plant is embryonic primary roots, and the rest are seminal roots.

They are the sole root tissues that provide water and nutrients during the first 2–3 wk of seedling growth. The embryonic root functions are supplemented by post-embryonic roots starting around 1 month after planting, although embryonic roots remain functional throughout the maize life cycle (Hetz et al., 1996).

Post-embryonic roots emerge from shoot nodes, initiated in the primordia that form opposite to the collateral vascular bundles in the nodal region of the coleoptile, controlled by the *rtcs* gene (Fig. 1. 1a). Crown roots appear around 10 – 14 d after seed germination from underground nodes, while brace roots initiate approximately 40 d after seed germination in aboveground nodes, with variations observed among maize genotypes and environmental conditions such as soil moisture and temperature. After the V3 growth stage, crown roots elongate, controlled by the *rtcl* (*rootless concerning crown and seminal roots like*) gene, and gradually become the main rootstock, with up to six whorls of crown roots and two to three whorls of brace roots forming during the maize lifespan (Hoppe et al., 1986; Hochholdinger et al., 2004). These shoot-borne roots contribute to upright growth, helping the plants resist lodging (McCully and Canny, 1988). In addition, post-embryonic roots are the main conductors of water and solutes since they contain >75% of metaxylem vessels in the vascular system (Hoppe et al., 1986).

Root hairs cover the surface of primary, seminal, and crown roots. Each root hair is a unicellular structure of trichoblasts in a root epidermal cell. The surface of axial roots has up to 200 hairs mm⁻², varying in length from 0.2 – 1.0 mm (Hey et al., 2017), regulated by *rth* (*root hair less*) genes. The presence of root hairs amplifies the contact between the root surface and surrounding soil, as they increase the surface area of roots by hundreds to thousands of times.

1.1.2 Lateral roots

Lateral roots are fine, absorptive extensions that extend from axial roots of all types (primary, seminal, crown, and belowground part of brace roots). Lateral roots originate from the endodermal and pericycle cells, under regulation of the *rum1* and *lrt1* (lateral root less 1) genes. Emergence of lateral roots is an intricate process that involves anticlinal cell division of the phloem pole pericycle cells, followed by periclinal division of pericycle cells, anticlinal division of endodermal cells, and ultimately, the formation of the lateral root primordium (Yu et al., 2016). As a result, the epidermis and columella of newly formed lateral roots originate from endodermal cells, while the vascular tissue is derived from pericycle cells (Bell and McCully, 1970).

Energetically, it is less resource-demanding for maize to produce laterals than extend the length of the axial roots. Maize lateral roots, with a diameter less than 0.68 mm, are typically thinner than axial roots from the embryonic and post-embryonic tissues (0.5–3 mm dia. for primary, seminal and crown roots) and brace roots (2–5 mm dia., Cahn et al., 1989). Lateral roots are 15 – 35 times longer than axial roots, accounting for >70% of root length and surface area but only 20% of root weight at V7 –V9 stages (Guo and York, 2019). Moreover, the growth rate of lateral roots surpasses that of axial roots by 2 to 5 times, as controlled by the *slr1* and *slr2* (*short lateral roots1 and 2*) genes (Cahn et al., 1989; Hochholdinger et al., 2001). In addition, development of lateral roots increases the absorptive root surface area because about 70–90% of lateral root surface is covered by root hairs (Gilroy and Jones, 2000). Whereas axial roots are a foundational support for transport of substrates throughout the root system, the main function of lateral roots is for water and nutrient uptake from the soil.

New lateral roots emerge from the axial root tissue, and they can also be produced from the existing lateral root tissue. Throughout the maize life cycle, the root system develops up to five orders of lateral roots. The first-order lateral roots, originating directly from axial roots, develop

continuously from the V1 stage to the reproductive stage. Approximately 29% of these first-order lateral roots give rise to higher-order lateral roots (Pages and Pellerin, 1994). The higher-order lateral roots tend to be thinner (dia. <0.3 mm) than the first-order lateral roots. Propagation of extensive lateral roots is another way that maize can anchor itself securely and maximize contact with the soil volume for acquisition of water and nutrient resources.

1.2 The anatomy of maize root tissue

All maize roots, including primary, seminal, crown, brace axial roots, and lateral roots, have three anatomical zones in their longitudinal direction: meristematic zone, elongation zone, and differentiation zone (Fig. 1. 1c). The youngest, undifferentiated cells in the root apex exist in the meristematic zone. The genetic regulation of meristematic cells governs the determinate growth of roots by controlling the timing and extent of cell division and elongation (Dowd et al., 2020). As these cells elongate, accompanied by division, they form an elongation zone. The meristematic and elongation zones overlap because cell expansion also occurs in the meristem (Ishikawa and Evans, 1995). Root cells reach their final size in the differentiation zone, where they develop into lateral roots and root hairs (Marzec et al., 2015). This anatomical structure creates a longitudinal gradient of the youngest cells and undifferentiated cell in the root apex and the oldest cells in the basal area.

The different root types (axial and laterals associated with the primary, seminal, crown, and brace roots) exhibit distinctive anatomical features that align with their specific functions (Fig. 1. 1d). The epidermis serves as the crucial interface connecting the root systems with the rhizosphere at the outermost layer of maize roots. As the roots get older, the deposition of lignin and suberin within the epidermis gives rise to the exodermis, a hardened layer that is visually apparent due to

its dark color near the root surface (Barberon, 2017). Epidermal cells differentiate into two types: root hair trichoblasts, which develop root hairs that extend into the soil pores and make contact with soil particles, and non-root hair atrichoblasts that contribute to the overall structural integrity of the root. Moving inward, cortical cells fill the space between the epidermal and endodermal layers. The endodermal layers surround the pericycle at the outermost layer of the central cylinder. The central vascular cylinder (as known as the stele) contains the xylem and phloem vessels responsible for the transportation of water and nutrients to stems and subsequently into the vascular system in leaves and other aboveground tissues. This transport system comprises two to three early metaxylem elements alongside one late metaxylem element, ensuring the efficient movement of water and solutes to the shoots (Hochholdinger, 2009). However, the number of xylem elements varies among root types. Shoot-born roots have up to 48 metaxylem elements, representing 63% more meta and proto-xylem elements than present in embryonic roots (Tai et al., 2016). This abundance of xylem elements enables crown roots to generate five times higher suction and radial water flow rates than seminal roots in 30-day-old maize seedlings (Doussan et al., 1998).

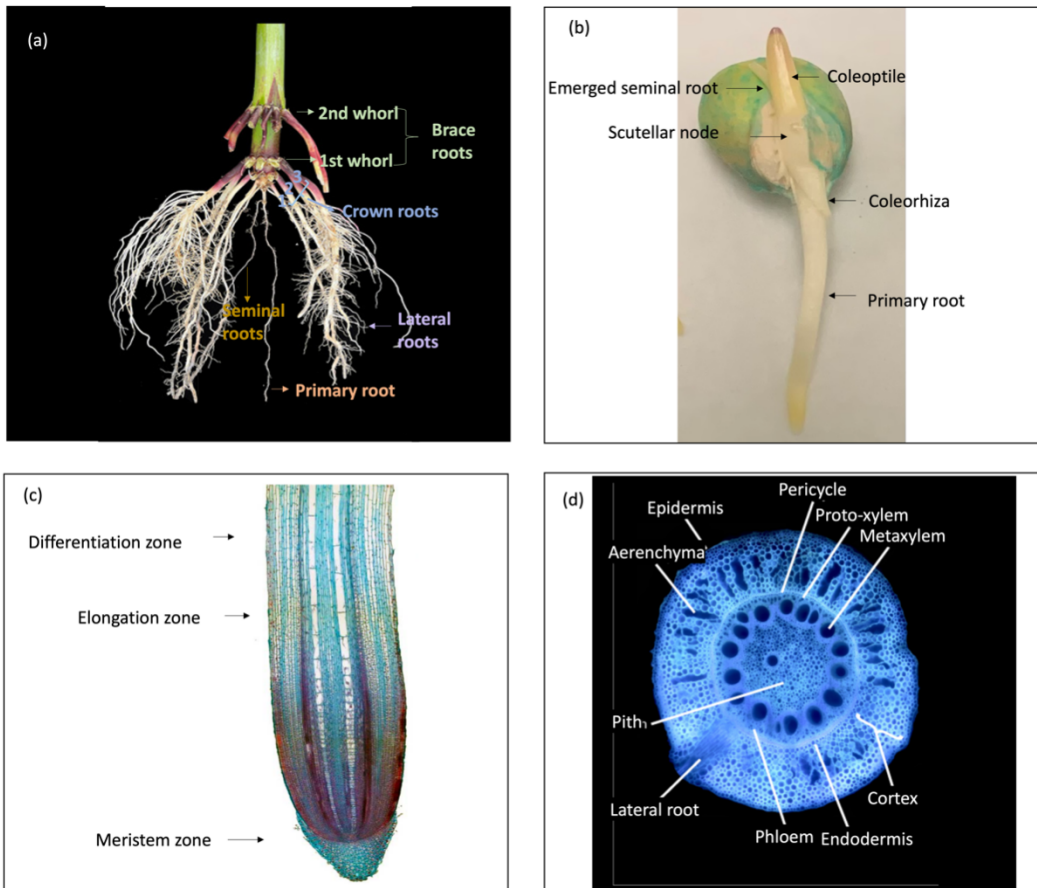


Fig. 1. 1 (a) Maize root types, taken from Viana, G., Scharwies, J.D., Dinneny, J.R. 2022. Deconstructing the root system of grasses through an exploration of development, anatomy and function. *Plant Cell Environ.* **45**: 602–619. Doi: <https://doi.org/10.1111/pce.14270>. (b) emergence of the maize embryonic roots, (c) the longitudinal anatomy of maize roots, image from Jen Dixon, (d) cross-sectional anatomy, taken from Lynch, J.P., Strock, C.F., Schneider, H.M., et al. 2021. Root anatomy and soil resource capture. *Plant Soil* **466**: 21–63. doi: <https://doi.org/10.1007/s11104-021-05010-y>.

Table 1. 1 Genes and their functions in maize root development

Type	Root types	Genes	Developmental process	Gene function	Reference
Axial root	Crown root	<i>rtcl</i>	Elongation	Auxin signaling	Xu et al., 2015
	Seminal root, crown root	<i>rtcs</i>	Initiation	Auxin signaling	Xu et al., 2015
	Seminal root, Lateral root	<i>rum1</i>	Initiation	Auxin signaling	Woll et al., 2005
Lateral root	Crown lateral root	<i>lrt1</i>	Initiation	Unknown	Hochholdinger et al., 1998
	Crown lateral root	<i>slr1</i>	Elongation	Unknown	Hochholdinger et al., 2001
	Crown lateral root	<i>slr2</i>	Elongation	Unknown	Hochholdinger et al., 2001
Root hair	Root hair	<i>rth1</i>	Elongation	Exocytotic vesicle fusion	Wen et al., 2005
	Root hair	<i>rth3</i>	Elongation	Cellulose organization	Hochholdinger et al., 2008
	Root hair	<i>rth5</i>	Elongation	Cell wall loosening	Nestler et al., 2014
	Root hair	<i>rth6</i>	Elongation	Cellulose synthesis	Li et al., 2016

1.3 Root plasticity in the soil environment

Sessile maize roots exhibit a remarkable capacity for adaptation to complex soil environments because gradients in soil water and nutrient concentrations trigger specific growth responses. This results in changes to root morphology and anatomical traits, such as root length, root angle, branching of lateral roots, the number of xylem vessels and cortical area. For instance, maize lateral root length can increase by up to 35% when exposed to a low N concentration (<4 mM) and water deficit (<-0.25 MPa, Jiang et al., 2023; Dowd et al., 2019). Meanwhile, water deficit reduces the xylem diameter by up to 80% within maize roots of 3-wk-old pot-grown maize (Jafarikouhini and Sinclair, 2023). These plastic adaptations, regulated by phytohormones like auxin (indole-3-acetic acid) and cytokinin represent strategic responses to facilitate water and nutrient acquisition in resource-limited environments (Wang et al., 2020). For example, when maize radicles were exposed to heterogeneous soil moisture conditions, the expression of the cytokinin oxidase gene was upregulated on the wet side than the dry side, resulting in enlarged meristem and forming the lateral roots (Schmülling, 2002; Wang et al., 2020).

1.3.1 Roots respond to soil water limitation

Water is the most limiting factor for maize growth because the soil water supply frequently falls below the threshold of sustained transpiration loss ($2 - 3.2 \text{ g s}^{-1} \text{ cm}^{-2}$, Cai et al., 2022b). Below this critical soil water value, transpiration exhibits a linear decrease due to the partial closure of stomata, denoting the onset of water deficit. The critical soil water value depends upon the soil texture. For example, sandy soil has a critical value of about $130 \text{ g water kg}^{-1}$, loam is about $185 \text{ g water kg}^{-1}$ and sandy loam is about $215 \text{ g water kg}^{-1}$ (Cai et al., 2022a, b). Water deficit in maize

reduces the dry matter accumulation in both shoot and root, particularly in the shoot system, resulting in a greater root-to-shoot ratio (Kou et al., 2022). However, maize roots adapt to this condition by growing toward regions with higher water availability, a phenomenon termed “hydropatterning” (Fig. 1. 2a). Hydropatterning involves axial root bending and lateral root positioning, and occurs in response to variation in water availability through the soil profile induced by topography (hillslopes), presence of soil organisms and vegetation, or pore discontinuities (Hart et al., 2021). Moreover, the anatomy of axial roots, including features such as decreasing xylem diameter in maize roots, responds to soil water deficit (Jafarikouhini and Sinclair, 2023). These adaptive responses allow for continued maize growth despite the water-deficit in soil.

1.3.1.1 Plasticity in axial root morphology

Axial roots direct their growth into moist soil by bending, with cells on the dry side elongating faster than those on the wet side. This was observed in maize root tips that detected a moisture gradient in a chamber wetted with a water-filled tubing along one side of the primary root (Wang et al., 2020). Differential wetting activated the Ca signaling pathway in root cells, which led to auxin accumulation and increased the cell length by 23–44% through the extension of cell wall on the dry side, within the 2 to 4.5 cm region from axial root tip during the next 4 h (Wang et al., 2020). Despite bending, the root length remained constant along the moisture gradient, implying no net change in growth and biomass accumulation. Upon the detection of water deficit, the transcriptomic changes occur across all root zones, with the root tip undergoing cell wall reorganization that enables sustained root growth despite water deficit (Opitz et al., 2016). The length of primary and seminal axial roots was unchanged when exposed to water potentials from

-0.1 to -0.3 MPa (equivalent to 2.5 – 6 g water g⁻¹ peat), and it was not until the water potential declined to -0.35 MPa (2 g water g⁻¹ peat) that root length diminished (Dowd et al., 2019). Thus, axial root bending is a strategic response of maize to water deficit.

1.3.1.2 Plasticity in lateral root morphology

Maize produces more lateral root branches on the wet side than the dry side of a soil moisture gradient ($\Delta = 0.03 - 0.32$ MPa) that spans the radial plane of the differentiation zone (Robbins and Dinneny, 2018). This adaptation is the result of activation of auxin response factor, triggering the expression of the LBD16 gene in dry side root cells that suppressed lateral root initiation (Orosa-Puente et al., 2018; Bao et al., 2014). This mechanism resulted in a 20% increase in lateral root initiation on the wet side of the root, compared to the dry side of the root (Orosa-Puente et al., 2018). By growing more lateral roots, maize greatly increases water uptake. The water uptake rate was 5 orders of magnitude faster in lateral roots (1.64×10^{-5} cm s⁻¹) than seminal axial roots (5.34×10^{-10} cm s⁻¹) of 16-d-old maize (Ahmed et al., 2016).

Water deficit also affects the lateral root elongation, depending on the maize genotype. For instance, the first-order primary laterals of the FR697 genotype were longer under mild water deficit 7 d after transplanting, whereas the length of laterals of transplanted B73 remained constant in well-watered peat (-0.1 MPa, ~6 g g⁻¹ peat) or media with a mild water deficit (-0.28 MPa, ~2.8 g g⁻¹ peat, Dowd et al., 2020). Longer lateral roots in FR697 were related to less meristematic activity, which extended the growing time of lateral roots (Dowd et al., 2019; Dowd et al., 2020). Longer lateral roots have greater access to soil resources, as evidenced by a 32% higher yield of maize with long lateral roots than a related maize variety with short lateral roots in soil with a low N fertilizer dose (33 kg N ha⁻¹ of urea; Zhan and Lynch, 2015).

1.3.1.3 Plasticity in root anatomy

In response to water deficit, roots have a reduced xylem area, less cortical area, and form more cortical aerenchyma, i.e., intercellular space within the cortical layer. When exposed to water-deficit, xylem area had a 20 – 46% reduction in crown roots and 50 – 63% reduction in seminal roots, while primary roots showed no response to water deficit in four sweet maize hybrids (Hazman and Kabil, 2022). Similarly, in different genotypes (cv. CML538), 80% reduction in the diameter of xylem vessels in maize root tips exposed to water deficit for 9 d (Jafarikouhini and Sinclair, 2023). The plasticity of xylem in response to abscisic acid involves processes such as xylem lignification and developmental switches in xylem identity, although the specific mechanisms underlying these processes in maize roots are not yet fully understood (Ramachandran et al., 2021). Since root hydraulic conductance is proportional to the fourth power of xylem diameter (Hagen-Priseuille's law), reducing xylem diameter greatly limits water extraction from soil. This anatomical adaptation of the vesicular tissues acts as a negative feedback, effectively forcing the maize plant to conserve water by preventing excessive water removal from water-deficit soils. The cortical area of lateral roots, and the basal area of crown and seminal roots, also decrease in plants grown under water deficit (Hazman and Kabil, 2022). A smaller root cortex is associated with the development of thinner, longer roots. According to Chimungu et al. (2014), field-grown maize with fewer cortical cells had 33–40% deeper rooting, which accessed and transferred more water to the leaves (10–35% greater water content in leaf tissues), resulting in 33–114% greater yield at harvest under water-deficit. In addition, maize roots had 5 times more cortical aerenchyma when exposed to water-deficit (about 130 g water kg⁻¹ soil) than under well-watered condition (about 250 g water kg⁻¹ soil; Zhu et al., 2010). The formation of cortical

aerenchyma contributes to the deep rooting of maize in water-limited soils, as this structure reduces root respiration and promotes root growth.

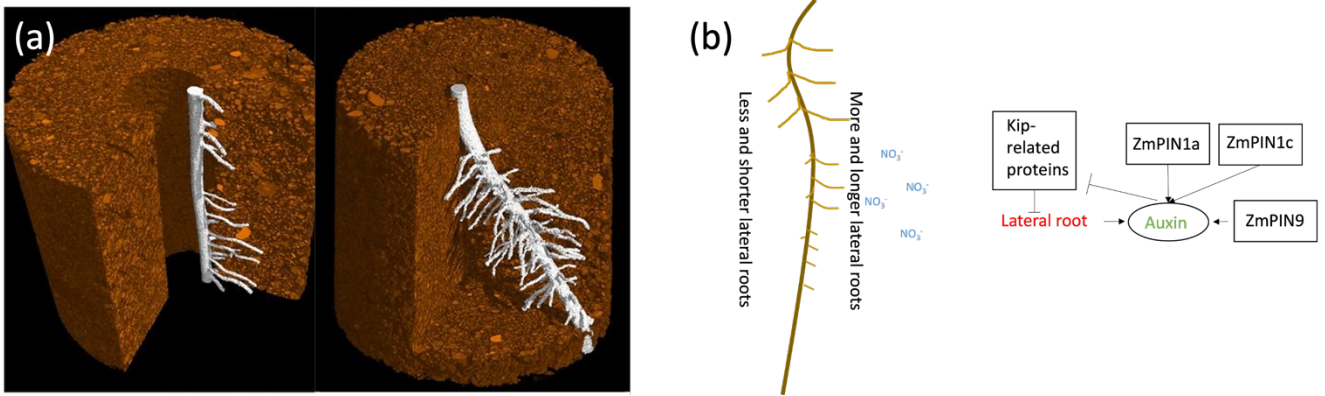


Fig. 1. 2 (a) Hydropatterning of maize roots revealed by microscale computed tomography (bars = 5 cm), taken from Bao, Y., Aggarwal, P., Robbins, N.E., et al. 2014. Plant roots use a patterning mechanism to position lateral root branches toward available water. *Pro. Natl. Acad. Sci.* **111**: 9319–9324. doi: <https://doi.org/10.1073/pnas.1400966111>. (b) Plasticity of maize lateral roots to heterogenous NO_3^- concentration, revised from Yu, P., Hochholdinger, F., Li, C. 2019. Plasticity of lateral root branching in maize. *Front. Plant Sci.* **10**: 363. <https://doi.org/10.3389/fpls.2019.00363>.

1.3.2 Roots respond to low N concentration

1.3.2.1 Morphological plasticity

Root phenotypic responses are regulated by the concentration of NO_3^- , the dominant ionic N form in field soil. However, root types differ in their growth when exposed to variable NO_3^- concentrations. When exposed to low NO_3^- concentration, young maize seedling (16-d-old) produced primary roots that were 10% longer than those grown in high NO_3^- concentration due to the regulation of brassinosteroids (Xing et al., 2021). As maize growing, axial root growth appears

to become less sensitive to the environmental NO_3^- concentration. A study on 30-d-old maize (cv. PS2790) revealed that primary, seminal, and crown axial roots had a constant length and surface area across a range of NO_3^- concentrations (0 to 7.8 mmol L^{-1}) in a perlite-based growth substrate (Jiang et al., 2023). The insensitivity of axial roots to the environmental NO_3^- concentration may be attributed to the determinate growth of primary, seminal, and the first whorl of crown roots in maize during its vegetative growth (e.g., from germination to the V3 – V4 growth stage). Similarly, studies on maize (cv. B73) showed that the growth of 2nd, 5th, and 7th whorl-shoot borne axial roots remained relatively stable when exposed to locally high NO_3^- concentrations (Yu et al., 2015). However, the responses of axial roots to NO_3^- concentration vary among different genotypes. For example, maize (cv. Zhengdan 985) produced longer 1st to 3rd whorl crown axial roots when exposed to low NO_3^- concentrations (40 $\mu\text{mol L}^{-1}$) than those grown in normal NO_3^- concentrations (4 mmol L^{-1}). While many of these studies were conducted in hydroponic systems, further observations in field settings are necessary to fully understand the response of axial roots to NO_3^- , considering that the primary functions of axial roots, such as solute translocation and anchorage, are crucial for absorbing mobile NO_3^- from deep soil layers.

Laterals of different maize root types showed plasticity to soil NO_3^- concentration. For example, lateral roots along seminal and crown roots of the V3 maize (cv. PS2790) elongate according to a quadratic relationship when the external NO_3^- concentrations increase from 0 to 7.8 mmol L^{-1} , but primary lateral roots did not showed any plastic responses (Jiang et al., 2023). However, the plastic responses are various among the genotypes. All types of lateral roots from maize cv. 478 were 20 – 41% longer as the NO_3^- concentration decreased from 20 mmol L^{-1} to 5 mmol L^{-1} , which was associated with the increased auxin concentration from 20 to 60 ng g^{-1} fresh root (Tian et al., 2008). Similarly, lateral roots were twice as long in a non-fertilized soil column

(containing 2.7 mg NO₃⁻ kg⁻¹) than the soil column fertilized with 10 mmol L⁻¹ Ca(NO₃)₂, according to X-ray microcomputed tomography (Griffiths et al., 2022). These suggest that auxin regulates the lateral root growth in N-limited environments.

Although auxin is biosynthesized in both shoot and root, the growth of lateral roots is mainly controlled by the auxin signaling from the N-demanding shoot tissue. Auxin synthesized in the shoot flows periodically through the central cylinder of the basal meristem and acts as a signal for initiating lateral root development, revealed by the real time DR5-luciferase reporter (Moreno-Risueno et al., 2010). Shoot-to-root auxin transport decreases as the soil NO₃⁻ concentration increases. Specifically, auxin transport rate decreased by 64% in lateral root initiation region and 70% in the root tip when the maize was exposed to 0.5 mmol L⁻¹ NO₃⁻ for 1 d compared to 0 mmol L⁻¹ NO₃⁻, as revealed by the radiolabeled auxin (³H-indole-3-acetic acid, Liu et al., 2010). Moreover, auxin level decreased 2 times more in NO₃⁻ rich microsites than in NO₃⁻ free microsites, adjusting auxin to the optimum level (40 – 60 ng g⁻¹ fresh weight in root tips) suitable for lateral root initiation (Liu et al., 2010). This adjustment is due to increased basipetal auxin transport by inducing the auxin transporters *ZmPIN1a* and *ZmPINc* in root tips (Fig. 1. 2b, Yu et al., 2015). In addition, the PIN9 gene in maize phloem pole cells modulates auxin efflux to the pericycle cells and activates the cell cycle by alleviating the inhibition of Kip-related proteins coding genes, which increases the lateral root length of brace root (5 – 30 cm from the root tip) by 50 – 200% (Yu et al., 2016). The plasticity of lateral roots to NO₃⁻ gradients is a functional response, since more than 60% of NO₃⁻ uptake is transported through laterals when the maize primary root is exposed to 0.1 or 10 mmol L⁻¹ ¹⁵N-NO₃ solution (Lazof et al., 1992). Thus, auxin flows act as a sensor of NO₃⁻ concentration in the environment and prime the root for lateral root initiation,

determining the number and length of lateral roots, presumably for maximum acquisition of NO_3^- since N is the most limiting nutrient for maize in most field environments.

1.3.2.2 Anatomical plasticity

Maize roots adapt to soil N deficiencies by adjusting the xylem area, the number of xylem vessels and cortical aerenchyma. Under low N conditions (no N fertilization), four out of eight genotypes produced 25–60% less xylem area in crown roots than under high N conditions (213 kg N ha^{-1} , Yang et al., 2019). Anatomical plasticity varied among whorls, with the fifth whorl of crown roots having 28% fewer xylem vessels under low N, while the first and second whorl crown roots remained constant (Yang et al., 2019). Moreover, maize roots have more cortical aerenchyma in soil with limited N concentration, based on 200% greater cortical aerenchyma formation in a pot study and 100% more cortical aerenchyma in the field (Saengwilai et al., 2014). Specifically, when grown in a N-limited soil with 30 kg N ha^{-1} , cortical aerenchyma increased in the primary (62%), seminal (218%), and crown roots (74%) than in the fertilized soil receiving 150 kg N ha^{-1} (Saengwilai et al., 2014). This adaptive response is associated with deep rooting, which presumably helps maize to access NO_3^- from deeper soil layers. Maize genotypes with more cortical aerenchyma had a 50% higher NO_3^- uptake than those with 3 times less cortical aerenchyma in a N-limited soil (Postma and Lynch, 2011).

1.3.3 Roots respond to phosphorous, potassium, and micronutrient availability

Maize must absorb essential nutrient ions (macro and micronutrients) for proper metabolism, biomass accumulation and production of yield components. Limited access to phosphorus (P) ions (H_2PO_4^- and HPO_4^{2-}) restricts primary root elongation while increasing lateral

roots and root hair production (Sánchez-Calderón et al., 2006). This response is due to the key role of P ions in plant physiological processes, such as the production of antioxidants to inhibit reactive oxygen species, and the synthesis of nitric oxide, ethylene, auxin, and cytokinin that regulate the cellular structure of root meristem, pericycle cells, and trichoblast cells (Niu et al., 2013). Maize P nutrition determines carbohydrate allocation in shoots to the roots, with total root length and biomass increasing after 3 d of P starvation due to increased carbon transfer to the roots (Mollier and Pellerin, 1999). Similarly, 18-d-old maize had 95% longer roots and 60% more root biomass (dry weight) when grown in a P-starvation solution culture for 6 d (Anghinoni and Barber, 1980). However, prolonged P starvation (>3 d) restricted carbohydrate biosynthesis in maize seedlings, which reduced the axial root and lateral root emergence (Mollier and Pellerin, 1999). Therefore, the short-term response of maize roots to soil P availability is regulated by carbon partitioning between shoots and roots.

Maize roots also respond to potassium (K) availability, as ionic K^+ regulates several phytohormones involved in root development. At the tasselling stage, D937 maize lateral root length decreased by 13% in K-free soil, with 15% less indole-3-acetic acid content and 25% more abscisic acid content (Zhao et al., 2016). However, roots of maize genotypes vary in their response to K availability. For instance, lateral roots of maize genotype 90-21-3 did not respond to the soil K concentration, and the indole-3-acetic acid and abscisic acid content of roots was not affected by the soil K supply (Zhao et al., 2016).

Micronutrients such as boron, copper, iron, manganese, molybdenum and zinc are essential cofactors in enzyme-mediated reactions and energy relations in maize, with potential to impact root growth. Micronutrient deficiencies may impact root hair development by altering the root hair proteome. For example, zinc is a cofactor for enzymes involved in primary carbon metabolism

such that Zn deficiency represses glycolysis and carbohydrate metabolism. Maize roots were 14% shorter in a Zn free environment than in the control containing 0.5 μM Zn (Mallikarjuna et al., 2020). Further research is needed to confirm how maize root systems may detect and respond to micronutrient deficiencies in soil.

1.4 Water uptake

1.4.1 Water uptake by maize roots

Water moves from the soil into the roots due to evapotranspiration. Evapotranspiration is the result of cohesive water molecules moving under tension through the xylem vessels and exiting the leaf stomata before evaporating from the leaf surface. The cohesion and tension forces generate a water potential gradient, resulting in root hydraulic conductance, which describes the overall capacity of a root system or a root type to conduct water. It is important to distinguish between root hydraulic conductance and root hydraulic conductivity, the latter representing the intrinsic ability of per unit area of root surface to conduct water. As water reaches the root surface, it is absorbed through the epidermis, including root hairs or non-root hair atrichoblasts. Water moves through the radial axis of roots via the apoplastic or cell-to-cell pathway to reach xylem vessels. The apoplastic pathway, facilitated by tension (up to -1 MPa) from the xylem, accounts for approximately 60% of water uptake, showing a velocity about 17 times greater than the cell-to-cell pathway (Steudle, 2001). The main barrier to water movement from soil to leaf surfaces is the Casparian strip, of the hydrophobic suberin and hydrophilic lignin band lining the exodermal and endodermal cells (Hose et al., 2001). Although all root types have a Casparian strip, primary roots have a larger Casparian strip than seminal and crown roots, as revealed by the berberine-ailine blue staining, which indicates a slower water flow rate within the primary roots than other root tissues (Tai et al., 2016).

Casparian strip greatly reduces the hydraulic conductance, given that maize seminal roots without an exodermis having 1.5–3.6 times more hydraulic conductance than the one with an exodermis containing aliphatic suberin (Zimmermann et al., 2000). Consequently, the cell-to-cell pathway is used for water transport when the apoplastic pathway is blocked by Casparian strip, or limited transpiration because leaf stomata are closed due to water shortage. The amount and activity of aquaporins, the specific protein channels that allow water to pass through cell membranes, tightly regulate the cell-to-cell pathway. Still, the activity of aquaporins depends upon environmental conditions. The *ZmPIP2* (plasma membrane intrinsic proteins) gene was upregulated when maize roots were exposed to water deficit, indicating a greater role for aquaporins in water transport when water moved through the cell-to-cell pathway (Hachez et al., 2012).

1.4.2 Root hydraulic conductance under water deficit

Root hydraulic conductance declines when there is a water-deficit, for several reasons. First, water deficit regulates the activity of aquaporins. In maize, plasma membrane intrinsic protein aquaporins were upregulated 5-fold, whereas tonoplast intrinsic protein aquaporins were downregulated 6-fold when the soil water available for transpiration decreased by 80% (Devi and Reddy, 2020). Second, water deficit induces suberization of the exodermis, restricting apoplastic water movement and redirecting water uptake to the cell-to-cell pathway (Steudle, 2000). More aliphatic suberin was formed under the -0.8 MPa osmotic stress, reducing the hydraulic conductance by 2.5-fold (Kreszies et al., 2019). Third, water deficit causes mechanical damage to cortical cells because it forms gaps called lacunae, which reduces the root hydraulic conductance due to discontinuities in water flow. Less water absorption is accompanied by stomatal closure,

controlled by abscisic acid (200 to 800 pmol g⁻¹ fresh weight) to minimize transpiration and prevent desiccation (Devi and Reddy, 2020).

In drier soil, the air gaps that form at the root-soil interface may further reduce root hydraulic conductance. The 0.2–0.6 mm air gap between the root and soil surfaces formed when soil water content dropped to 32.5 g kg⁻¹ (sandy soil) as revealed by the X-ray tomography (Carminati et al., 2009). The shrinkage mainly occurs in root hairs or cortical cells, with root hairs also shrinking as soil water content decreases from -0.01 MPa to -1 MPa (equivalent to 400 g kg⁻¹ to 120 g kg⁻¹), resulting in the linear reduction of water uptake into maize roots (Duddek et al., 2023). However, variations in shrinkage levels among root types may occur due to differences in the cortical area (Carminati et al., 2013). Seminal roots, with 33% less cortical area than primary and crown roots, might experience less shrinkage. Therefore, seminal roots may maintain the root hydraulic conductance, whereas primary and crown roots significantly decrease the root hydraulic conductance in water-limited soil.

1.5 N uptake by roots

1.5.1 N movement from soil to the root surface

Maize relies on N to synthesize essential components such as proteins, nucleic acids, and chlorophyll, contributing to biomass accumulation and grain yield. Typically, Canadian maize production is supplied with 120–180 kg N ha⁻¹ throughout its life cycle in the form of urea, ammonium nitrate, ammonium sulfate or other N salts that release ammonium (NH₄⁺) or NO₃⁻. Upon the dissolution of NH₄⁺ ions in soil pore water, active ammonia oxidizers and nitrifiers facilitate the conversion of NH₄⁺ into NO₃⁻ within hours to days. Ammonia oxidizers, including autotrophic and heterotrophic bacteria, and autotrophic archaea, produce ammonia

monooxygenase to form NH_2OH and hydroxylamine oxidoreductase to form nitrite (NO_2^-). The generated NO_2^- is then excreted outside the cells and absorbed by nitrifiers, which include autotrophic and heterotrophic bacteria and fungi. Nitrifiers use nitrite oxidoreductase to convert NO_2^- into NO_3^- , which can either be retained in microbial cells or released into the soil pore water. Consequently, NO_3^- and NH_4^+ are available N sources for maize growth, with NO_3^- being the dominant ion in well-aerated agricultural soils.

Ammonium and NO_3^- follow different processes as they move from the soil to reach plant roots. Immobile NH_4^+ is transported by diffusion and root interception, which means the ions move across the concentration gradient and require contact with the root surface (Barber et al., 1963). In contrast, mobile NO_3^- is primarily transported by mass flow, facilitated by plant transpiration that moves ions into the extensive root system (Barber, 1962). During plant transpiration, the water column within the xylem vessels moves upward from the root to the leaf surface, reducing the water potential inside the root xylems. As a result, roots generate a force that draws water and mobile ions (e.g., NO_3^-) towards the root surface.

Each active root exerts a transpiration pull on water molecules and NO_3^- ions, but the magnitude of the transpiration pull varies among different root types. The xylem suction and radial flow rate were estimated to be 1 to 2 MPa and 2.2 to $4.3 \times 10^5 \text{ cm}^3 \text{ cm}^{-2} \text{ s}^{-1}$ in crown root, and 0.05 to 0.6 MPa and 0.05 to $1.2 \times 10^5 \text{ cm}^3 \text{ cm}^{-2} \text{ s}^{-1}$ in the seminal root of 30-d old maize seedlings (Doussan et al., 1998). This is because crown roots have 63% more meta- and protoxylem elements and larger xylem vessels, which allows them to create a negative pressure gradient that can effectively transfer water from soil pore to root xylem (Tai et al., 2016; Ahmed et al., 2018). Furthermore, since the hydraulic conductance drive mass flow, the number and area of the xylem also enhance NO_3^- uptake rate. This was supported by the evidence that barley roots with 150%

more metaxylem vessels and 36% increased xylem cell area had a 97% higher low-affinity NO_3^- uptake rate (Liu et al., 2020). Moreover, as maize grows, crown roots become the main rootstock (>50%) after the V3 growth stage. As a result, crown roots become the main location for water and mineral nutrient uptake as the crown roots have higher hydraulic conductance.

1.5.2 NO_3^- uptake by roots

Once reaching the root surface, NO_3^- is absorbed through an energy-demanding active uptake process. This process requires 13 kJ mol^{-1} as root cells (5 mmol L^{-1} cytoplasmic NO_3^-) absorb NO_3^- ($10 \text{ mmol L}^{-1} \text{ NO}_3^-$) from the surrounding environment, working against an electrical potential gradient of -150 mV at $20 \text{ }^\circ\text{C}$ (Crawford and Glass, 1998). Facilitated by the proton gradient (H^+), active NO_3^- uptake involves the coupling of NO_3^- influx to the influx of protons at a 2:1 ratio ($\text{H}^+:\text{NO}_3^-$, Miller and Smith, 1996).

Absorption of NO_3^- occurs through high-affinity and low-affinity transport systems. The high affinity transport is activated when external NO_3^- concentration is $<250 \text{ } \mu\text{M}$. The high-affinity transporter is further classified as constitutive transporter ($k_m = 6 - 20 \text{ } \mu\text{M}$, $V_{\text{max}} = 0.3 - 0.82 \text{ } \mu\text{M g h}^{-1}$) and inducible ($k_m = 20 - 250 \text{ } \mu\text{M}$, $V_{\text{max}} = 3 - 8 \text{ } \mu\text{M g h}^{-1}$, Crawford and Glass 1998). Four higher-affinity NRT2 genes were characterized in maize: *ZmNRT2.1*, *ZmNRT2.2*, *ZmNRT2.3*, *ZmNRT2.5* (Plett et al., 2010). The inducible transporter *ZmNRT2.1* was identified in the root cortex and epidermis, whereas *ZmNRT2.2* (constitutive or inducible) was identified in root cortex, stele, and lateral root primordia (Trevisan et al., 2008). The spatial distribution of the high-affinity transporters suggests that transmembrane transport of NO_3^- occurs during the uptake of roots and xylem loading (Orsel et al., 2002). NO_3^- uptake capacity of *ZmNRT2.1* and *ZmNRT2.2* increases when soil N availability is reduced (Garnett et al., 2013). This fact suggests that the high-affinity

transporters are responsible for N influx into maize roots, particularly when N is limited in the surrounding environment.

When the external NO_3^- concentration is $> 250 \mu\text{M}$, the low-affinity transporters (NRT1 and NPF families) are activated. The low-affinity NO_3^- transport mediates a higher NO_3^- transport rate ($700 \mu\text{mol h}^{-1} \text{g}^{-1}$ root fresh weight) than high-affinity transporters ($4 \mu\text{mol h}^{-1} \text{g}^{-1}$ root fresh weight), resulting in about 3mmol L^{-1} cytoplasmic NO_3^- concentration in maize (Miller and Smith, 1996). Low-affinity transporters do not saturate even at NO_3^- concentrations as high as 50mM . Low-affinity NO_3^- transporters are usually not saturated by the external NO_3^- concentration because soil NO_3^- concentrations are typically below 30mmol L^{-1} ($\theta_g = 100 \text{g kg}^{-1}$, Nájera et al., 2014).

The kinetics of nitrate uptake vary among different segments of roots and between root types, likely due to differences in the abundance and activity of transporters on the root surface. For example, in a 20-d-old maize seedling, crown roots had 22% higher and lateral roots had 34% higher maximum influx rates than seminal roots, indicating the faster NO_3^- uptake kinetics in crown roots and lateral roots (York et al., 2016). Within an individual root, NO_3^- uptake rate decreased as the distance from root tips increased. In a maize primary root, the 2–4 mm segment behind the root tip had a NO_3^- uptake rate of $2.81 \mu\text{mol m}^{-1} \text{h}^{-1}$, whereas the segment 4–6 mm from the root tip absorbed $1.86 \mu\text{mol NO}_3^- \text{m}^{-1} \text{h}^{-1}$ (Rao et al., 1997). Similarly, when soaking the maize primary root (7-d-old) in the solution contained $50 \mu\text{M NO}_3^-$, the root tip (0 – 2 cm, $0.043 \mu\text{mol NO}_3^- \text{cm}^{-2} \text{h}^{-1}$) showed 25% higher NO_3^- maximum uptake rate of inducible high-affinity transport system than root regions (4–6 cm, $0.035 \mu\text{mol NO}_3^- \text{cm}^{-2} \text{h}^{-1}$, Sorgona et al., 2011). Therefore, measurements of NO_3^- uptake kinetics are needed for specific root types and root segments, as they cannot be generalized for the whole root system.

Within the root cells, NO_3^- can be used to produce amino acids that synthesize the proteins and other N-containing compounds (e.g., chlorophyll). First, NO_3^- is reduced into NO_2^- by nitrate reductase in the cytosol, which consumes NADH as an electron donor. Then, NO_2^- is reduced to NH_4^+ in a reaction catalyzed by enzyme nitrite reductase. The NH_4^+ is further assimilated into amino acids through various enzymatic reactions. However, the excess NO_3^- can be stored in the vacuole with a capacity of 100 mmol L^{-1} or pumped out of the root cells into the apoplasm (Miller and Smith, 1996). Some NO_3^- can be transported to the xylem for long-distance translocation. Once in the xylem vessels, NO_3^- is transported upward along with the transpiration pull, which is driven by the loss of water vapor from leaf stomata through transpiration. Finally, NO_3^- reaches mesophyll cells, where NO_3^- is reduced and assimilated into amino acids or stored in the vacuole.

1.6 Conclusions and future directions

Maize grows primary, seminal, and crown axial roots, each with associated lateral roots responsible for early-stage N uptake. Variations in morphological and anatomical traits of these root types means that each type has a distinct root hydraulic conductance. This conductance facilitates water flow toward the roots, pulling mobile NO_3^- ions to the root surface. Shoot-borne crown roots with larger xylem vessels than embryonic primary and seminal roots should have higher root hydraulic conductance and NO_3^- uptake rate in water-sufficient conditions. However, as the soil dries, the hydraulic conductance of the crown axial root could decrease significantly. In response to water and N limitations, maize adapts its root traits to sustain resource uptake. Questions remain regarding how maize roots adapt to water-limited and N-deficient soils and how NO_3^- is delivered to the roots in water-limited soil. Therefore, the objectives of my dissertation are to (1) assess the responses of lateral and axial roots, associated with primary, seminal, and crown

roots of maize, to varying NO_3^- concentrations in the perlite growth medium; (2) investigate how root morphological and anatomical traits in response to N fertilizer rates and soil water contents; (3) quantify NO_3^- uptake rate of maize primary, seminal, and crown roots in soil conditions with sufficient and deficient water in a split-root system. My dissertation will focus on the following hypotheses:

- Increasing the NO_3^- concentration induces peak growth of lateral roots of all root types, while axial root growth is insensitive to the NO_3^- concentration of the environment.
- In well-watered soils, maize roots would exhibit plasticity by increasing lateral root length, crown root number, and xylem area with higher N fertilizer rates. However, we expected a lack of plastic responses to N fertilization in the dry soil because of maize has lower shoot biomass and root hydraulic conductance, which reduce the N uptake.
- Crown roots have a higher NO_3^- uptake rate than embryonic roots in relatively wet soil ($\Psi_{\text{soil}} = -5$ kPa) due to their higher hydraulic conductance during vegetative growth. However, in relatively dry soil ($\Psi_{\text{soil}} = -30$ kPa), we expect that embryonic roots acquire more NO_3^- than crown roots due to their proximity to pores containing occluded water, as well as the lower hydraulic conductance of crown roots in dry soil.

FORWARD TO CHAPTER 2

Growth of maize root types depends on the soil physio-chemical environment. The NO_3^- concentration of the growth media is expected to affect the growth rate and morphology of embryotic roots, as well as post-embryotic crown roots. Root traits were evaluated in relation to the maize N uptake in the first 30 d of vegetative growth, up to the 3-leaf stage (V3). The experiment was done in a controlled greenhouse experiment with one maize cultivar that was grown in perlite, a mineral-based porous media that provides physical support for the root system, and the NO_3^- concentration was controlled by adding a well-characterized NO_3^- solution.

Chapter 2 is available as a published article: Jiang, Y., Hung, C.-Y. and Whalen, J.K. 2023. Distinctive plasticity of maize (*Zea mays*) root types to variable nitrate concentration. Canadian Journal of Plant Science 103:319-323. doi: 10.1139/CJPS-2022-0246

CHAPTER 2

Distinctive plasticity of maize (*Zea mays*) root types to variable nitrate concentrations

Yutong Jiang¹, Chih-Yu Hung¹, Joann K. Whalen^{1*}

Address: ¹Department of Natural Resource Sciences, Macdonald Campus of McGill University,
21111 Lakeshore Road, Ste-Anne-de-Bellevue, Quebec, Canada H9X 3V9

Corresponding author: Joann K. Whalen, joann.whalen@mcgill.ca, tel: 001-514-398-7943

2.1 Abstract

Maize roots vary their growth in response to nitrate (NO_3^-) concentrations in the environment, but growth plasticity differs among root tissues. We assessed the morphological response of lateral and axial roots associated with primary, seminal, and crown roots exposed to 0, 1, 2, 3.9 and 7.8 $\text{mmol L}^{-1} \text{NO}_3^-$. Higher NO_3^- concentration did not change the growth of all axial roots and laterals of primary roots but caused positive quadratic growth in laterals of the seminal and crown root types. Maize root plasticity to NO_3^- concentrations is the result of differential growth of laterals on seminal and crown root types.

Keywords: Auxin, Axial roots, Nitrogen uptake, Perlite, Phenotypic plasticity, Root architecture

2.2 Introduction

Growth plasticity in the root system allows plants to optimize their acquisition of nitrate (NO_3^-) from soil solution. In a hydroponic study, maize lateral roots were 23% longer after 22 days when the hydroponic nutrient solution contained 0.02 mmol L^{-1} compared to 2 mmol L^{-1} (Liu et al. 2008). Elongation of maize lateral roots is associated with auxin sensing of the NO_3^- concentration in soil solution (Casimiro et al. 2001; Moreno-Risueno et al. 2010). As the external NO_3^- concentration increases, the acropetal transport of auxin decreases to $<45\text{--}80 \text{ ng auxin g}^{-1}$ root (fresh weight) in the whole root system (Tian et al. 2008), which inhibits further elongation of lateral roots. However, not all root types have growth plasticity in a complex root system. Root types that grow under genetic control will be insensitive to NO_3^- fluctuations. Identifying root types that respond to NO_3^- , other nutrients, and soluble molecules in the environment supports a trait-based approach to explain the origins of root phenotypic variation. Growth plasticity may also reveal functions, since lateral roots absorb more NO_3^- than structural root tissues (Lazof et al. 1992).

This study assessed the morphology of lateral and axial roots associated with three maize root types (primary, seminal, and crown) when exposed to variable NO_3^- concentration (0, 0.1, 1, 2, 4, and 8 mmol L^{-1}) in perlite growth media. We hypothesized that increasing the NO_3^- concentration will lead to peak growth of lateral roots associated with all root types due to auxin sensing, but axial root growth is under genetic control.

2.3 Materials and methods

The experimental unit was a pot (12.7 cm diameter, 15 cm depth) with drainage. It was filled with 200 g coarse perlite (2–5 mm; Perlite Canada Inc., Lachine, QC, Canada) with

0.11 g cm⁻³ bulk density and 1.5 g g⁻¹ water holding capacity, containing 0.003 g NH₄⁻ kg⁻¹ and no detectable NO₃⁻ (<0.001 g NO₃⁻kg⁻¹). Maize seed (*Zea mays* L. cv. PS2790, not genetically modified, not treated with fungicide or insecticide) was pre-treated by soaking (in biostimulant or water) or not soaked before planting. Maize seed was soaked for 10 h at 22 °C in 100 mL of 0.6% v/v biostimulant solution in deionized water (Humic Land™, Rogitex Inc., Pointe-Claire, QC, Canada) or 100 mL deionized water. Soaked seed was oven-dried (8 h at 45 °C) to 8% ± 1% moisture content, the same moisture content as non-soaked seeds.

One maize seed was planted at a depth of ~3 cm in each pot. Pots were in a greenhouse with natural lighting plus supplemental fluorescent lighting (400 μmol⁻² s⁻¹ of photon flux density) with 16 h light at 25 ± 2 °C and 8 h dark at 18 ± 1 °C. Pots were assigned randomly to an NO₃⁻ concentration (0, 0.1, 1, 2, 4, or 8 mmol L⁻¹ NO₃⁻), in a complete factorial design with 3 soaking treatments × 6 NO₃⁻ concentrations × 5 replicates, resulting in 90 experimental pots. The NO₃⁻ concentrations were chosen because they represent N limitation to N luxury consumption for maize seedlings based on a preliminary test. Solutions containing 0.1–8 mmol L⁻¹ NO₃⁻ were made by adding Ca(NO₃)₂ to the modified Hoagland nutrient solution (2 mmol L⁻¹ MgSO₄, 1 mmol L⁻¹ KH₂PO₄, 2 mmol L⁻¹ K₂SO₄, 46 μmol L⁻¹ H₃BO₃, 14.3 μmol L⁻¹ MnCl₂, 0.8 μmol L⁻¹ ZnSO₄, 0.32 μmol L⁻¹ CuSO₄, 0.6 μmol L⁻¹ Na₂MoO₄, 0.5 mmol L⁻¹ Fe-EDTA, pH = 6.0). The control (0 mmol L⁻¹ NO₃⁻) was the modified Hoagland nutrient solution without Ca(NO₃)₂. The calcium supply was balanced with CaCl₂ to maintain a constant 4 mmol L⁻¹ Ca²⁺ in all solutions.

Pots were watered with 150 mL deionized water to the maximum water-holding capacity every 2 days for the first 14 days. From day 15 to day 29, each pot received 500 mL of the NO₃⁻ plus Hoagland solution every 2 days to maintain the nominal NO₃⁻ concentration. Leachate (around 320 mL) was collected in pot drainage to assess the NO₃⁻ concentration by the modified indophenol

blue method (Sims et al. 1995). This confirmed that the measured NO_3^- concentration was within $\pm 10\%$ of the nominal NO_3^- concentration added to the pot (Table S2. 1).

Chlorophyll content in the mid-blade of the newest fully formed leaf was recorded 27 days after seeding with a SPAD 502 m (Spectrum Technologies, Plainfield, IL, USA). Maize was harvested at the V3 stage (30 days after seeding). Stems were cut at the perlite surface, while roots were removed from the pots, rinsed thoroughly with deionized water until all root-associated perlite were removed, and kept at 4 °C. The NO_3^- concentration in perlite was determined after extracting 6 g perlite (1:5 perlite: 2 mol L⁻¹ KCl solution), according to Sims et al. (1995).

Shoots were oven-dried (48 h at 55 °C), weighed, ground (<1 mm), and analyzed for total N concentration (Thermo Finnigan Flash EA 1112, Carlo Erba, Milan, Italy). Shoot N content was the mass (g dry matter) × N concentration (mg N g⁻¹). Fresh roots were divided manually into primary, seminal, and crown root types. The axial root length was measured with a ruler. Lateral root length and surface area were quantified by analyzing root segments on an Epson perfection V700 Photo scanner and WinRhizo software (Regent Instruments, QC, Canada). Total length from the software was $\pm 4\%$ of the total length measured with a ruler on 10 root segments selected at random from primary, seminal, or crown root types ($P > 0.05$, pairwise t test, Fig. S2. 2). For each root type, lateral root length was the total root length minus axial root length (Chun et al. 2005). The lateral root surface area was assumed to be the total surface area of fine roots with diameter <0.5 mm in WinRhizo software, because >95% of lateral roots had a diameter <0.5 mm in maize at the V3 stage (Cahn et al. 1989). This slightly overestimated the lateral root surface area because <5% of total roots are smaller axial roots with a diameter <0.5 mm (Cahn et al. 1989). We did not measure the weight of the lateral and axial roots for each root type, because it is difficult to manually separate all lateral roots from the axial roots.

Data were normally distributed (Shapiro–Wilk test, $P > 0.05$) with homogeneous variance (Levene’s test, $P > 0.05$). The seed soaking treatment had no effect on the dependent variables (shoot biomass, chlorophyll content, plant N content, and root length and surface area; analysis of variance (ANOVA), $P > 0.05$). Hence, we pooled data for each independent NO_3^- concentration ($n = 15$, except for $n = 14$ in the $8 \text{ mmol L}^{-1} \text{NO}_3^-$ concentration, because one maize plant died during the experiment). Relationships between the measured NO_3^- concentrations and each dependent variable were described with the best-fit line. The statistical analysis was done with SAS statistical software, version 9.4.

2.4 Results

Shoot biomass, N content, and chlorophyll content increased to an exponential plateau when roots were exposed to higher NO_3^- concentrations (Fig. 2. 1). Axial root growth did not vary with NO_3^- exposure for any root type (Figs. 2. 2a–c). Laterals of the primary root type were unaffected by NO_3^- , but laterals of seminal and crown root types tended to be longer when they were exposed to higher NO_3^- concentrations (Figs. 2. 2d–f). There were 82% longer laterals on the seminal roots and 59% longer laterals on crown roots as exposure increased from 0 to $2 \text{ mmol L}^{-1} \text{NO}_3^-$. Lateral root length reached a maximum at $3.9 \text{ mmol L}^{-1} \text{NO}_3^-$ for seminal roots and $4.5 \text{ mmol L}^{-1} \text{NO}_3^-$ for crown roots (Figs. 2. 2e and 2. 2f). Similarly, seminal and crown root types had larger lateral root surface area that increased from 0 to $2 \text{ mmol L}^{-1} \text{NO}_3^-$, plateauing at $4.2 \text{ mmol L}^{-1} \text{NO}_3^-$ (seminal roots) and $4.5 \text{ mmol L}^{-1} \text{NO}_3^-$ (crown roots; Figs. 2. 2g–i).

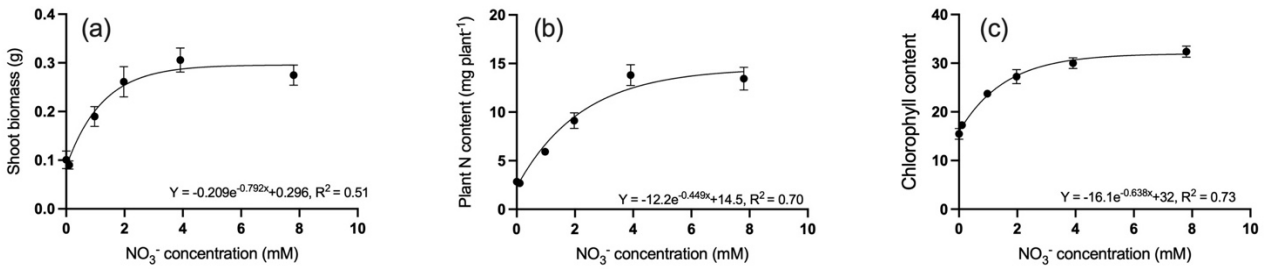


Fig. 2. 1 Shoot biomass (a) and plant N content (b) at harvest, plus the chlorophyll content (c) after 27 days of maize planting. Maize was harvested at the V3 stage, after roots were exposed to variable NO_3^- concentrations (mean value of measured NO_3^- concentration from 15 to 29 days) in perlite-filled pots for 30 days. Error bars are standard error of the mean (n=15)

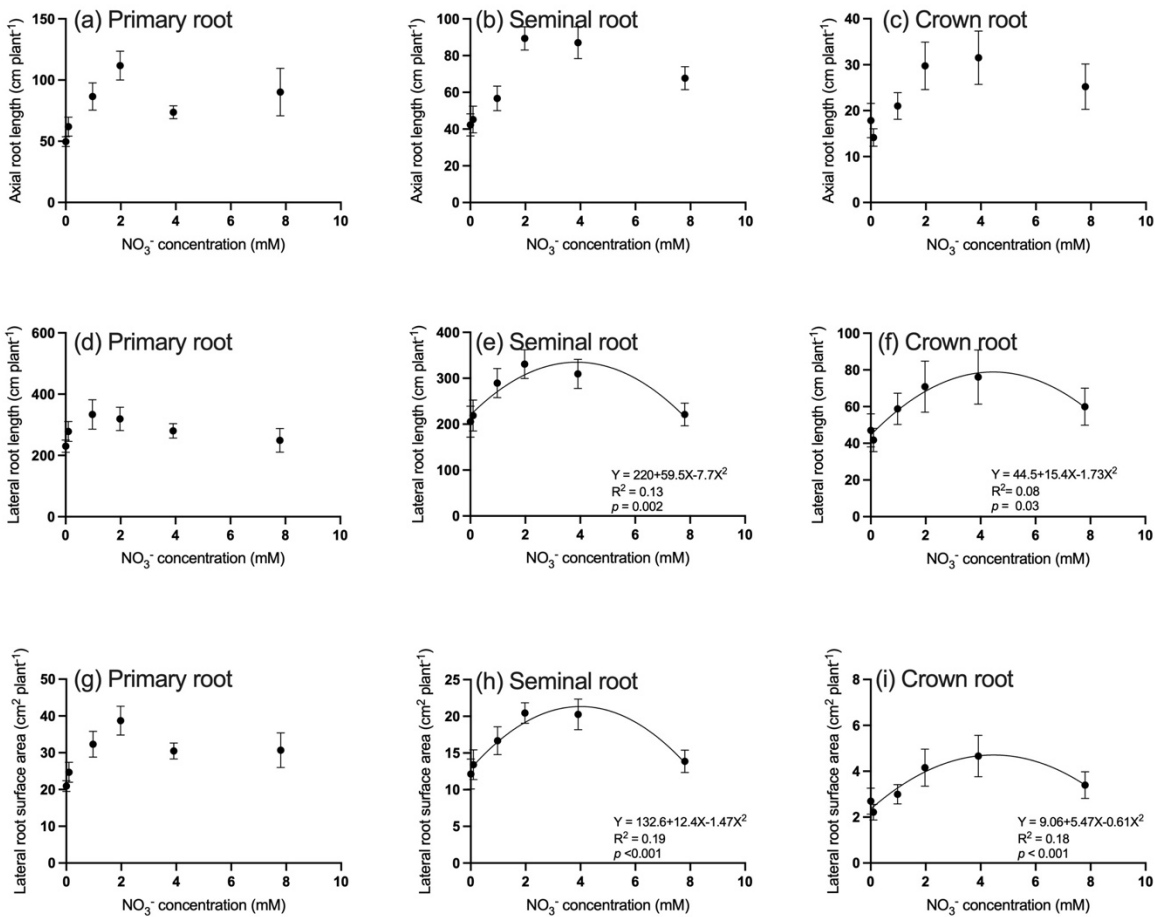


Fig. 2. 2 Length of primary axial root (**a**), seminal axial roots (**b**) crown axial roots (**c**), length of primary lateral roots (**d**), seminal lateral roots (**e**) and crown lateral roots (**f**), and surface area of primary lateral roots (**h**), seminal lateral roots (**i**) and crown lateral roots (**j**) at V3 stage after roots were exposed to variable NO_3^- concentrations (mean value of measured NO_3^- concentration from 15 to 29 days) in perlite-filled pots for 30 ddays. Error bars are standard error of the mean (n=15)

2.5 Discussion

Seminal and crown root types had a plastic growth response to variable NO_3^- concentration in perlite growth media. Total lateral roots were longer and had a larger surface area as the NO_3^- concentration increased, reaching the maximum length and surface area at 3.9–4.5 $\text{mmol L}^{-1} \text{NO}_3^-$ and declining thereafter. Another hydroponic study found that 5 $\text{mmol L}^{-1} \text{NO}_3^-$ was optimal for laterals growing on seminal and crown root types of 12-day-old maize, and lateral root growth was associated with the presence of 60 ng auxin g^{-1} fresh root mass (Tian et al. 2008). Lateral root initiation requires auxin sensing of the NO_3^- concentration in soil solution, which may come from basipetal or acropetal auxin transport (Casimiro et al. 2001). Since plasticity in lateral roots with variable NO_3^- concentration results from acropetal auxin transport (Guo et al. 2005; Liu et al. 2010), the auxin response may originate in the N-demanding shoot tissues. Our maize seedlings required 3.7–3.8 $\text{mmol L}^{-1} \text{NO}_3^-$ to reach the maximum shoot N content and chlorophyll content, which is greater than the amount needed for maximum shoot biomass (2.3 $\text{mmol L}^{-1} \text{NO}_3^-$), suggesting that shoots controlled NO_3^- uptake in maize seedlings. There was little evidence of basipetal auxin transport, as a constant number of lateral root tips were found at all NO_3^- concentrations (Table S2. 2). Thus, we suggest that the N-demanding shoot tissues or chlorophyll initiate the acropetal auxin

process, which detects the NO_3^- concentration around the roots and triggers lateral growth in seminal and crown root types.

Primary lateral roots did not respond to variable NO_3^- concentrations. This was surprising because primary and seminal root types had a similar lateral root length, e.g., ~ 300 cm of laterals with $2 \text{ mmol L}^{-1} \text{ NO}_3^-$, and about $4\times$ longer laterals than the crown roots, e.g., ~ 75 cm of laterals with $2 \text{ mmol L}^{-1} \text{ NO}_3^-$. This indicated that lateral growth on primary roots might be controlled by genetic factors rather than the NO_3^- concentration in soil solution. The slow transport of water and solutes into the xylem of maize primary root is due to its wider Casparian strip than in seminal and crown root types (Tai et al. 2016; Calvo-Polanco et al. 2021). Furthermore, primary roots have a lower ratio of meta-xylem vessels in the whole stele area, compared to seminal and crown root types (Tai et al. 2016). If the stele of the primary root is mainly a conduit for photosynthates rather than water or solutes like NO_3^- , this could explain the insensitivity of laterals in the primary root to variable NO_3^- concentrations. Hence, we suggest that lateral roots have specialized functions in the complex maize root system, depending on whether they are associated with primary, seminal, or crown root types. The plasticity of root types is a useful trait that may help to develop maize root systems with a superior ability to absorb NO_3^- .

We did not expect axial roots to respond to the variable NO_3^- concentration, because axial root morphology is controlled by genetic rather than environmental factors (Hochholdinger et al. 2004; Yu et al. 2015). Determinate axial root growth occurred up to the V3 stage (this study) and during vegetative and silking stages in the B73 inbred line (Yu et al. 2015). We noticed that Gao et al. (2015) reported 46%–60% longer axial roots of the primary, seminal, and crown root types when 12-day-old maize seedlings were exposed to hydroponics solution containing $4 \text{ mmol L}^{-1} \text{ NO}_3^-$ than $0.04 \text{ mmol L}^{-1} \text{ NO}_3^-$. Still, there is variation in axial growth among root types, with

longer axials on the primary root > seminal root > crown root at the same NO_3^- concentration (Figs. 2. 2a–c). Extension of axial roots is also affected by the container and growth media. However, the total root length (590–950 cm root⁻¹) in our study is comparable to the total root length of maize grown in 20× larger containers (500–1200 cm root⁻¹; Liu et al. 2008). Perlite provides a solid support for axial root elongation, although it is more porous (bulk density = 0.11 g cm⁻³) than typical field soil that has a natural bulk density of 1.0–1.4 g cm⁻³ with patchier nutrient concentrations in soil solution. In a minimally constrained growth media, we conclude that maize axial roots will reach the maximum determinate growth according to genetic programming rather than the NO_3^- concentration.

2.6 References

- Cahn, M.D., Zobel, R.W., and Bouldin, D.R. 1989. Relationship between root elongation rate and diameter and duration of growth of lateral roots of maize. *Plant Soil*. **119**: 271-279. doi: <http://www.jstor.org/stable/42938280>.
- Calvo-Polanco, M., Ribeyre, Z., Dauzat, M., Reyt, G., Hidalgo-Shrestha, C., Diehl, P., Frenger, M., Simounneau, T., Muller, B., Salt, D.E., Franke, R.B., Maurel, C., and Boursiac, Y. 2021. Physiological roles of Casparian strips and suberin in the transport of water and solutes. *New Phytol*. **232**: 2295–2307. doi: <https://doi.org/10.1111/nph.17765>.
- Casimiro, I., Marchant, A., Bhalerao, R.P., Beeckma, T., Dhooge, S., Swarup, R., Graham, N., Inzé, D., Sandberg, G., Casero, P.J., and Bennett, M. 2001. Auxin transport promotes Arabidopsis lateral root initiation. *Plant Cell*. **13**: 843–852. doi: <https://doi.org/10.1105/tpc.13.4.843>.
- Chun, L., Mi, G., Li, J., Chen, F., and Zhang, F. 2005. Genetic analysis of maize root characteristics in response to low nitrogen stress. *Plant Soil*. **276**: 369–382. doi: <https://doi.org/10.1007/s11104-005-5876-2>.
- Gao, K., Chen, F., Yuan, L., Zhang, F., and Mi, G. 2015. A comprehensive analysis of root morphological changes and nitrogen allocation in maize in response to low nitrogen stress. *Plant Cell Environ*. **38**: 740–750. doi: <https://doi.org/10.1111/pce.12439>.
- Guo, Y., Chen, F., Zhang, F., and Mi, G. 2005. Auxin transport from shoot to root is involved in the response of lateral root growth to localized supply of nitrate in maize. *Plant Sci*. **169**: 894–900. doi: <https://doi.org/10.1016/j.plantsci.2005.06.007>.

- Hochholdinger, F., Woll, K., Sauer, M., and Dembinsky, D. 2004. Genetic dissection of root formation in maize (*Zea mays*) reveals root-type specific developmental programmes. *Ann. Bot.* **93**: 359–368. <https://doi.org/10.1093/aob/mch056>.
- Lazof, D.B., Rufty, Jr.T.W., and Redinbaugh, M.G. 1992. Localization of nitrate absorption and translocation within morphological regions of the corn root. *Plant Physiol.* **100**: 1251–1258. doi: <https://doi.org/10.1104/pp.100.3.1251>.
- Liu, J., An, X., Cheng, L., Chen, F., Bao, J., Yuan, L., Zhang, F., and Mi, G. 2010. Auxin transport in maize roots in response to localized nitrate supply. *Ann. Bot.* **106**: 1019–1026. doi: <https://doi.org/10.1093/aob/mcq202>.
- Liu, J., Li, J., Chen, F., Zhang, F., Ren, T., Zhuang, Z., and Mi, G. 2008 Mapping QTLs for root traits under different nitrate levels at the seedling stage in maize (*Zea mays* L.) *Plant Soil.* **305**: 253–265. doi: <https://doi.org/10.1007/s11104-008-9562-z>.
- Moreno-Risueno, M.A., Van Norman, J.M., Moreno, A., Zhang, J., Ahnert, S.E., and Benfey, P.N. 2010. Oscillating gene expression determines competence for periodic Arabidopsis root branching. *Science.* **329**: 1306–1311. doi: <https://doi.org/10.1126/science.1191937>.
- Sims, G.K., Ellsworth, T.R., and Mulvaney, R.L. 1995. Microscale determination of inorganic nitrogen in water and soil extracts. *Commun. Soil Sci. Plant. Anal.* **26**: 303–316. doi: <https://doi.org/10.1080/00103629509369298>.
- Tai, H., Lu, X., Opitz, N., Marcon, C., Paschold, A., Lithio, A., Nettleton, D., and Hochholdinger, F. 2016. Transcriptomic and anatomical complexity of primary, seminal, and crown roots highlight root type-specific functional diversity in maize (*Zea mays* L.). *J. Exp. Bot.* **67**: 1123–1135. doi: [10.1093/jxb/erv513](https://doi.org/10.1093/jxb/erv513).

Tian, Q., Chen, F., Liu, J., Zhang, F., and Mi, G. 2008. Inhibition of maize root growth by high nitrate supply is correlated with reduced IAA levels in roots. *J. Plant Physiol.* **165**: 942–951. doi: <https://doi.org/10.1016/j.jplph.2007.02.011>.

Yu, P., Hochholdinger, F., and Li, C. 2015. Root-type-specific plasticity in response to localized high nitrate supply in maize (*Zea mays*). *Ann. Bot.* **116**: 751–762. doi: <https://doi.org/10.1093/aob/mcv127>.

FORWARD TO CHAPTER 3

Chapter 2 revealed the distinctive plasticity of maize root types, with crown and seminal lateral roots showed a quadratic response to NO_3^- concentrations in a controlled growing environment. However, this experimental system may be too simplistic to predict the response of maize roots to NO_3^- concentration in soil, which contains minerals and organic matter. Furthermore, the movement of NO_3^- in soil is linked to the water mass flow process that is controlled by transpiration. Maize root plasticity with respect to morphology and anatomy is likely affected by the interactive effects of soil water content and NO_3^- concentrations. Therefore, the objectives of Chapter 3 are (1) to investigate the morphological and anatomical plasticity of maize root types growing in water-deficient and N-limited soils; (2) to determine which root types are responsible for the root hydraulic conductance, which is associated with maize N uptake. To achieve these objectives, I analyzed results from maize root systems in a controlled growth chamber experiment and a two-year field experiment.

CHAPTER 3

Plasticity of maize (*Zea mays*) roots depends on water content in nitrogen fertilized soil

Yutong Jiang¹, Joann K. Whalen^{1*}

Address: ¹Department of Natural Resource Sciences, Macdonald Campus of McGill University,
21111 5 Lakeshore Road, Ste-Anne-de-Bellevue, Quebec, Canada H9X 3V9

Corresponding author: Joann K. Whalen, joann.whalen@mcgill.ca, tel: 001-514-398-7943

3.1 Abstract

Growth of maize (*Zea mays*) roots respond to soil nitrate (NO_3^-) concentration to optimize nitrogen (N) uptake. However, soil water content may influence plastic root responses by regulating plant N demand. Maize root growth was assessed in response to variable soil water content and N fertilizer rates. The growth chamber experiment was factorial with N fertilizer (equivalent to 85 or 170 kg N ha⁻¹) × water treatments (soil water potential at -5 kPa and -15 kPa), with five replicates per treatment. Field plots were fertilized with 0, 30, 40 or 50 kg N ha⁻¹, banded at seeding in four replicated blocks, in 2021 and 2022. In relatively wet soil (-5 kPa), pot-grown maize maintained had 23% longer lateral roots, 16% greater lateral root surface area, and 15% more crown root number with 170 kg N ha⁻¹ than 85 kg N ha⁻¹. In relatively dry soil (-15 kPa), lateral root surface area and crown roots were similar with both N fertilizer levels. In the wetter growing season (2022), field-grown maize with 30–40 kg N ha⁻¹ had 21–25% longer lateral roots on the seminal and crown roots than with 0 kg N ha⁻¹. Maize exhibited higher hydraulic conductance in wetter soil, which positively correlated with N uptake in pot and field conditions. Maize roots show more growth plasticity to N fertilizer treatments in wetter soil conditions, indicating that water management is the key to optimize root development for maximum N uptake.

Keywords: adaption, lateral roots, nitrate, nitrogen uptake, root hydraulic conductance, xylem

3.2 Introduction

Maize (*Zea mays*) is a globally significant crop with multiple economic and nutritional purposes. As the world's largest single recipient of nitrogen (N) fertilizer, maize requires about 200 kg N ha⁻¹ to synthesize essential N-containing compounds and produce high-quality grains. However, the uptake of soluble nitrate (NO₃⁻) relies on transpiration-driven mass flow process, which is limited by soil water deficit. Many maize-growing regions have annual precipitation of 300–500 mm, which is near or below the optimal level for maize growth (Hanjra and Qureshi 2010). The combined N limitation and water deficit can cause a yield reduction of 7 – 15% (Plett et al. 2020; Flynn et al. 2023).

Maize roots display plasticity, adjusting their morphological and anatomical structures to optimize the N uptake according to the growing conditions. For example, maize laterals along seminal and crown root types elongate following a quadratic relationship as the external NO₃⁻ concentrations increase from 0 to 7.8 mM, regulated by auxin (Tian et al., 2008; Jiang et al. 2023). The plasticity is functional, given that more than 60% of NO₃⁻ uptake is absorbed by laterals when the maize primary root is exposed to ¹⁵N-NO₃⁻ solution (Lazof et al. 1992). Moreover, xylem area of crown roots was decreased, while cortical aerenchyma increased in the primary (62%), seminal (218%), and crown roots (74%) in a N-limited soil, which helped maize acquire up to 50% more NO₃⁻ (Postma and Lynch 2011; Saengwilai et al. 2014a).

Soil water is the most limiting factor for maize growth in most of the world, due to the plant need for water in structural tissues and cellular process, and as a solute that transports NO₃⁻, other nutrients and growth promoting substances. A decrease in soil water content results in decreased shoot biomass, leading to reduced N demand in maize. In addition, lower soil water content is associated with reduced transpiration pull to NO₃⁻ and root hydraulic conductance (Jafarikouhini

and Sinclair 2023). This reduced root hydraulic conductance limits the movement of N, particularly NO_3^- ions, in the soil. For example, in sandy loam soil, maize's transpiration rate experiences a twofold decrease, dropping from approximately $2.5 \text{ g s}^{-1} \text{ cm}^{-2}$ to $1 \text{ g s}^{-1} \text{ cm}^{-2}$, while root hydraulic conductance decreases by 10-fold when soil water potential decreases from -5 to -50 kPa (Cai et al. 2022). These reductions contribute to a 4% decrease in total N removal from the soil (Lai et al. 2011). Given the reduced N demand in maize under water deficit, it is expected that maize will exhibit less root plasticity when soil NO_3^- concentration varies under water-deficit than in well-watered condition.

This study aims to evaluate the maize root plasticity in response to N fertilizer inputs and investigate its interaction with soil water content in growth chamber and field environments. We hypothesized that under well-watered soils, maize roots would exhibit plasticity by reducing lateral root length, crown root number, and xylem area in response to decreased N fertilization. However, we expected a lack of plastic responses to N fertilization in the dry soil because of the reduced N uptake by maize resulting from decreased shoot biomass and root hydraulic conductance.

3.3 Materials and methods

3.3.1 Soil

The 2-year field experiment (2021, 2022) occurred at the Emile A. Lods Agronomy Research Centre in Sainte-Anne-de-Bellevue, Québec ($45^{\circ}25'N$, $73^{\circ}55'W$, 39 m elevation). Climate at this site is cold and humid with an average of 1000 mm precipitation per year (based on 30-year climate data). During the growing seasons (May to October), the average air temperature was 18°C , with 368 mm precipitation in 2021 and 530 mm precipitation in 2022. Soil at this location is a sandy-loam Humic Gleysol of the St. Amable series containing $620 \text{ g sand kg}^{-1}$, $60 \text{ g clay kg}^{-1}$, and 48 g

organic C kg⁻¹, with pH 6.3, field capacity of 23% and an average bulk density of 1110 kg m⁻³. The top soil (0 – 15 cm) has 138 g organic C kg⁻¹, 166 kg Mehlich-III P ha⁻¹ and 412 kg Mehlich-III K ha⁻¹, with a P/Al ratio of 8.1%. The area used for the field experiment was planted with clover forage and perennial grass (2017–2020), which was plowed down in early spring before maize was planted in 2021. The same site was used for maize cultivation in 2022. Prior to the field experiment, we collected soil (0 –15 cm) from this location in October 2019 for a controlled growth chamber experiment.

3.3.2 Growth chamber experiment

The controlled growth chamber experiment was designed to regulate soil water content during maize growth, up to the vegetative 6-leaf stage (V6). The experiment was designed as a full factorial study with 4 biostimulant treatments (seed soaking only, soil application only, seed soaking plus soil application, or control), 2 levels of N fertilizer (equivalent to 85 kg N ha⁻¹ and 170 kg N ha⁻¹), and 2 levels of watering (-5 kPa and -15 kPa, measured as gravimetric water content and estimated as soil water potential, Ψ_{soil}) with 5 replicates of each (n = 5), for a total of 80 pots (12.7 cm dia., 15 cm depth). The soil water retention curve was reported in Fig. S3. 1. Moist field soil (680 g dry weight, sieved < 8 mm) was adjusted to the same moisture content (about -15kPa), packed into the pots at field bulk density, and the weight of each pot and soil was recorded. After seed soaking in 0.6% v/v biostimulant solution (Humic LandTM, Rogitex Inc., Pointe-Claire, Quebec, Canada) or water for 10 h at 22°C, 5 maize seeds per pot (cv. MZ3877 containing *Bacillus thuringiensis* and *Roundup Ready* transgenes) were planted at a depth of ~ 2 cm in each pot. Forty pots were planted with the biostimulant-soaked seed and 40 pots had water-soaked seed.

Pots were then placed in a controlled growth chamber (E15, Conviron Inc., Manitoba, Canada) with a daytime temperature of 27 °C, a nighttime temperature of 17 °C with 16h: 8h day: night cycle under fluorescent light (800 $\mu\text{mol}^{-2} \text{s}^{-1}$ of photon flux density). Ten days after planting, the two largest maize plants per pot were kept for the experiment and the rest were removed from the pot. Soil application was done by dribbling the 1 mL pot^{-1} biostimulant solution (0.5 % v/v) on the soil surface beside the maize stem. Also at this time, 10 mL of 61.6 g L^{-1} NH_4NO_3 solution was sprayed uniformly on the soil surface of 40 pots to supply 170 kg N ha^{-1} on an equivalent surface area basis, and the other 40 pots were sprayed with 5 mL of 61.6 g L^{-1} NH_4NO_3 solution, representing 85 kg N ha^{-1} on the soil surface. Each pot received 10 mL of 14.5 g L^{-1} KHPO_4 uniformly applied to soil surface, in accordance with agronomic recommendation for maize in a low fertility soil, commonly used in pot studies due to high nutrient demand of maize in limited soil volumes (Terman 1974; CRAAQ 2010).

Two wk after seeding, soil moisture was adjusted to the target levels of -5 kPa (n = 40 pots) and -15 kPa (n = 40 pots). In growth chamber studies, maize requires daily watering to about 80% of the soil water-holding capacity to avoid growth limitation, and ~60% of the soil water-holding capacity induces a water deficit, although this soil moisture level is above the permanent wilting point. Thus, soil water potential at -5 kPa contained about 260 g water kg^{-1} soil, representing 80% soil water-holding capacity, while soil water potential at -15 kPa contained about 200 g water kg^{-1} , representing 60% soil water-holding capacity. From 14–28 d after seeding, the entire pot was weighed to determine the water loss every 2–3 d, and tapwater was added to replenish the mass (1 g water = 1 mL water). We did not account for the extra mass from plant biomass because maize produced 3 – 5 g fresh mass pot^{-1} by 28 d and that is only 10% of the water lost every 2–3 d (30 – 50 g). After 28 d, watering was done at a constant rate of 30–50 g per pot every 2–3 d, according

to the average water loss in the previous weeks. By 48 d, the pots with $\Psi_{\text{soil}} = -5$ kPa received 977 mL of water in total, and the pots with $\Psi_{\text{soil}} = -15$ kPa moisture content received 636 mL in total. The experiment ended 48 d after seeding when 80% of maize plants reached the V6 stage.

3.3.3 Field study

The complete factorial design had four biostimulant treatments (seed soaking only, soil application only, seed soaking plus soil application, or control) and three N fertilizer levels (72 kg N ha⁻¹, 96 kg N ha⁻¹, 120 kg N ha⁻¹). An unfertilized control (0 kg N ha⁻¹) was included in 2022. The highest N fertilizer rate is within the 120–170 kg N ha⁻¹ recommended for maize production in Quebec, adjusted for the N credit of approximately 50 kg N ha⁻¹ following the plow-down of the legume-based forage crop (CRAAQ 2010). Each factorial plot was 5 m × 6 m, and treatments were assigned in a randomized complete block design with four blocks separated by 3 m buffers, for a total of 48 experimental plots. On 13 May 2021, starter N fertilizer was banded into the seed row at rates of 30, 40 or 50 kg N ha⁻¹ with granular ammonium sulfate (21-0-0-24), but no P and K fertilizers were applied because soil test indicated an adequate supply for field-grown maize (Parent et al. 2020). On 7 June 2021, maize (*Zea mays* L. cv. PS2790, not genetically modified, not treated with fungicide or insecticide) was seeded at 5 cm depth with a planter (75 cm row spacing with 8 rows per plot) at a seeding rate of 80 000 seeds ha⁻¹, to replace maize seedlings that were accidentally terminated by glyphosate application the previous week. On 12 May 2022, we applied the starter N fertilizer at of 30, 40 or 50 kg N ha⁻¹ with granular ammonium sulfate (21-0-0-24), along with 87 kg ha⁻¹ triple super phosphate (0-46-0) and 67 kg ha⁻¹ potash (0-0-60). The same seeding procedure and cultivar was used in 2022. At the V6 growth stage, calcium-ammonium nitrate (27.5-0-0) was side-dressed beside the planted row at the rates of 0 kg N ha⁻¹

(only in 2022), 42 kg N ha⁻¹, 56 kg N ha⁻¹ and 70 kg N ha⁻¹, which supplied 0 kg N ha⁻¹, 72 kg N ha⁻¹, 96 kg N ha⁻¹ and 120 kg N ha⁻¹ during the growing season. During the vegetative 1-leaf, 3-leaf, 5-leaf and 7-leaf growth stages, referred to as V1, V3, V5 and V7, 10 maize plants and their root-associated soil were collected at random from each plot.

3.3.4 Plant and soil sampling

The maize shoot was cut at the soil surface, dried (55 °C for 48 h), weighed, and ground (<1 mm). Maize roots were separated from soil by carefully shaking and brushing off the root-associated soil. In the field experiment, the root was excavated to 25 cm depth with a shovel, which recovers an estimated 80% of the lateral roots from field-grown maize at V1 to V7 growth stages (Sobat and Whalen 2021). Root-associated soil was refrigerated upon removal from pots in the growth chamber study, or transferred in a cooler with ice when collected in the field. Root-associated soil was stored at 4 °C for up to 3 d.

3.3.5 Plant and soil analyses

Roots were scanned on a Photo scanner (V700, Epson Inc., Markham, Canada) at 400 dpi resolution and analyzed by WinRhizo software (Regent Instruments, Quebec, Canada) to determine the root morphological traits, including total root length and surface area. Further, roots collected from the field in 2022 were manually dissected the fresh roots into primary, seminal, and crown roots, before measuring the length and surface area of each root type. The length and surface area of lateral roots was assumed to be the sum of the fine roots with a diameter < 0.5 mm measured in WinRhizo software (Cahn et al. 1989; Jiang et al. 2023). After measuring the morphological traits, roots were oven-dried (55°C for 48 h), weighed (dry mass), and ground (<1 mm). Shoot and

root N concentration (mg g^{-1}) was determined by combustion at $900\text{ }^{\circ}\text{C}$ (Thermo Finnigan Flash EA 1112, Carlo Erba, Milan, Italy). The N uptake (mg plant^{-1}) was the total N contained in shoot plus root dry mass.

Soil moisture content was measured after drying ($105\text{ }^{\circ}\text{C}$ for 24 h). About 6 g of moist soil was extracted (1:5 w:v extracts of soil: 2M KCl) and soil mineral N (changeable NH_4^+ and NO_3^- concentrations) were determined colorimetrically at 650 nm on a μQuant microplate reader (BioTek, Winooski, VT, USA) according to Sims et al. (1995).

3.3.6 Xylem measurements

Xylem diameter was measured on the same maize cultivar, grown in soil from the field site, in a controlled greenhouse bench (a light/darkness photoperiod of 16/8 h at $28/18\text{ }^{\circ}\text{C}$, $400\text{ }\mu\text{mol}^{-2}\text{ s}^{-1}$ of photon flux density, and 60% relative humidity). One set of pots (12.7 cm dia., 15 cm depth) was planted with maize cv. MZ3877 and received 2×2 factorial experiment with two levels of N fertilizer (equivalent to 85 kg N ha^{-1} and 170 kg N ha^{-1}), and two levels of watering ($\Psi_{\text{soil}} = -5\text{ kPa}$ and -15 kPa), with 4 replicates of each ($n = 4$). Maize was fertilized, watered and sampled at the V6 stage following the same procedure as in the growth chamber experiment. The second set of pots (22 cm dia., 25 cm depth) was seeded with maize cv. PS2790 and watered to similar soil water content level (+5%) as the average moisture in the 2021 and 2022 field environments, monitored by a soil moisture sensor (TDR 100, Spectrum Technologies, Aurora, IL, USA). Urea fertilizer was split-given at seeding (0.413 g pot^{-1}) and V6 (0.578 g pot^{-1}) to give a total rate of 120 kg N ha^{-1} , or 0 kg N ha^{-1} , with 4 replicates of each ($n = 4$). The roots of four individual plants ($n = 4$) were destructively sampled at V1, V3, V5, and V7 stages according to the procedure followed for the field experiment.

A cross-section of tip (0 – 20 mm from root tip), mid (50 – 70 mm from root tip), base (0 – 20 mm from root base) of one root from each root type (primary root, seminal root, and crown root) were prepared for anatomical analysis. The root segments were fixed in 4% paraformaldehyde in 1× phosphate buffer saline solution while shaking (3 h, 22°C), and washed 3 times (30 min, 22°C) in 1× phosphate buffer saline solution. The root segments were thin sectioned, stained by 0.1% Toluidine Blue O and washed by 1× phosphate buffer saline solution before sealing with a cover slip. Root anatomy images were taken with light microscopy (ZEISS imager Z1, Germany) with ×10 magnification. Xylem area, number, and diameter were analyzed by ImageJ (version Fiji for Mac OS X, U. S. National Institutes of Health, Bethesda, Maryland, USA).

Theoretical hydraulic conductance through each root type was calculated by the modified Hagen-Poiseuille Law (Strock et al. 2021):

$$k = \frac{\pi\rho}{128\eta} \sum_{i=1}^n (d_i^4) \quad (1)$$

where ρ is the xylem sap fluid density assumed to be water (1000 kg m⁻³, at 20°C), and η is the viscosity of the xylem sap assumed to be water (1 × 10⁻⁹ MPa s, at 20°C), d is the mean diameter of each metaxylem vessel (m).

3.3.7 Maize transpiration calculation

We estimated maize transpiration in field studies with the Shuttleworth-Wallace algorithm in the Root Zone Water Quality Model (RZWQM2, Kuang et al., 2021). The root mean square error (RMSE) and relative RMSE of shoot dry mass was used to quantify the goodness fit of the simulated values and observed values over n observations (equation S3.1). The relative RMSE of shoot dry mass was within 20% (equation S3.2), and the R² (equation S3.3) and index of agreement

(equation S3.4) were more than 0.7, meaning the model calibration was appropriate to measure maize growth and transpiration (Supplementary Table S3. 1).

3.3.8 Statistical analyses

Data were normally distributed (Shapiro-Wilk test, $p > 0.05$) with homogeneous variance (Levene's test, $p > 0.05$). Analysis of variance revealed no effect ($p > 0.05$) of the biostimulant exposure on any dependent variable (shoot and root dry mass, root morphological traits, soil moisture content, soil mineral N concentrations, and maize N uptake (Supplementary Table S3. 2). Thus, data were pooled among biostimulant treatments, which gave more replicates ($n = 20$ in the growth chamber experiment, and $n = 16$ in the field experiment) for the soil water and N fertilizer treatments. In the growth chamber experiment, the main and interactive effects of soil water content and N fertilizer levels were evaluated by two-way analysis of variance. In the field experiment, N fertilizer levels were considered as fixed effects, whereas block, and block \times N fertilizer levels were treated as random effect. The effects of N fertilizer levels on plant growth parameters and soil mineral N were evaluated with one-way analysis of variance. When the fixed effects were significant ($p < 0.05$), mean values were compared with Tukey's HSD test. Correlation with Pearson coefficient was used to describe the best-fit lines of the relationship between root hydraulic conductance and N uptake. Statistical tests were done with SAS statistical software, version 9.4.

3.4 Results

3.4.1 Root development in pot-grown maize responds to N fertilization in well-watered soil

The longest roots in pot-grown maize were laterals, which maize were 746 –1000 cm in length with a surface area of 130 – 171 cm², while axial roots were much shorter, from 108 – 141 cm in length with a similar surface area of 138 – 160 cm² (Fig. 3. 1). When soil moisture was limited to -15 kPa, maize had 14% longer lateral roots and similar root surface area with 170 kg N ha⁻¹ than 85 kg N ha⁻¹. Well-watered soil had 23% longer lateral roots and 16% greater root surface area with 170 kg N ha⁻¹ than 85 kg N ha⁻¹. Maize axial root length, axial surface area and number of 2nd whorl-crown axial roots did not respond to N fertilizer treatments ($p > 0.05$), except for a 15% increase in the number of 1st whorl-crown axial roots with 170 kg N ha⁻¹ at -5 kPa. Maize growth and N uptake was greater, and the soil mineral N concentration was lower in pots with soil water potential at -5 kPa (wet soil) than -15 kPa (dry soil, Table 3. 1, Fig. 3. 2a).

3.4.2 Root hydraulic conductance associated with crown roots in pot-grown maize

Pot-grown maize had root hydraulic conductance of 45–76 (kg m MPa⁻¹ s⁻¹) ×10⁻⁵ across the soil water content and N fertilizer treatments (Fig. 3. 2a). Maize had 47–64% greater root hydraulic conductance when grown in the wet soil than the dry soil. Furthermore, there was 14% gain in root hydraulic conductance in the well-watered soil that received 170 kg N ha⁻¹ than 85 kg N ha⁻¹ (Fig. 3. 2a), due to more 1st whorl crown roots in the maize treated with 170 kg N ha⁻¹ (Fig. 3. 1 e, f). Because crown roots had 25 – 120% more xylem vessels and 300 – 660% greater xylem area than other root types (Tables S3. 2 and S3. 3), each crown root had 10–30 times more root hydraulic conductance than the primary and seminal roots. In a V6 maize plant with 19 – 23 1st whorl crown roots and about 10 2nd whorl crown roots, about 90% of the root hydraulic conductance was due to water acquisition by crown roots. As crown roots became more numerous, the increased root hydraulic conductance was correlated positively with greater N uptake in maize

grown in relatively wet soil ($p < 0.05$, Fig. 3. 2b). In addition, there was 21% greater N uptake and 35% less soil mineral N when maize was amended with 170 kg N ha⁻¹ than 85 kg N ha⁻¹ (Fig. 3. 2A, Table 3. 1).

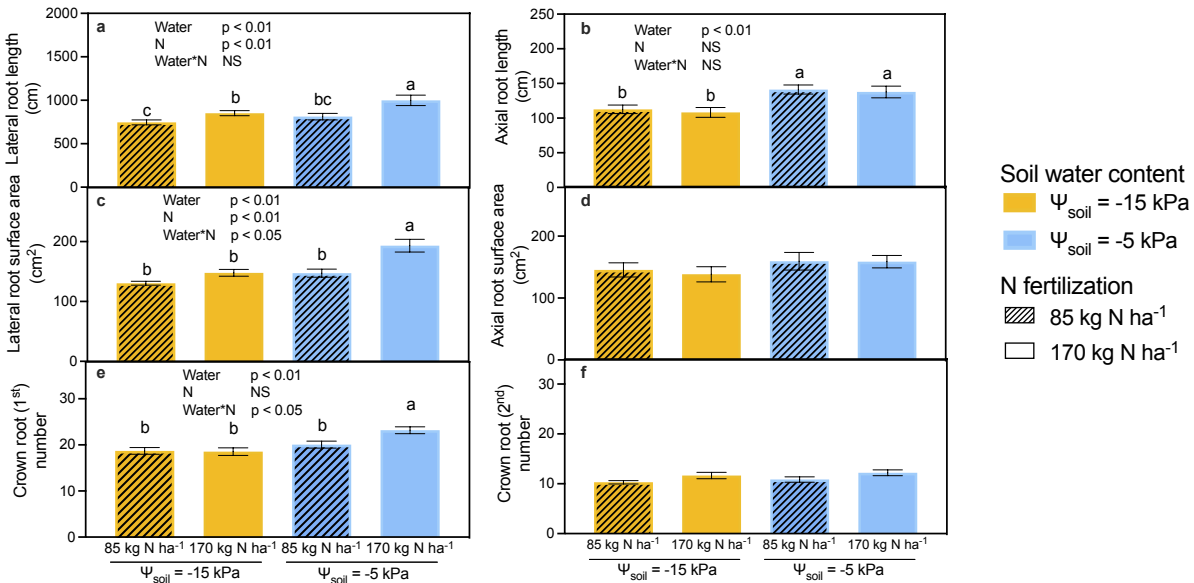


Fig. 3. 1 Root morphological traits, including (a) Lateral root length, (b) axial root length, (c) lateral root surface area, (d) axial root surface area, (e) number of crown roots (1st whorl), (f) number of crown root (2nd whorl) from maize (V6 stage) in a growth chamber environment. Bars noted by a different letter are significantly different ($p < 0.05$). Maize was grown in pots with two levels of N fertilizer (equivalent to 85 and 170 kg N ha⁻¹) and watered to a constant water potential of -15 or -5 kPa. NS, not significant ($p > 0.05$). Error bars represent standard error of means, $n = 20$.

Table 3. 1 Soil moisture, soil mineral N concentration, maize properties at V6 stage in a growth chamber experiment.

		$\Psi_{\text{soil}} = -15 \text{ kPa}$		$\Psi_{\text{soil}} = -5 \text{ kPa}$	
		85 kg N ha ⁻¹	170 kg N ha ⁻¹	85 kg N ha ⁻¹	170 kg N ha ⁻¹
Soil	Moisture content (g kg ⁻¹)	170 ± 5	167 ± 5	174 ± 7	171 ± 8
	NH ₄ ⁺ (mg kg ⁻¹)	1.7 ± 0.1	2.1 ± 0.2	2.1 ± 0.2	1.7 ± 0.1
	NO ₃ ⁻ (mg kg ⁻¹)	33 ± 5 ^{ab}	40 ± 6 ^a	20 ± 3 ^{bc}	13 ± 2 ^c
Plant	Shoot dry mass (g)	10.4 ± 0.7 ^c	12.6 ± 0.8 ^{bc}	16.8 ± 1.2 ^{ab}	19 ± 2.1 ^a
	Root dry mass (g)	1.31 ± 0.05 ^b	1.41 ± 0.06 ^b	1.38 ± 0.05 ^b	1.89 ± 0.05 ^a
	Shoot N concentration (g kg ⁻¹)	27.8 ± 0.7 ^b	33.0 ± 0.4 ^a	23.9 ± 0.6 ^c	29.8 ± 0.7 ^b

Data is the mean ± standard error (n = 20). Within a row, values followed by a different letter are significantly different ($p < 0.05$).

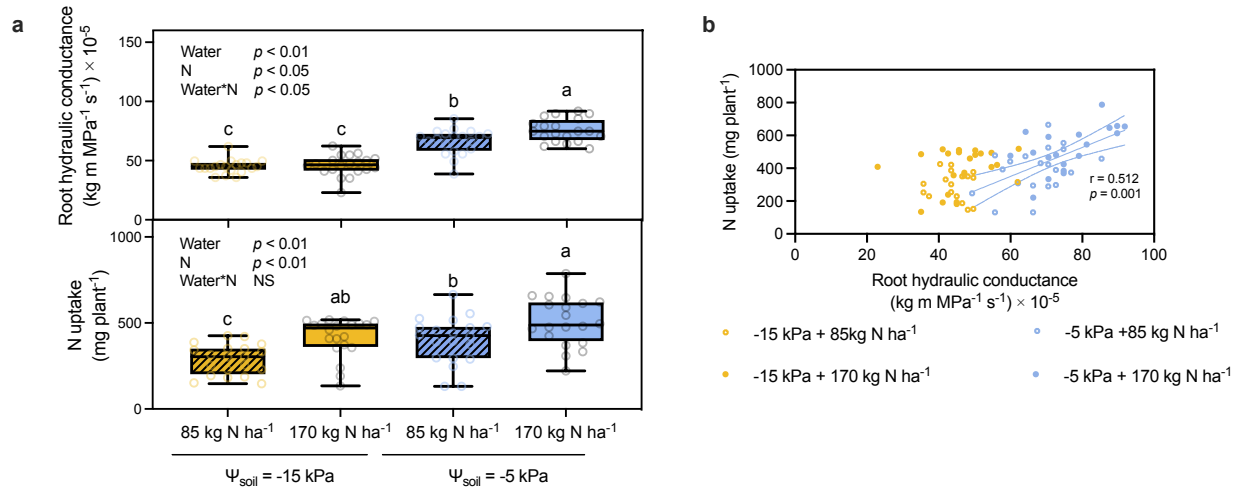


Fig. 3. 2 (a) The N uptake of maize (V6 stage) grown in pots with two levels of N fertilizer (equivalent to 85 and 170 kg N ha⁻¹) and watered to a constant water potential of -15 or -5 kPa. Boxplots show the minimum, median and maximum values, and bars with different letters were significantly different ($p < 0.05$). NS, not significant ($p > 0.05$). (b) The N uptake was related to the root hydraulic conductance of maize, where r is the Pearson correlation coefficient for $n=20$ observations for water potential of -15 or -5 kPa. The procedure for measuring root hydraulic conductance is explained in Table S3.4.

3.4.3 Root development in field-grown maize generally does not respond to N fertilization

Root development of field-grown maize was evaluated in two growing seasons. Maize grown in the drier season (2021) received 102 mm precipitation from seeding until the V7 stage (Fig. 3. 3a), while the wetter season (2022) had 235 mm precipitation, greater soil water content and 14–38% greater cumulative transpiration during the same development period (Fig. 3. 3b). The farmer practice in this region is to apply $\leq 50 \text{ kg N ha}^{-1}$ as starter fertilizer at planting and the remaining N fertilizer at the V6 stage. Consequently, field-grown maize was exposed to similar N

fertilizer regimes and the lateral and axial root growth rates were generally the same among N fertilizer treatments from V1 to V7 (Fig. 3. 4a, b). The only observed difference was at the V5 stage in 2022 when maize receiving 0 kg N ha⁻¹ had 21–25% shorter lateral roots on the seminal and crown roots (Fig. S3. 3) than maize receiving 30–40 kg N ha⁻¹, but this was not sustained at the V7 stage (Fig. 3. 4a). Crown root development by the V5 and V7 stages resulted in more 1st whorl crown roots in the N fertilized than unfertilized control during the wetter 2022 season, with extra 2nd whorl crown roots recorded at the V7 stage in N-fertilized plots, relative to the unfertilized control (Fig. 3. 4c).

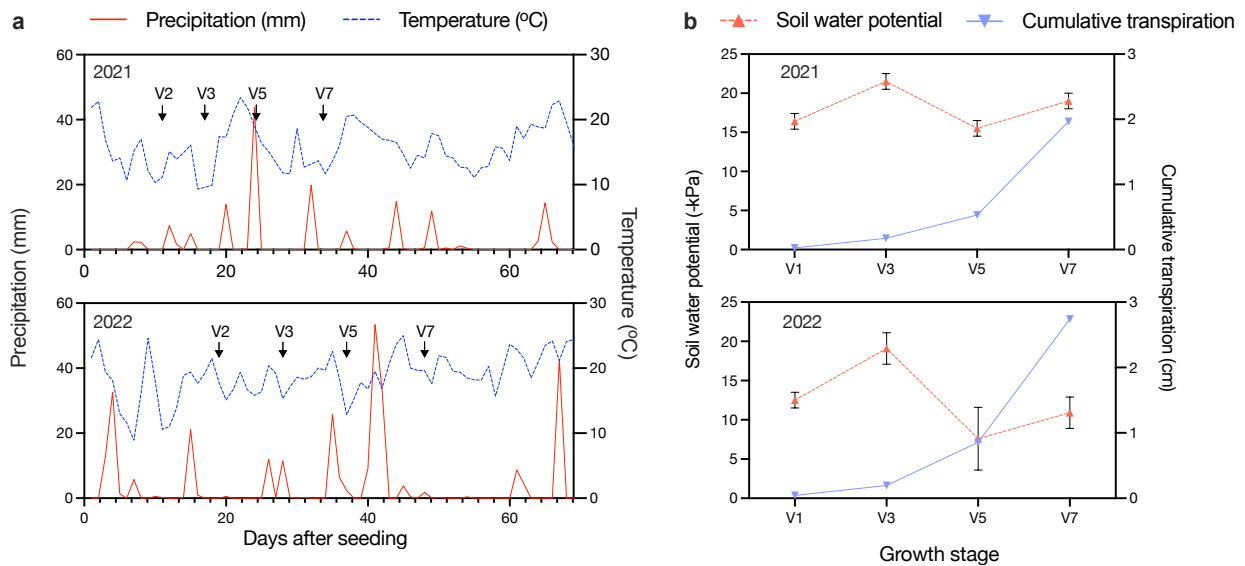


Fig. 3. 3 Rainfall and temperature (a), and soil water potential and cumulative transpiration (b) of two field growing seasons at Sainte-Anne-de-Bellevue, Québec, Canada. Data was collected at the V1 to V7 stages of maize growth in 2021 and 2022. Maize was seeded on June 7, 2021, and May 12, 2022. Soil water potential in the root-associated soil at the V1, V3, V5 and V7 growth stages was averaged among N fertilization treatments (0, 72, 96 or 120 kg N ha⁻¹ during the growing season), and reported as mean \pm standard error (n = 48 in 2021, and n = 64 in 2022).

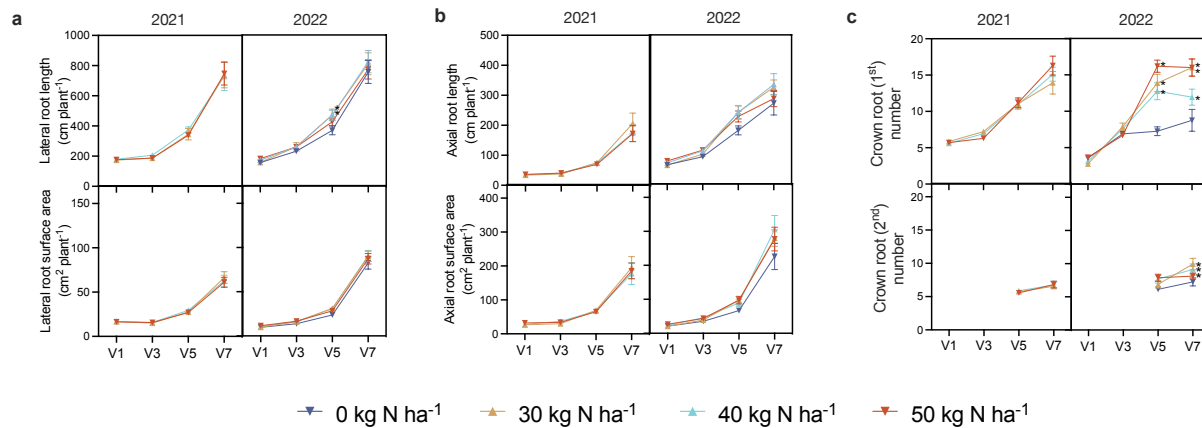


Fig. 3. 4 Root morphological traits, including lateral root length and surface area (a), axial root length and surface area (b), number of 1st whorl and 2nd whorl crown roots (c) of field-grown maize from the V1 to V7 growth stages during the 2021 and 2022 seasons at Sainte-Anne-de-Bellevue, Québec, Canada. The fertilizer treatment delivered about 40% of the target N rate banded as ammonium sulfate at planting (0, 32, 40 or 50 kg N ha⁻¹) and the remaining 60% side-dressed as calcium ammonium nitrate at the V6 stage, supplying 0, 72, 96 or 120 kg N ha⁻¹ during the growing season. Data points are the mean with standard error bars, n= 16. Asterisk (*) indicates significant difference (p <0.05) compared to control plot received 0 kg ha⁻¹.

3.4.4 Root hydraulic conductance associated with crown roots in field-grown maize

When grown under simulated field conditions, maize crown roots had 150 – 560% larger xylem area and more than 5 times the root hydraulic conductance than primary and seminal roots at the V5 stage (Tables S3. 5 and S3. 6). Simulated field-grown maize produced 6 – 16 1st whorl crown roots with 13 to 17 (kg m MPa⁻¹ s⁻¹) × 10⁻⁶ hydraulic conductance and 6 – 10 2nd whorl crown roots having 14 to 20 (kg m MPa⁻¹ s⁻¹) × 10⁻⁶ hydraulic conductance (Table S3. 6). Consequently, crown root development was responsible for the increase in root hydraulic

conductance from V1 to V7 in field-grown maize, which was similar among N fertilizer levels in 2021 and greater in the N fertilized than unfertilized control in 2022 (Fig. 3. 5a). The N uptake increased during maize growth, with similar N uptake among N fertilizer treatments and less N uptake in the unfertilized control during 2022 (Fig. 3. 5b). Maize N uptake at V5 and V7 stages was not related to root hydraulic conductance in 2021, which had a relatively dry growing season (102 mm precipitation from V1 to V7; Fig. 3. 5c). The N uptake was positively correlated with root hydraulic conductance at the V5 and V7 stages in field-grown maize that received 235 mm precipitation by the V7 stage in 2022 (Fig. 3. 5c). Thus, greater N uptake of field-grown maize was related to more rainfall and starter N fertilizer, which resulted in almost 50% greater N uptake than the unfertilized control in 2022.

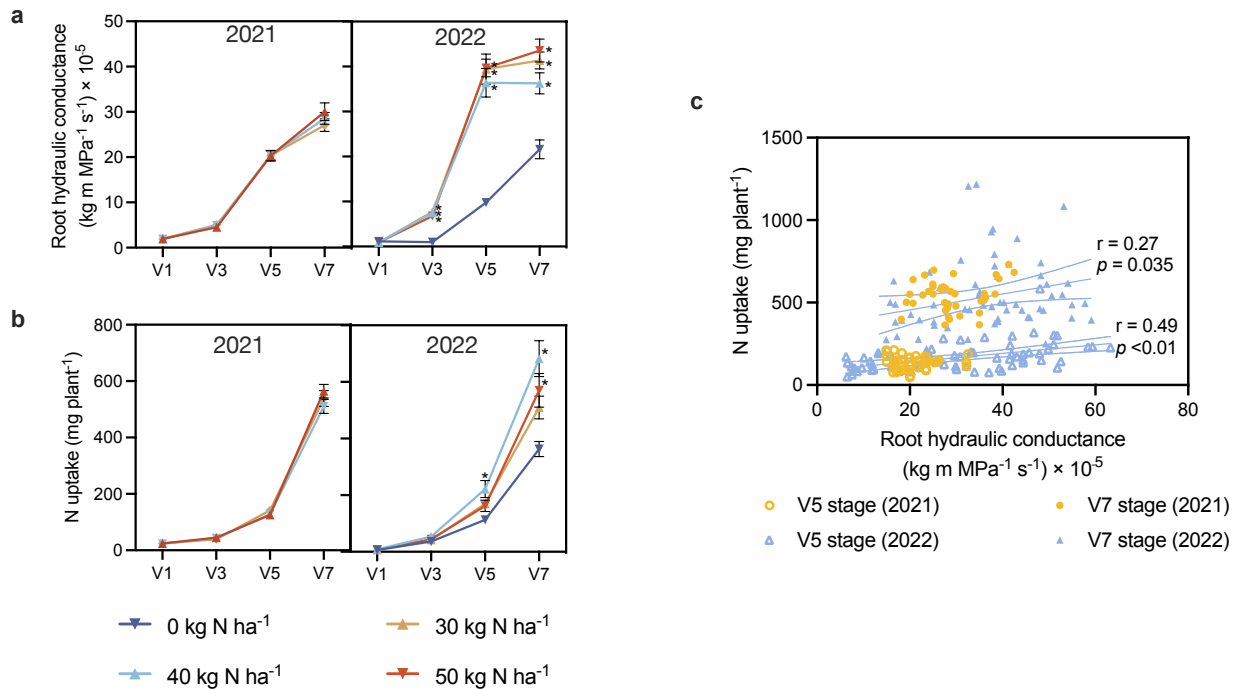


Fig. 3. 5 Root hydraulic conductance (a) and the N uptake (b) at the V1, V3, V5, and V7 stages of maize growth in a field at Sainte-Anne-de-Bellevue, Québec, Canada. The fertilizer treatment

delivered about 40% of the target N rate banded as ammonium sulfate at planting (0, 32, 40 or 50 kg N ha⁻¹) and the remaining 60% side-dressed as calcium ammonium nitrate at the V6 stage, supplying 0, 72, 96 or 120 kg N ha⁻¹ during the growing season. Data points are the mean with standard error bars. Asterisk (*) indicates significant difference ($p < 0.05$) compared to control plot received 0 kg ha⁻¹. The relationship between maize N uptake and root hydraulic conductance (c) was fitted to best-fit lines (with 95% confidence intervals) when r , the Pearson correlation coefficient, was significant ($p < 0.05$). The procedure for measuring root hydraulic conductance is explained in Table S 3. 6.

3.5 Discussion

3.5.1 Root plasticity to N fertilizer inputs under well-watered condition

We expected root system plasticity in response to N fertilizer inputs. In well-watered soil, there were shorter lateral roots in the pot- and field-grown maize in response to reduced N fertilization, aligning with the hypothesis. The field experiment allowed us to observe root plasticity at multiple growth stages. During the V1 – V3 stages, maize roots exhibited no plastic response to soil NO₃⁻ concentration, as the plant primarily depended on embryonic resources, acquiring only 5% of its total N from the soil before the V3 growth stage (Bender et al. 2013). Notably, plasticity in seminal and crown lateral roots was observed at the V5 stage, consistent with findings by Jiang et al. (2023). The adaptive adjustments in lateral roots for N uptake at this stage may be attributed to an acropetal auxin process triggered by N-demanding shoot tissues (Guo et al. 2005). This is supported by the observation that the shoot N concentration was 18 – 20% lower in maize receiving 0 kg N ha⁻¹ compared to those receiving 30 to 50 kg N ha⁻¹ at the V5 stage ($p < 0.05$, Fig. S3. 2). Surprisingly, maize lateral roots did not exhibit plasticity in response to N

fertilizations at the V7 stage, despite the plant experiencing a 200 – 300% increase in N uptake than previous stages. This may be attributed to varying N fertilizer rates resulting in similar shoot N concentrations, possibly due to dilution effects caused by 12 – 46% more shoot biomass in fertilized plots compared to non-fertilized plots. The current N fertilizer rates of 120 kg N ha⁻¹, 96 kg N ha⁻¹, and 72 kg N ha⁻¹ over the growing season did not impose any N limitation on maize growth or yield as evidenced by grain yields from fertilized plots similar to the regional average of 9.94 Mg ha⁻¹ (Table S3. 7; CRAAQ 2010; Institut de la statistique du Québec 2023). Therefore, future field experiments in this humid temperate region should consider lowering the N fertilization levels to < 50 kg N ha⁻¹ to impose N stress treatments and including a well-fertilized control with 170 kg N ha⁻¹ to ensure maize reaches its maximum yield and growth potential.

In well-watered soil, maize produced more crown roots, but the axial root length and its xylem structure was constant across N fertilizer levels. Thus, the hypothesis is partially accepted. This finding is in line with Gaudin et al. (2011), who observed a 60% more crown roots in maize after tasseling under high N conditions (20 mmol L⁻¹) than low nitrogen conditions (8 mmol L⁻¹). Maize with fewer crown roots may develop of a deeper root system, facilitating the access of maize roots to mobile NO₃⁻ ions from deeper soil layer (Saengwilai et al. 2014b; Gao et al. 2016). We did not determine the root depth of field-grown maize, as our sampling method focused on the top 25 cm of soil. Moreover, the xylem number and area of axial roots were constant in both pot- and field grown maize in response to various soil mineral N, which did not align with the expectations. In our study, maize sampling was conducted before the V7 stage, during which only 1st and 2nd whorl crown roots were produced. These early whorls may be less representative of subsequent whorls, given that maize can produce up to 6 whorls throughout its lifespan (Yang et al. 2019). Since maize enters the rapid growth phase and absorbs 90% of its total N after the V6 stage, it is

possible that vascular traits of higher-order crown roots are more plastic in response to soil mineral N. Consequently, we encourage future research to investigate whether maize develops a deeper root system and exhibits plasticity in higher-order crown roots under N-limited soil conditions to optimize N uptake.

3.5.2 Roots were insensitive to N fertilizer inputs under dry soil

In relatively dry soil, root traits were insensitive to N fertilization, possibly due to reduced demand for N uptake resulting from decreased shoot biomass and root hydraulic conductance under insufficient water conditions. Our study indicates that maize grown in the dry soil produced 56% less shoot biomass than those in the wet soil, resulting in a 22% reduction in N uptake. In addition, maize grown in dry soil probably had reduced transpiration pull to take up mobile NO_3^- ions due to the stomatal closure (Cai et al., 2022; Fig. S3. 4). This decreased transpiration resulted in less root hydraulic conductance, with pot-grown maize grown in the dry soil experiencing a 36% reduction compared to maize grown in the relatively wet soil. This result aligns with Cai et al. (2022), reporting a 10-fold reduction in root hydraulic conductance in maize roots as the water potential of sandy loam decreased from -5 to -50 kPa. The limited movement of soluble NO_3^- ions toward the roots, indicated by 65 – 210% higher mineral N left in the dry soil than the wet soil, suggests that maize N uptake is constrained by soil water content.

3.5.3 Crown roots are responsible for maize N uptake during vegetative growth

Crown roots, characterized by larger xylem area and root hydraulic conductance, represent the main conduit for N uptake in maize. The greater capacity of crown roots to conduct water than other root types are consistent with Tai et al. (2016), who reported that crown roots exhibit a 63%

increase in meta- and protoxylem elements and possess larger xylem vessels than primary and seminal roots. The abundance of larger xylem vessels contributes to higher axial hydraulic conductivity, leading to upward water flow from the root xylem to the leaf surface. This process generates radial hydraulic conductance, facilitating the movement of NO_3^- as water flows towards the root surface (Steudle 2001; Liu et al. 2013). Liu et al. (2020) demonstrated that roots with a 150% increase in metaxylem vessels and a 36% expansion in xylem cell area exhibited elevated root hydraulic conductance and a 97% higher low-affinity NO_3^- uptake rate. York et al. (2016) reported 20% higher NO_3^- uptake kinetics in crown root tips compared to seminal root tips in hydroponically grown maize. More N uptake is associated with greater root hydraulic conductivity in pot-grown and field-grown maize, and most of this water movement was conducted through crown roots, which had 5-fold higher hydraulic conductance than primary and seminal roots. This suggests that crown roots are the main transporter of water and dissolved NO_3^- from the soil into maize plants. Future research could measure N uptake by different root types in soil-grown maize using a split-root system combined with ^{15}N isotope labeling.

3.6 Conclusions

Maize roots respond to N fertilizer inputs by growing longer lateral roots and more crown roots, but only in wetter soil conditions, consistently in pot and field studies. Since soil water is the key regulator of maize root development and nutrient uptake, soil water management has to be the priority in maize production systems. Future research on the topic root system plasticity across various maize genotypes must consider the interactive effects of soil water and N fertilization.

3.7 References

- Bender RR, Haegele JW, Ruffo ML, Below FE.** 2013. Nutrient uptake, partitioning, and remobilization in modern, transgenic insect-protected maize hybrids. *Agronomy Journal* **105**, 161–170. <https://doi.org/10.2134/agronj2012.0352>
- Cai G, Ahmed MA, Abdalla M, Carminati A.** 2022. Root hydraulic phenotypes impacting water uptake in drying soils. *Plant, Cell & Environment* **45**, 650–663.
- Cahn MD, Zobel RW, Bouldin DR.** 1989. Relationship between root elongation rate and diameter and duration of growth of lateral roots of maize. *Plant and Soil* **119**, 271–279. <https://doi.org/10.1007/BF02370419>
- CRAAQ.** 2010. Guide de référence en fertilisation (in French). 2nd ed. Centre de référence en Agriculture et Agroalimentaire du Québec, Québec, Canada.
- Flynn NE, Comas LH, Stewart CE, Fonte SJ.** 2023. High N availability decreases N uptake and yield under limited water availability in maize. *Scientific report* **13**, 14269
- Gao Y, Lynch JP.** 2016. Reduced crown root number improves water acquisition under water deficit stress in maize (*Zea mays* L.). *Journal of experimental botany* **67**, 4545–4557. <https://doi.org/10.1093/jxb/erw243>
- Griffiths M, Mellor N, Sturrock CJ, et al.** 2022. X-ray CT reveals 4D root system development and lateral root responses to nitrate in soil. *The Plant Phenome Journal* **5**, e20036.
- Guo Y, Chen F, Zhang F, Mi G.** 2005. Auxin transport from shoot to root is involved in the response of lateral root growth to localized supply of nitrate in maize. *Plant Sci* **169**, 894–900. <https://doi.org/10.1016/j.plantsci.2005.06.007>
- Hanjra MA, Qureshi ME.** 2010. Global water crisis and future food security in an era of climate change. *Food policy* **35**, 365–377.

- Jafarikouhini N, Sinclair TR.** 2023. Hydraulic conductance and xylem vessel diameter of young maize roots subjected to sustained water-deficit. *Crop Science* **63**, 2458–2464.
- Jiang Y, Hung CY, Whalen JK.** 2023. Distinctive plasticity of maize (*Zea mays*) root types to variable nitrate concentration. *Canadian Journal of Plant Science* **103**, 319-323. <https://doi.org/10.1139/cjps-2022-0246>
- Kuang N, Ma Y, Hong S, Jiao F, Liu C, Li Q, Han H.** 2021. Simulation of soil moisture dynamics, evapotranspiration, and water drainage of summer maize in response to different depths of subsoiling with RZWQM2. *Agricultural Water Management* **249**, 106794. <https://doi.org/10.1016/j.agwat.2021.106794>
- Lai WL, Wang SQ, Peng CL, Chen CH.** 2011. Root features related to plant growth and nutrient removal of 35 wetland plants. *Water research* **45**, 3941–3950. <https://doi.org/10.1016/j.watres.2011.05.002>
- Lazof DB, Rufty TWJ, Redinbaugh MG.** 1992. Localization of nitrate absorption and translocation within morphological regions of the corn root. *Plant Physiol* **100**, 1251–1258. <https://doi.org/10.1104/pp.100.3.1251>
- Liu Z, Giehl RFH, Hartmann A, Hajirezaei MR, Carpentier S, von Wirén N.** 2020. Seminal and nodal roots of barley differ in anatomy, proteome and nitrate uptake capacity. *Plant and Cell Physiology* **61**, 1297–1308. <https://doi.org/10.1093/pcp/pcaa059>
- Liu XF, Zhang SQ, Shan L.** 2013. Heterosis for water uptake by maize (*Zea mays* L.) roots under water deficit: responses at cellular, single-root and whole-root system levels. *Journal of Arid Land* **5**, 255–265. <https://doi.org/10.1007/s40333-013-0158-y>
- Lobell DB, Schlenker W, Costa-Roberts J.** 2011. Climate trends and global crop production since 1980. *Science* **333**, 616–620.

- Ordóñez RA, Castellano MJ, Danalatos GN, Wright EE, Hatfield JL, Burras L, Archontoulis S V.** 2021. Insufficient and excessive N fertilizer input reduces maize root mass across soil types. *Field Crops Research* **267**, 108142. <https://doi.org/10.1016/j.fcr.2021.108142>
- Parent SÉ, Dossou-Yovo W, Ziadi N, Leblanc M, Tremblay G, Pellerin A, Parent LE.** 2020. Corn response to banded phosphorus fertilizers with or without manure application in Eastern Canadian Journal of Agronomy **112**, 2176–2187. <https://doi.org/10.1002/agj2.20115>
- Postma JA, Lynch JP.** 2011. Root cortical aerenchyma enhances the growth of maize on soils with suboptimal availability of nitrogen, phosphorus, and potassium. *Plant physiology* **156**, 1190–1201. <https://doi.org/10.1104/PP.111.175489>
- Plett DC, Ranathunge K, Melino VJ, Kuya N, Uga Y, Kronzucker HJ.** 2020. The intersection of nitrogen nutrition and water use in plants: new paths toward improved crop productivity. *Journal of experimental botany*, **71**, 4452-4468. <https://doi.org/10.1093/jxb/eraa049>
- Saengwilai P, Nord EA, Chimungu JG, Brown KM, Lynch JP.** 2014. Root cortical aerenchyma enhances nitrogen acquisition from low-nitrogen soils in maize. *Plant Physiology* **166**, 726–735. <https://doi.org/10.1104/pp.114.241711>
- Sandhu S, Ranjan R, Sharda R.** 2023. Root plasticity: an effective selection technique for identification of drought tolerant maize (*Zea mays* L.) inbred lines. *Scientific Reports* **13**, 5501. <https://doi.org/10.1038/s41598-023-31523-w>
- Sobat E, Whalen JK.** 2022. Mycorrhizal colonization associated with roots of field-grown maize does not decline with increasing plant-available phosphorus. *Soil Use Management* **38**, 1370–1379. <https://doi.org/10.1111/sum.12786>

- Stedle E.** 2001. The cohesion-tension mechanism and the acquisition of water by plant roots. Annual review of plant biology **52**, 847–875. <https://doi.org/10.1146/annurev.arplant.52.1.847>
- Strock CF, Burridge JD, Niemiec MD, Brown KM, Lynch JP.** 2021. Root metaxylem and architecture phenotypes integrate to regulate water use under drought stress. Plant, Cell & Environment **44**, 49–67. <https://doi.org/10.1111/pce.13875>
- Saengwilai P, Tian X, Lynch JP.** 2014. Low crown root number enhances nitrogen acquisition from low-nitrogen soils in maize. Plant physiology **166**, 581–589. <https://doi.org/10.1104/pp.113.232603>
- Terman GL.** 1974. Amounts of nutrients supplied for crops grown in pot experiments. Communications in Soil Science and Plant Analysis **5**, 115–121. <https://doi.org/10.1080/00103627409366487>
- Wang Y, Mi G, Chen F, Zhang J, Zhang F.** 2005. Response of root morphology to nitrate supply and its contribution to nitrogen accumulation in maize. Journal of Plant Nutrition **27**, 2189–2202. <https://doi.org/10.1081/PLN-200034683>
- York LM, Silberbush M, Lynch JP.** 2016. Spatiotemporal variation of nitrate uptake kinetics within the maize (*Zea mays* L.) root system is associated with greater nitrate uptake and interactions with architectural phenes. Journal of Experimental Botany **67**, 3763–3775. <https://doi.org/10.1093/jxb/erw133>
- Yu P, Hochholdinger F, Li C.** 2015. Root-type-specific plasticity in response to localized high nitrate supply in maize (*Zea mays*). Annals of Botany **116**, 751–762.

FORWARD TO CHAPTER 4

Chapter 3 reported greater plasticity of maize root growth in wetter soil than drier soil conditions. The reduction in root hydraulic conductance resulted in less N uptake in the dry soil. However, questions persist regarding how maize roots acquire N under varying soil moisture conditions. The objective of Chapter 4 is to distinguish the relative importance of embryonic and crown roots of maize in acquiring NO_3^- from both drier and wetter soil conditions. To achieve the objective, I used ^{15}N stable isotope tracing to calculate N uptake by embryonic and crown root types under two contrasting water conditions (-5 kPa and -30 kPa), tracking growth until the V3 and V6 stages, employing a customized split-root system.

CHAPTER 4

Water-conducting roots responsible for nitrogen uptake in maize (*Zea mays*)

Yutong Jiang¹, Joann K. Whalen^{1*}

Address: ¹Department of Natural Resource Sciences, Macdonald Campus of McGill University,
21111 5 Lakeshore Road, Ste-Anne-de-Bellevue, Quebec, Canada H9X 3V9

Corresponding author: Joann K. Whalen, joann.whalen@mcgill.ca, tel: 001-514-398-7943

4.1 Abstract

Nitrate (NO_3^-) uptake, primarily driven by mass flow, varies among maize root types. Yet, the relative importance of embryonic and crown roots in acquiring NO_3^- and nitrification around these root types was determined in wet and dry soil conditions. Maize was grown in a split-root pot that segregated the embryonic roots and crown roots and maintained at water potential of -5kPa or -30kPa. A partial N mass balance was made by destructively sampling shoots, roots, and soils after 0, 24 and 48 h following $^{15}\text{N-KNO}_3$ injection at the V3 and V6 stages. Gross nitrification was assessed using a ^{15}N isotope dilution technique. At the V3 stage, crown roots had a 202% more N uptake than embryonic roots in wet soil (-5 kPa). In dry soil (-30kPa), N uptake was similar for embryonic and crown roots, possibly due to 80% reduction of hydraulic conductance in crown roots. By the V6 stage, crown roots dominated N uptake, with embryonic roots supplying <20% of the N uptake. Soil gross nitrification rate was similar across the root types. We conclude that maize NO_3^- uptake depends primarily on the crown root system, due to its capacity to extract water and NO_3^- from soil, even under dry conditions.

Keywords: Embryonic roots, N stable isotope, Root hydraulic conductance, Split-root system

4.2 Introduction

Maize (*Zea mays*) requires nitrogen (N) to produce chlorophyll and protein for maximum growth and to reach its yield potential. Maize acquires more than 90% of its N supply through mass flow, primarily in the form of nitrate (NO_3^- , Barber 1962; McMurtrie and Näsholm 2018). Transpiration is responsible for NO_3^- movement in water that flows from soil into the roots and thereafter in xylem vessels that connect the root system to the leaf surface. Continuous water flow creates tension in the xylem, producing a water gradient that draws water and associated solutes, including mobile NO_3^- ions. However, the root hydraulic conductance cannot transfer NO_3^- effectively from dry soil that contains less freely flowing water in its soil pores, which breaks the continuity of water flow between soil pores to leaves. The agricultural soil water deficit is predicted to intensify under future climate (Plett et al. 2020), investigating how maize acquires NO_3^- under such conditions provides information on soil water management to ensure sustainable N uptake.

Maize forms primary and seminal roots during embryogenesis, and crown roots and brace roots during post-embryonic development. Each root type is expected to have a unique capacity to absorb NO_3^- . Shoot-borne crown roots have about 63% more meta- and protoxylem elements and about 200% larger xylem vessels than embryonic primary and seminal roots (Tai et al. 2016; Hazman and Kabil 2022). This anatomical structure translates to a 5-fold higher hydraulic conductance in crown roots, inducing a faster water flow from soil pores to the root xylem (Doussan 1998; Ahmed et al. 2018b). For example, water uptake rate was 1.8 to $2.4 \times 10^{-5} \text{ cm s}^{-1}$ in crown roots and $<5 \times 10^{-8} \text{ cm s}^{-1}$ in seminal roots of a 35-d-old maize (V3 – V4 growth stage, Ahmed et al. 2018b). The higher hydraulic conductance should result in greater NO_3^- uptake by crown roots. In a hydroponic environment, crown roots had 22% higher maximum NO_3^- influx rate than seminal roots of a 20-d-old maize (V2 – V3 stage, York et al. 2016). This suggests that

crown roots should be responsible for NO_3^- uptake in the early vegetative growth (~V3 growth stage) of maize, but it should be confirmed for a soil environment. Furthermore, if N uptake varies among the root types, then soil N transformations may vary around embryonic and crown roots due to potential differences in soil pH and the associated microbial community within adjacent soil. Currently, we are not aware of any studies that have attempted to assess the spatial variability of gross nitrification surrounding the maize root system.

Dry soil conditions are characterized by less flow of water and solutes, including NO_3^- , to root surfaces. As soil dries, there was a 50% reduction in the hydraulic conductance of crown roots, but the hydraulic conductance of primary and seminal roots did not change 4 wk after exposure to water deficit (Hazman and Kabil, 2022). Recent research has revealed that the hydraulic conductance of both seminal and primary roots immediately decreased when exposed to mild water deficit, followed by full recovery in seminal roots and a 60% recovery in primary roots after 4 d of prolonged water deficit (Protto et al. 2024). The area of xylem vessels in crown roots decreased up to 80%, while there was no change in the xylem area of primary roots (Jafarikouhini and Sinclair, 2023; Hazman and Kabil, 2022). In addition, root may shrink and form the airgaps under water-deficit, which limits water flow between root-soil interfaces (Carminati et al. 2013). Crown roots may suffer from more shrinkage than the seminal roots due to their 10 – 40 % thicker diameter and about 30% additional cortex cell layer (Tai et al. 2016). Consequently, it is possible that embryonic roots acquire more NO_3^- than crown roots during the early vegetative growth stage under water deficit.

The objective of this study is to quantify NO_3^- uptake rates by embryonic roots versus crown roots at V3 and V6 growth stages under two contrasting soil water conditions ($\Psi_{\text{soil}} = -5$ and -30 kPa) using a customized split-root system combined with the ^{15}N isotope technique. We

hypothesized that crown roots have a higher NO_3^- uptake rate than embryonic roots in relatively wet soil ($\Psi_{\text{soil}} = -5$ kPa) at both V3 and V6 growth stages due to their higher hydraulic conductance. However, in relatively dry soil ($\Psi_{\text{soil}} = -30$ kPa), we expect that embryonic roots acquire more NO_3^- than crown roots at V3 growth stage because crown roots have decreased hydraulic conductance when exposed to the dry soil. We also expect a higher nitrification around crown roots than embryonic roots in the relatively wet soil.

4.3 Materials and methods

4.3.1 Soil and maize

Soil (0–15 cm) was collected from the Emile A. Lods Agronomy Research Centre in Sainte-Anne-de-Bellevue, Québec (45°25'N, 73°55'W, 39 m elevation) in October 2022 following maize harvest. The soil is a sandy-loam Humic Gleysol of the St. Amable series containing 620 g sand kg^{-1} , 60 g clay kg^{-1} and 48 g organic C kg^{-1} , with pH 6.3. Soil (sieved < 6 mm) was pre-mixed with urea (46-0-0), triple superphosphate (0-46-0) and potassium chloride (0-0-60) at rates of 17 mg N kg^{-1} , 27 mg P_2O_5 kg^{-1} plus 17 mg K_2O kg^{-1} soil. The maize variety was *Zea mays* L. cv. PS2790, not genetically modified and not treated with fungicide or insecticide.

4.3.2 Split-root pot design

The split-root pot was designed to segregate the embryonic root system (i.e., primary and seminal roots) from the crown roots (Fig. S3. 1). An inner chamber (PVC pipe with 5 cm diameter, 25 cm height) was placed in the middle of the outer chamber (PVC pipe with 10 cm diameter, 30 cm height). Field-moist soil was packed into the inner chamber (0.54 kg dry weight basis) and the outer chamber (2.05 kg dry weight basis), with a constant bulk density of 1100 kg m^{-3} . An aluminum foil cone (3 cm height) was placed on top of the inner chamber. There was a small hole

(0.5 cm dia.) on the top of the cone, allowing the primary and seminal roots (i.e., the embryonic roots) to grow through the hole into the inner chamber, while the crown roots are directed to grow in the outer chamber. There was no drainage in the split-root pot to avoid water and soluble nutrient losses by leaching.

4.3.3 Experimental treatments

The experiment was a two-way factorial designed to evaluate the N acquisition by maize as influenced by soil moisture (-5 kPa or -30 kPa, measured as soil water potential, Ψ_{soil}) and the maize root type (embryonic roots or crown root), with four replicates per treatment. The maize root types were separated spatially within the split-root pot, and each pot was considered to be a replicate in the experiment. Soil water potential was monitored in 8 additional split-root pots at 2 water levels (n=4 for each water level) with tensiometers (MLT, Irrrometer Inc., Riverside, California, US) inserted into the inner chamber and the outer chamber (Fig. S4. 2). We confirmed that the maize root growth was similar in a split-root pot as a regular pot by growing maize in 8 pots (2 water levels \times 4 replicates) that were PVC pipe (10 cm diameter, 30 cm height) containing 2.4 kg soil (dry weight basis) and no inner chamber (Fig. S4. 3).

Maize seeds were pre-germinated in pots (12.7 cm dia., 15 cm depth) for 10 d before transplanting to the split-root pots. Embryonic roots emerged within 10 d after seeding, but crown roots did not. Thus, embryonic roots were manually introduced to the inner chamber through the small hole on the aluminum foil cone, while the crown roots were emerged 3 – 5 d later and naturally grew into the outer chamber. All pots were placed in a growth bench with a fluorescent lightening system ($400 \mu\text{mol}^{-2} \text{s}^{-1}$ of photon flux density) with controlled light and temperature of 16 h light ($25 \pm 2^\circ\text{C}$) and 8 h dark ($18 \pm 1^\circ\text{C}$). Distilled water was added every 2 d by a syringe

with a long needle (12 cm, HaBeuniver Inc., Fuzhou, Fujian, China) to maintain the soil water potential at target levels ($\Psi_{\text{soil}} = -5$ or -30 kPa) according to the average tensiometer readings in the 8 monitoring pots.

At the V3 and V6 growth stages, N acquisition by each maize root type was evaluated using ^{15}N -labeled KNO_3 . When maize had 3 fully-formed leaves (V3), we injected KNO_3 solution (0.33 g N L^{-1} , 18.4% atom ^{15}N excess) either in the inner (26 mL) or the outer chamber (112 mL) of the pots, targeting at $\Psi_{\text{soil}} = -5$ kPa. We injected KNO_3 solution (0.67 g N L^{-1} , 18.7% atom ^{15}N excess) either in the inner (13 mL) or the outer chamber (56 mL) of the pots that targeted at $\Psi_{\text{soil}} = -30$ kPa to deliver 0.02 g N kg^{-1} soil. We injected non-labeled KNO_3 solution (0.33 g N L^{-1} or 0.67 g N L^{-1}) into the chamber that was not exposed to the ^{15}N - KNO_3 solution, so the total N input was the same for the inner and outer chambers of each pot. Controlled pots were handled identically except that both inner and outer chambers received non-labeled KNO_3 solution to establish the ^{15}N natural abundance in maize. Pots ($n = 56$) were destructively sampled 0, 24 and 48 h post-labeling. The pots that were kept until the V6 stage ($n = 56$) received ^{14}N - KNO_3 in inner and outer chambers at the V3 stage. At the V6 growth stage, these pots were labeled and sampled following the procedure described for the V3 growth stage.

4.3.4 Plant sampling and analysis

Following exposure to ^{15}N - KNO_3 , pots were destructively sampled by cutting maize stems at the soil surface, then shoots were rinsed, dried (55°C for 72 h) and ground ($<1 \text{ mm}$). Roots were removed from the soil by gently shaking and rubbing off most of the root-associated soil. A single crown root, seminal root, and primary root from each pot was immediately removed under the deionized water for root hydraulic conductance analysis. The rest of roots were washed thoroughly

with deionized water to remove the attached soil particles, and then rinsed with 1 mM CaSO₄ to remove apoplastic ¹⁵N, stored in a refrigerator at 4°C for up to 7 d, while the following analysis were underway.

Root hydraulic conductance was measured within 1 h of sampling by the root exudation method (Knipfer et al. 2010). The single primary root, seminal root, and crown root were connected to the glass microcapillary tube (0.3-, 0.5- or 1-mm diameter). Then, the roots sampled from pots with $\Psi_{\text{soil}} = -5$ or -30 kPa were bathed in 0.069 or 4 g L⁻¹ sucrose solution. The movement of exudate in the capillary was recorded every 15 min for 3 h and the water flow rate (mm³ min⁻¹) was the slope of linear part of the flow vs time plot. After 3 h, the exudate was collected from the capillary tube with a syringe needle. The osmotic pressure of the bath medium (ψ_{medium} , MPa) and the xylem exudates (ψ_{xylem} , MPa) were determined by measuring the osmolality using a vapor pressure osmometer (Model 5520, Wescor Vapro, Utah, the United States). The surface area (m²) and length (m) of the single root used for hydraulic conductance measurement was determined by a Photo scanner (V700, Epson Inc., Markham, Canada) and WinRhizo software (Regent Instruments, Quebec, Canada). The root hydraulic conductance (m³ s⁻¹ MPa⁻¹) was calculated as:

$$\text{Root hydraulic conductance} = \frac{\text{Water flow rate} \times 10^{-9} \div 60}{(\psi_{\text{xylem}} - \psi_{\text{medium}})} \times \frac{\text{Surface area of total roots}}{\text{Surface area of single roots}} \quad (1)$$

Hand cross-section of tip (0 – 20 mm from root tip), mid (50 – 70 mm from root tip), base (0 – 20 mm from root base) of crown root, seminal root, and primary root was prepared for anatomical analysis. Root segments were fixed in 4% paraformaldehyde in 1× phosphate buffer saline solution while shaking (3 h, 22°C), and washed 3 times (30 min, 22°C) in 1× phosphate buffer saline solution. The root segments were thin sectioned, stained by 0.1% Toluidine Blue O and washed by 1× phosphate buffer saline solution before sealing with a cover slip. Root anatomy

images were taken with light microscopy (ZEISS imager Z1, Germany) with $\times 10$ magnification. Xylem area, number, diameter, stele area, and cross-section area were analyzed by ImageJ (version Fiji for Mac OS X, U. S. National Institutes of Health, Bethesda, Maryland, USA). The cortex area was calculated by subtraction the stele area from the cross-section area. The axial hydraulic conductance of tip (0 – 20 mm from root tip), mid (50 – 70 mm from root tip), base (0 – 20 mm from root base) segments was calculated by Hagen-Poiseuille Law (Strock et al., 2021):

$$k = \frac{\pi\rho}{128\eta} \sum_{i=1}^n (d_i^4) \quad (2)$$

where ρ is the xylem sap fluid density assumed to be water (1000 kg m^{-3} , at 20°C), and η is the viscosity of the xylem sap assumed to be water ($1 \times 10^{-9} \text{ MPa s}$, at 20°C), d is the mean diameter of each metaxylem vessel (m).

Morphological traits (length and surface area) of primary, seminal, and crown roots were measured by WinRhizo software. Total root length and total surface area also included the excised roots subsampled for root hydraulic and anatomy measurements. The length and surface area of lateral roots was assumed to be the sum of the fine roots with a diameter $< 0.5 \text{ mm}$ measured in WinRhizo software.

Shoots, embryonic roots and crown roots were oven-dried (55°C for 48 h), weighed (dry mass), ground ($< 1 \text{ mm}$). N content and ^{15}N excess (%) of shoot ($[APE]_{shoot}$), primary root ($[APE]_{primary}$), seminal root ($[APE]_{seminal}$), and crown root ($[APE]_{crown}$) was measured in shoot, primary root, seminal root and crown root tissue (2 – 5 mg) on an isotope ratio mass spectrometer at the UC Davis Stable Isotope Facility (Davis, CA, USA). N uptake rate (mg d^{-1}) was calculated following Barraclough (1996):

$$N \text{ uptake} = N_{shoot} \times \frac{[APE]_{shoot}}{[APE]_{KNO_3}} + N_{primary} \times \frac{[APE]_{primary}}{[APE]_{KNO_3}} + N_{seminal} \times \frac{[APE]_{seminal}}{[APE]_{KNO_3}} + N_{crown} \times \frac{[APE]_{crown}}{[APE]_{KNO_3}}$$

(3)

4.3.5 Soil sampling and analysis

Soil from the inner chamber and the outer chamber was removed separately and stored at 4 °C for up to 7 d until analysis. Soil NH₄⁺ and NO₃⁻ concentrations were analyzed in extracts from 20 g soil (1:4 soil: 0.5M K₂SO₄ solution) and measured calorimetrically at 650 nm on a μQuant microplate reader (BioTek, Winooski, VT, USA) following Sims et al. (1995). The ¹⁵N enrichment of NH₄⁺ and NO₃⁻ pools was determined by acid diffusion procedure according to Brooks et al. (1989), with >90% recovery of NH₄⁺ and NO₃⁻ from the extracts based on internal standard analysis. Acidified (15 μL of 2.5 M KHSO₄) glass filter paper disks (5 mm, Whatman GF/D, pre-ashed at 500 °C for 4 h) were sealed in Teflon tape (2 disks per Teflon packet). To attain the required 20 – 50 μg N in solution, considering the low NH₄⁺ concentration (<2 mg NH₄⁺ kg⁻¹) in soil extracts, we spiked 10 mL of soil extract with 10 mL ¹⁵N-(NH₄)₂SO₄ (4 mg N L⁻¹, 4.2 atom% excess ¹⁵N) in a 120-mL specimen cup prior to the diffusion procedure. The ¹⁵N enrichment of NO₃⁻ pool was evaluated after diluting the soil extract with 10 mL of 0.5M K₂SO₄ in a separate 120-mL specimen cup. Diffusion began after adding one Teflon packet and 0.1 g MgO (for ¹⁵N-NH₄) or one Teflon packet, 0.1 g MgO, and 0.4 g Devarda's alloy (for ¹⁵N-NO₃) and capping the specimen cup. Correction of the background ¹⁵N concentration and ¹⁵N recovery was done by including blanks (K₂SO₄) and spiking solution (¹⁵N-(NH₄)₂SO₄) with the same procedure. Specimen cups were mixed gently by hand twice a day for 7 d to ensure the MgO and Devarda's alloy reaction with the solution. After 7 d, filter paper disks were removed from the Teflon packet, dried over concentrated H₂SO₄ in a desiccator for about 48 h, and packaged into tin capsules for

isotopic enrichment $[APE]_{sample}$ determination on a Micro Cube elemental analyzer (Elementar Analysensysteme GmbH, Hanau, Germany) interfaced to a PDZ Europa 20-20 isotope ratio mass spectrometer (Sercon Ltd., Cheshire, UK) at the UC Davis Stable Isotope Facility.

4.3.6 Nitrogen calculations

The atom% ^{15}N in the $\text{NH}_4\text{-N}$ pool was:

$$[APE]_{sample} \times (N_{extract} + N_{spike}) = (N_{extract} \times [APE]_{NH_4}) + (N_{spike} \times [APE]_{spike}) \quad (4)$$

where $[APE]_{sample}$ is the atom% ^{15}N measured from the diffusion disks, $N_{extract}$ is the amount of $\text{NH}_4\text{-N}$ (μg) in soil extracts, $[APE]_{spike}$ is the atom% ^{15}N measured from the diffusion disks from the spike solution, and N_{spike} is the amount of $\text{NH}_4\text{-N}$ (μg) in the spike (Whalen et al., 2021). The unknown in the equation is $[APE]_{NH_4}$, the atom% ^{15}N in the $\text{NH}_4\text{-N}$ pool of soil extracts. Similarly, atom% ^{15}N in the $\text{NO}_3\text{-N}$ pool was calculated as:

$$[APE]_{sample} \times (N_{NH_4} + N_{NO_3} + N_{K_2SO_4}) = (N_{NH_4} \times [APE]_{NH_4}) + (N_{K_2SO_4} \times [APE]_{K_2SO_4}) + (N_{NO_3} \times [APE]_{NO_3}) \quad (5)$$

where N_{NO_3} is the amount of $\text{NO}_3\text{-N}$ (μg) in soil extracts, $N_{K_2SO_4}$ is the amount of N in the blank solution, and $[APE]_{K_2SO_4}$ is the atom% ^{15}N measured from the diffusion disks from the blank solution. The unknown in the equation is $[APE]_{NO_3}$, the atom% ^{15}N in the $\text{NO}_3\text{-N}$ pool of soil extracts.

Gross nitrification rate ($\text{mg of N kg}^{-1} \text{ soil d}^{-1}$) was calculated (Kirkham & Bartholomew, 1954):

$$\text{Gross nitrification} = \frac{[NO_3]_{t1} - [NO_3]_{t2}}{t_2 - t_1} \times \frac{\log([APE]_{NO_3-t1}/[APE]_{NO_3-t2})}{\log([NO_3]_{t1}/[NO_3]_{t2})} \quad (6)$$

Where $[NO_3]_{t1}$ and $[NO_3]_{t2}$ indicate total NO_3^- concentration ($mg\ N\ kg^{-1}$) at time 1 and time 2, $[APE]_{NO_3-t1}$ and $[APE]_{NO_3-t2}$ indicate atom% ^{15}N excess of NO_3^- pool at time 1 and time 2.

4.3.7 Statistical analyses

Data was normally distributed (Shapiro-Wilk test, $P > 0.05$) with homogeneous variance (Levene's test, $P > 0.05$). Analysis of variance revealed no effect ($p > 0.05$) of sampling time (0, 24 and 48 h post-labeling) on several dependent variables (root length, root hydraulic conductance). Thus, data were pooled among sampling times, which gave more replicates for root morphological measurement ($n = 20$, Fig.4. 1) and root hydraulic measurement ($n = 12$, Fig.4. 2) for each treatment. The main and interactive effects of root types and soil water potential were evaluated by analysis of variance. When the main effects or interactive effects were significant ($p < 0.05$), mean values were compared with Tukey's honestly significant test. The xylem number, xylem area and calculated hydraulic conductance under two water potential was compared by Student's t-test. Correlation with Pearson coefficient was used to describe the best-fit lines of the relationship between root hydraulic conductance of each root types and N uptake (R 3.6.1).

4.4 Results

4.4.1 Root morphology of primary, seminal and crown roots

By the V3 growth stage, crown roots emerged as the predominant root type, constituting 65–72% of total axial roots. When exposed to the wet soil ($\Psi_{soil} = -5kPa$), lateral roots were 2 – 3 times greater on the crown than on the primary and seminal roots (Fig. 4. 1c). However, in dry soil ($\Psi_{soil} = -30kPa$), all root types produced similar length and surface area of lateral roots ($p > 0.05$,

Fig. 4. 1c, e). At the V6 stage, the crown root system, comprising 1st and 2nd whorl crown roots, constituted 73–84% of axial root length and 68–81% of lateral root length. Lateral surface area was 300 – 328% greater for crown roots than embryonic roots, regardless of soil water potential. When exposed to dry soil, the 2nd whorl crown roots produced 58% shorter axial roots and 57% less lateral root surface than grown in the wet soil.

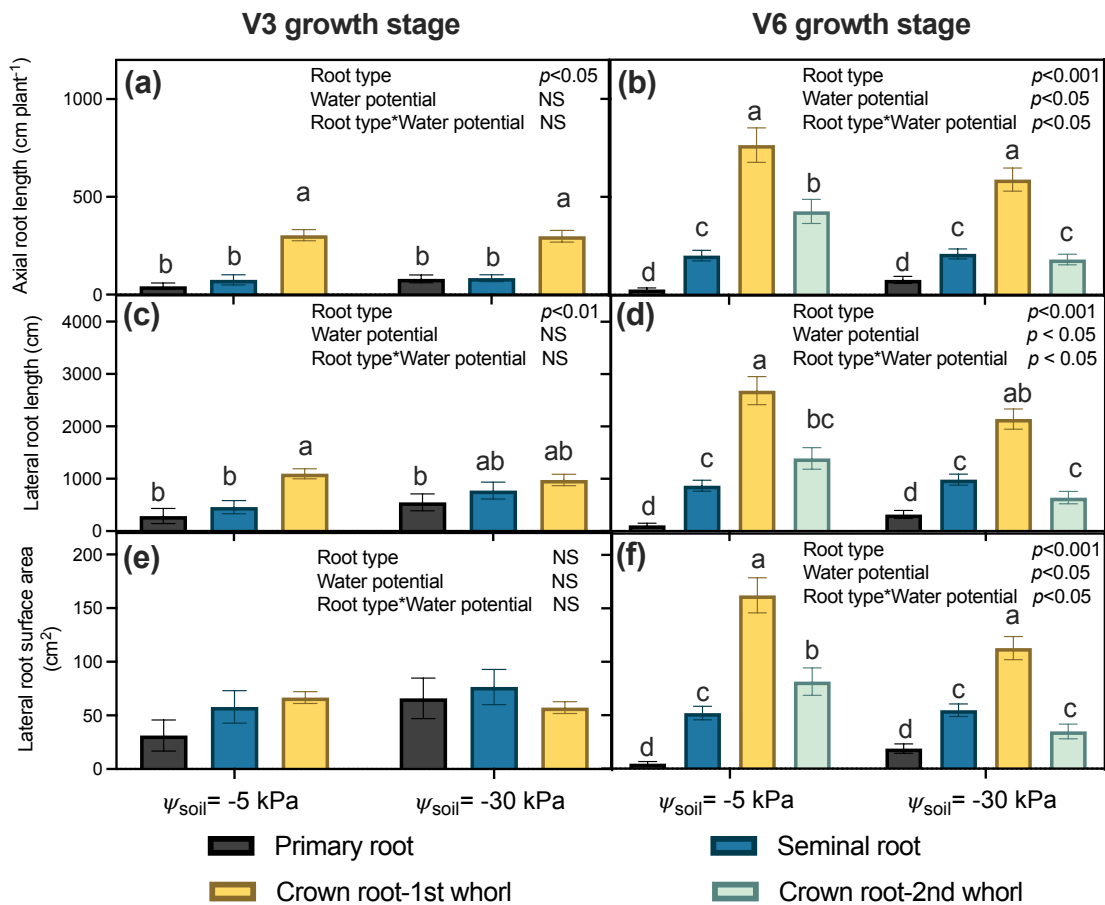


Fig. 4. 1 Root morphological traits, including axial root length (a, b), lateral root length (c, d), lateral root surface area (e, f) of maize grown in the split-root system to the V3 or V6 stages. Maize was grown in pots kept at a constant water potential (-5kPa or -30kPa). Data was pooled among N tracer treatments, and plants with the same water potential were pooled together (n = 20). Different

letters over the bars represent significant differences ($p < 0.05$, Tukey's honestly significant test). NS, not significant ($p > 0.05$).

4.4.2 Hydraulic conductance of crown roots declined in dry soil

At V3 growth stage, crown roots had 22% more xylem vessels and 56 – 120% larger xylem area than primary roots, and 75% more xylem vessels and 84 – 300% larger xylem area than seminal roots in wet soil (Table 4. 1). The larger xylem vessel area was associated with the 80 – 600 % greater calculated axial hydraulic conductance along the crown roots than along the primary and seminal roots. Dry soil had 1st whorl crown roots with 35% less xylem area at the root tip, leading to 46% lower axial hydraulic conductance at this region. In contrast, the axial hydraulic conductance was similar in primary and seminal roots growing in the dry soil ($p > 0.05$). At V6 stage, primary and seminal roots contributed < 5% of axial hydraulic conductance, regardless of soil water condition. The 1st and 2nd whorl crown roots had 16 – 45 times more calculated axial hydraulic conductance than primary and seminal roots. The 2nd whorl crown roots had 13% reduced xylem area and 25% reduced axial hydraulic conductance at the root tip region.

Measured root hydraulic conductance revealed a consistent pattern among different root types (Fig. 4. 2). At the V3 stage, crown roots had 10-times more hydraulic conductance than primary and seminal roots in wet soil. However, since root hydraulic conductance interacts with soil water potential (Root type \times Water potential effects, $p = 0.03$), the hydraulic conductance of crown roots decreased by 83% in dry soil. There was a similar hydraulic conductance in crown, primary and seminal roots in the dry soil. By the V6 stage, 1st and 2nd whorl crown roots dominated, contributing 90% of water-conducting capacity, despite a 37% reduction in 2nd-whorl crown root hydraulic conductance in dry soil.

Table 4. 1 Xylem number, xylem area, and calculated axial hydraulic conductance, determined from three segments (tip: 0–20 mm from root tip, mid: 40–60 mm from root tip, base: 0–20 mm from the base of the stem) of a representative thin-sectioned axial root for each type (primary, seminal and crown, 1st and 2nd whorls) of maize grown to the V3 or V6 stages in a split-root system. The split-root system was kept at a constant water potential (-5kPa or -30kPa). Values are the mean \pm standard error, n= 4. Different letters in the same column indicate significant differences among the same region of each root type within the same growth stage. Asterisks (*) indicate significant differences among water potential treatments of each root type within the same growth stage.

Axial root type	Root Segment	Xylem number		Xylem area (μm^2) $\times 10^4$		Calculated hydraulic conductance ($\text{kg m Mpa}^{-1} \text{s}^{-1}$) $\times 10^{-6}$		
		-5 kPa	-30 kPa	-5 kPa	-30 kPa	-5 kPa	-30 kPa	
V3	Primary	Tip	6 \pm 1 ^b	5 \pm 0 ^b	1.13 \pm 0.13 ^b	1.57 \pm 0.15 ^a	0.85 \pm 0.11 ^b	2.08 \pm 0.50 ^b
		Mid	6 \pm 1 ^b	6 \pm 1 ^b	1.66 \pm 0.01 ^b	1.73 \pm 0.18 ^a	1.89 \pm 0.20 ^b	2.31 \pm 0.61 ^a
		Base	6 \pm 1 ^b	6 \pm 0 ^b	2.16 \pm 0.40 ^a	1.29 \pm 0.39 ^a	3.26 \pm 1.08 ^a	1.50 \pm 0.95 ^a
	Seminal	Tip	5 \pm 0 ^b	4 \pm 0 ^c	1.35 \pm 0.12 ^b	0.86 \pm 0 ^b	1.56 \pm 0.26 ^b	0.77 \pm 0 ^b
		Mid	4 \pm 0 ^c	4 \pm 0 ^c	1.28 \pm 0.11 ^b	1.14 \pm 0.18 ^b	1.61 \pm 0.26 ^b	1.34 \pm 0.38 ^b
		Base	4 \pm 0 ^c	4 \pm 0 ^c	0.85 \pm 0.23 ^b	0.99 \pm 0.13 ^b	0.85 \pm 0.40 ^b	1.17 \pm 0.17 ^b

	Crown (1 st whorl)	Tip	8 ± 0 ^a	7 ± 1 ^a	2.49 ± 0.13 ^a	1.62 ± 0.12 ^{a*}	3.4 ± 0.48 ^a	1.85 ± 0.35 ^{a*}
		Mid	6 ± 1 ^b	6 ± 1 ^b	2.92 ± 0.75 ^a	2.33 ± 0.28 ^a	6.0 ± 2.7 ^a	3.44 ± 0.42 ^a
		Base	9 ± 1 ^a	7 ± 1 ^a	3.38 ± 0.39 ^a	2.49 ± 0.28 ^a	5.9 ± 1.1 ^a	3.97 ± 0.72 ^a
V6	Primary	Tip	6 ± 0 ^b	6 ± 0 ^b	1.56 ± 0.12 ^b	1.53 ± 0.24 ^b	1.6 ± 0.2 ^b	1.90 ± 0.58 ^b
		Mid	6 ± 0 ^b	6 ± 0 ^b	1.51 ± 0.19 ^b	1.24 ± 0.03 ^b	1.6 ± 0.41 ^b	1.13 ± 0.05 ^b
		Base	6 ± 1 ^{bc}	6 ± 0 ^b	1.26 ± 0.26 ^b	1.20 ± 0.13 ^b	1.02 ± 0.27 ^b	1.07 ± 0.20 ^b
	Seminal	Tip	4 ± 0 ^c	5 ± 0 ^c	1.07 ± 0 ^c	0.88 ± 0.18 ^b	1.43 ± 0 ^c	0.71 ± 0.26 ^b
		Mid	4 ± 0 ^c	4 ± 0 ^c	0.55 ± 0.19 ^b	0.66 ± 0.07 ^b	0.46 ± 0.23 ^b	0.44 ± 0.09 ^b
		Base	4 ± 0 ^c	5 ± 0 ^c	0.53 ± 0.22 ^b	0.58 ± 0.11 ^b	0.45 ± 0.33 ^b	0.32 ± 0.10 ^b
	Crown (1 st whorl)	Tip	10 ± 1 ^a	8 ± 1 ^a	8.77 ± 0.52 ^a	4.55 ± 1.92 ^{ab}	23.8 ± 4.6 ^a	13.1 ± 6.48 ^{ab}
		Mid	10 ± 2 ^a	10 ± 1 ^a	7.20 ± 1.90 ^a	6.08 ± 1.02 ^a	22.4 ± 7.7 ^a	16.9 ± 4.6 ^a
		Base	10 ± 1 ^a	10 ± 2 ^a	6.63 ± 1.52 ^a	6.07 ± 1.33 ^a	18.8 ± 5.9 ^a	15.7 ± 4.4 ^a
	Crown (2 nd whorl)	Tip	12 ± 1 ^a	12 ± 1 ^a	8.61 ± 0.28 ^a	7.53 ± 0.05 ^{a*}	26.5 ± 2.9 ^a	19.9 ± 1.3 ^{a*}
		Mid	12 ± 0 ^a	11 ± 0 ^a	8.44 ± 0.71 ^a	8.12 ± 0.23 ^a	25.2 ± 3.1 ^a	23.5 ± 1.6 ^a
		Base	12 ± 1 ^a	11 ± 1 ^a	8.93 ± 0.94 ^a	8.70 ± 0.44 ^a	28.3 ± 5.1 ^a	27.4 ± 1.9 ^a

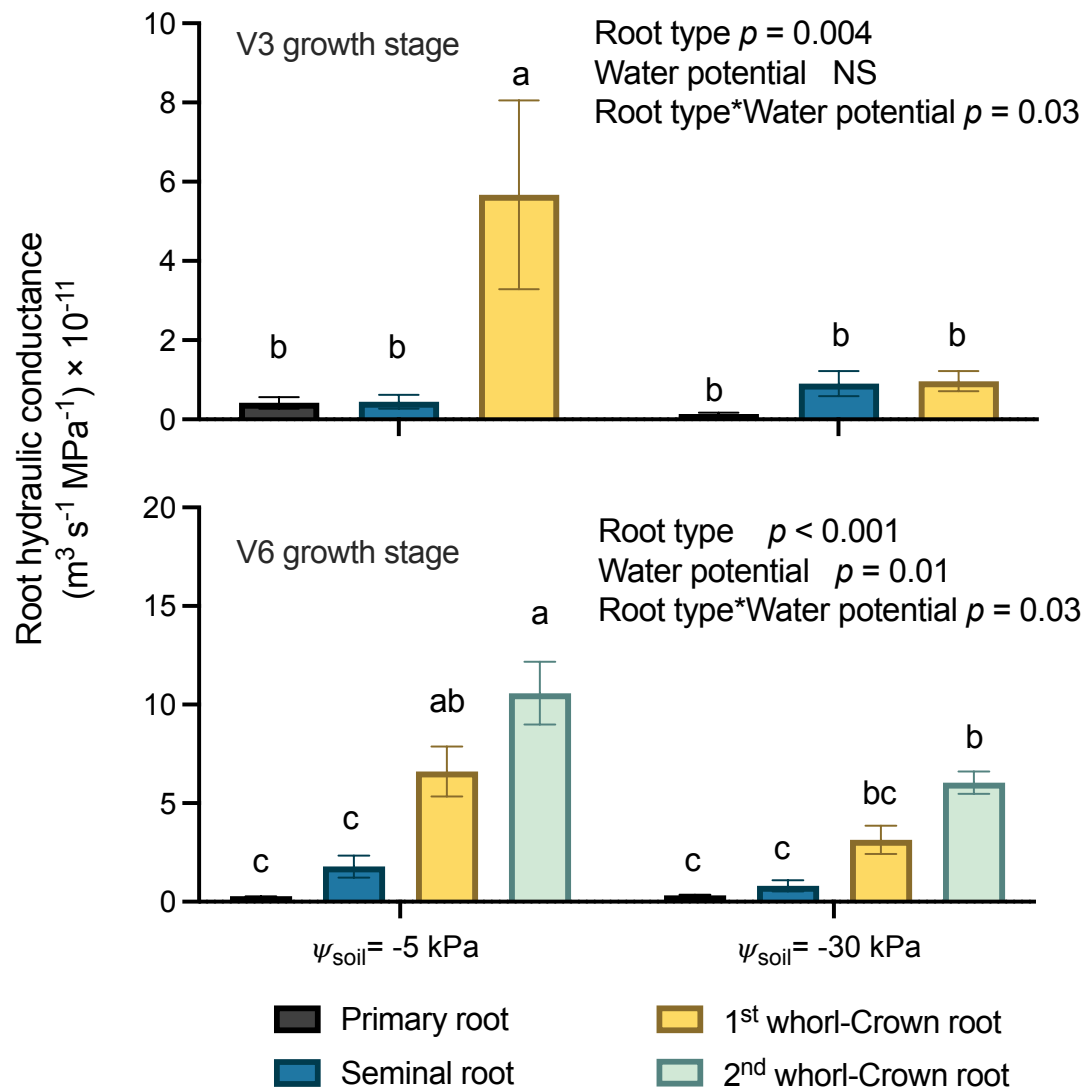


Fig. 4. 2 Measured hydraulic conductance of maize grown in the split-root system until the V3 (a) and V6 stages (b). Maize was grown in pots kept at a constant water potential (-5kPa or -30kPa). Hydraulic conductance was determined with the root exudation method, with one primary, seminal, 1st whorl crown root, and 2nd whorl crown root collected from each of the 12 individual plants grown under one water potential for analysis (n = 12). Error bars represent standard error of means. Different letters over the bars represent significantly differences ($p < 0.05$, Tukey's honestly significant test). NS, not significant ($p > 0.05$).

4.4.3 Crown roots responsible for N uptake, with help from embryonic roots in dry soil

Between 80% to 112% of the ^{15}N was recovered in the soil, shoot, and root pools from 0, 24, and 48 h after injection of the ^{15}N - KNO_3 solution at V3. Similarly, between 83% to 118% of the ^{15}N was recovered in the soil, shoot, and root pools up to 48 h after injection of the labeled solution at V6 (Table 4. 2). Maize shoot and root biomass was progressively enriched with ^{15}N in the hours after injection of the ^{15}N tracer (Fig. S4. 4). At the V3 growth stage, N uptake by crown roots was 2.7-fold higher than embryonic roots in the wet soil (Fig. 4. 3). However, in the dry soil, the N uptake rate was similar in crown and embryotic roots ($p > 0.05$), with embryonic roots supplying 38% of N uptake. By the V6 stage, the crown root system was the dominant pathway for N uptake that was responsible for about 80% of N uptake by maize growing in wet and dry soils.

Table 4. 2 Percentage of ^{15}N from added $^{15}\text{NO}_3\text{-N}$ in maize shoot, roots, and soil after 0, 24 and 48 h of exposure to ^{15}N enrichment. Maize was grown in split-root system with a constant water potential (-5kPa or -30kPa). At V3 and V6 stages, one of the chambers, either the inner or outer, received an injection of $^{15}\text{N-KNO}_3$ solution (18.4% atom ^{15}N excess), while the other chamber received $^{14}\text{N-KNO}_3$ solution, ensuring exposure of only one root type (either the embryonic seminal and primary roots, or the crown roots) to $^{15}\text{N-KNO}_3$ solution. Data are the mean \pm standard errors; n = 4.

Stage	Ψ_{soil} (kPa)	Chamber ^a	Time (h)	Shoots (%)	Crown roots (%)	Seminal roots (%)	Primary roots (%)	Soil (%)	^{15}N recovery (%)
V3	-5	-	0	0	0	0	0	94 \pm 4	94 \pm 4
	-30	-	0	0	0	0	0	97 \pm 17	94 \pm 17
	-5	Inner	24	12 \pm 2	2.1 \pm 0.4	0.1 \pm 0	0.1	66 \pm 7	80 \pm 6
	-30	Inner	24	13 \pm 4	2 \pm 0.2	0.5 \pm 0.1	0.5 \pm 0.1	71 \pm 14	88 \pm 12
	-5	Outer	24	6 \pm 1	0.5 \pm 0	0	0.1	88 \pm 16	95 \pm 15
	-30	Outer	24	4 \pm 1	0.4 \pm 0	0	0.1 \pm 0.1	100 \pm 18	105 \pm 18
	-5	Inner	48	40 \pm 7	5 \pm 1	0.4 \pm 0.2	0.1 \pm 0.1	66 \pm 12	112 \pm 16
	-30	Inner	48	20 \pm 5	2 \pm 1	0.9 \pm 0.3	0.2 \pm 0.1	70 \pm 24	93 \pm 20
	-5	Outer	48	23 \pm 7	0.6 \pm 0	0.4 \pm 0.2	0	80 \pm 26	104 \pm 22

V6	-30	Outer	48	7 ± 1	1 ± 0	0.1 ± 0.1	0.1	103 ± 11	112 ± 10
	-5	-	0	0	0	0	0	87 ± 4	87 ± 4
	-30	-	0	0	0	0	0	110 ± 13	110 ± 13
	-5	Inner	24	89 ± 5	9 ± 2	0 ± 0	0.3 ± 0.2	18 ± 4	116 ± 6
	-30	Inner	24	45 ± 7	4 ± 0.4	1 ± 0.5	1.0 ± 0.5	65 ± 5	118 ± 10
	-5	Outer	24	50 ± 5	25 ± 19	0.1 ± 0	0	15 ± 3	100 ± 22
	-30	Outer	24	30 ± 4	3 ± 0	0.1 ± 0	0	73 ± 16	106 ± 13
	-5	Inner	48	105 ± 3	8 ± 2	0.6 ± 0.1	0.2 ± 0.1	3 ± 1	116 ± 2
	-30	Inner	48	66 ± 4	5 ± 1	0.7 ± 0.1	0.4 ± 0.1	34 ± 11	105 ± 8
	-5	Outer	48	70 ± 4	7 ± 1	0.1 ± 0	0.1 ± 0.1	4 ± 2	83 ± 4
-30	Outer	48	33 ± 5	3 ± 1	0.3 ± 0.2	0.1 ± 0.1	59 ± 8	95 ± 8	

^a Chamber indicates the ¹⁵N labeling location, either the inner pot or the outer pot of the split-root pot.

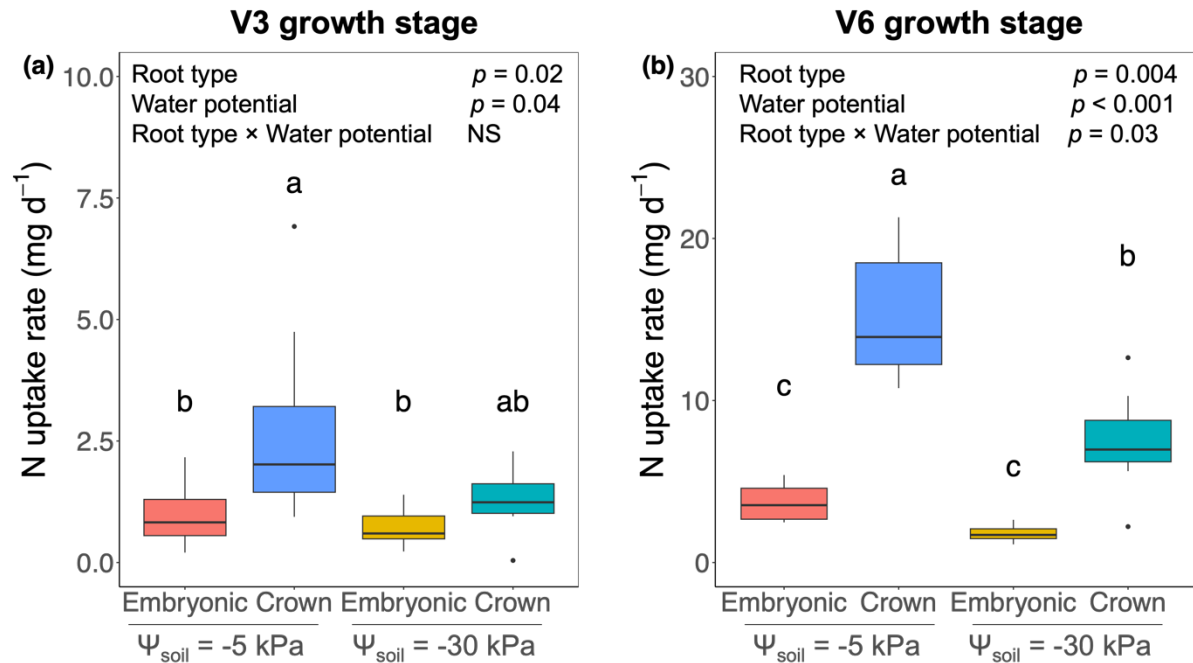


Fig. 4. 3 Nitrogen uptake by embryonic roots and crown roots of maize grown in the split-root system until V3 (a) and V6 stages (b). Maize was grown in pots kept at a constant water potential (-5kPa or -30kPa). Nitrogen uptake rate was calculated from the ^{15}N enrichment in maize shoot after 0h, 24h, and 48h ^{15}N enrichment periods. At V3 and V6 stages, one of the chambers, either the inner or outer, received an injection of $^{15}\text{N}\text{-KNO}_3$ solution (18.4% atom ^{15}N excess), while the other chamber received $^{14}\text{N}\text{-KNO}_3$ solution, ensuring exposure of only one root type (either embryonic or crown roots) to $^{15}\text{N}\text{-KNO}_3$ solution. Boxplots show minimum, median, maximum. The dots show outliers. Different letters over the bars indicate significantly different ($p < 0.05$, Tukey's honestly significant test). NS, not significant ($p > 0.05$).

4.4.4 Nitrification was uniform among the root types

Gross nitrification rates were similar at the V3 and V6 growth stages, ranging from 3.8 – 45.5 $\text{mg NO}_3^- \text{ kg}^{-1} \text{ d}^{-1}$ (Fig. 4. 4). Root types did not affect the nitrification rate at the V3 and V6 growth

stages. Nitrification rate was 330% higher around crown roots in the wet soil than in the dry soil at the V6 growth stage.

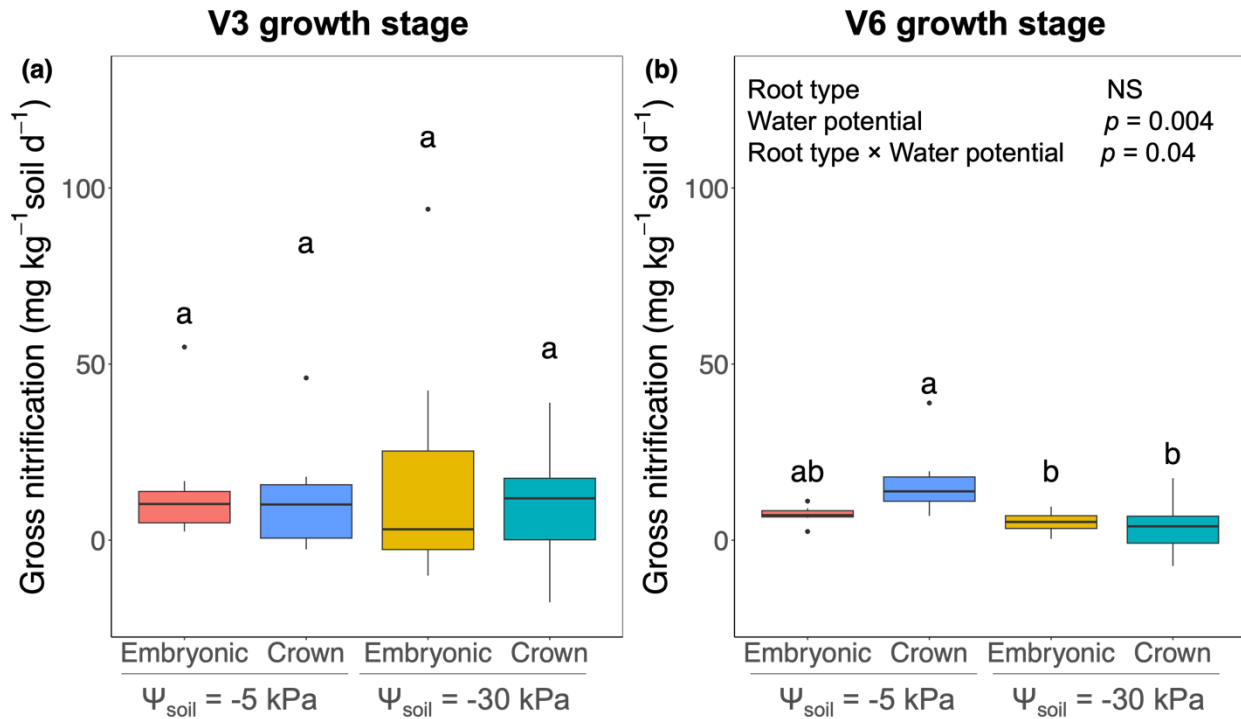


Fig. 4. 4 Gross nitrification arounds embryonic roots and crown roots of maize grown in the split-root system until (a) V3 and (b) V6 stages. Maize was grown in pots kept at a constant water potential (-5kPa or -30kPa). Gross nitrification rate was calculated from the ^{15}N isotope dilution after 0h, 24h, and 48h ^{15}N enrichment periods. At V3 and V6 stages, one of the chambers, either the inner or outer, received an injection of $^{15}\text{N}\text{-KNO}_3$ solution (18.4% atom ^{15}N excess), while the other chamber received $^{14}\text{N}\text{-KNO}_3$ solution, ensuring exposure of only one root type (either embryonic or crown roots) to $^{15}\text{N}\text{-KNO}_3$ solution. Boxplots show minimum, median, maximum. The dots show outliers. Different letters over the bars indicate significantly different ($p < 0.05$, Tukey's honestly significant test). NS, not significant ($p > 0.05$).

4.5 Discussion

We accept our hypothesis that crown roots have a higher NO_3^- uptake rate than embryonic roots in relatively wet soil at both V3 and V6 growth stage. In this study, NO_3^- was the source of plant-available N for maize because NO_3^- represented more than 95% of soil mineral N pool (Fig. S4. 5). Thus, we assume that mass flow was the dominant process for maize N uptake, and NO_3^- moved in the water that was extracted from soil pores by maize roots. We found NO_3^- was mainly taken up by crown roots in wet soil (-5 kPa), at both V3 and V6 growth stages. This is consistent with Ahmed et al. (2018b), who reported the water uptake rate was 1000 times greater in crown roots than seminal roots of 35-day-old maize, suggesting a greater mass flow capacity in crown roots. Our observation also aligns with Liu et al. (2020), showing that crown roots of barley (*Hordeum vulgare*) had 2-fold higher NO_3^- uptake and root-to-shoot translocation capacities than the seminal roots. Despite genetic differences between barley and maize, both cereals share similarities in root system, characterized by a typical fibrous root system comprising embryonic seminal roots and post-embryonic crown roots. By the V6 stage, we observed a 5-fold increase in plant NO_3^- uptake compared to the V3 stage, suggesting that maize enter the rapid N uptake phase at V6 (Bender et al. 2013). The crown root system dominates the N uptake in both wet and dry soil, accounting for about 80% of N uptake by maize. This result aligns with the fact that the contribution of embryonic roots decreases as maize growing beyond the V3 stage (Ahmed et al. 2016, 2018b).

We must reject the hypothesis that embryonic roots had higher N uptake than crown roots in dry soil. Yet, the contribution of the embryonic root system to plant N uptake at the V3 growth stage increases from 25% to 38% as the soil dried. Our results indicate a positive correlation between NO_3^- uptake and the root hydraulic conductance of shoot-derived crown roots, aligning

with the transport mechanism of NO_3^- ions (Fig. S4. 6, McMurtrie and Nasholm, 2018). This relation indicates that greater hydraulic conductance in crown roots facilitates the transport of NO_3^- to roots (Henriksson et al. 2021). However, the root hydraulic conductance of crown roots was decreased by 83% when exposed to dry soil, while primary and seminal roots maintain their root hydraulic conductance. This result is consistent with Hazman and Kabil, (2022), who reported that crown root hydraulic conductance had a 50% reduction, while embryonic root hydraulic conductance was insensitive when exposed to the water-deficit. The reduced root hydraulic conductance decreased N uptake, as we observed the 52% reduction of N uptake by crown roots in the dry soil at V6. This aligns with the findings of Hammad et al. (2017) and Flynn et al. (2023), who observed reductions in N uptake by maize in response to decreased soil water availability. Given the significant impact of the interaction between water potential and root types on N uptake at the V6 stage, our results underscore the critical importance of soil water management during this growth stage to optimize both water and N uptake in maize.

There are several explanations for the reduction of root hydraulic conductance in crown roots. This reduction is not related to the decreased root length or surface area under water-deficit, as only the root morphology of 2nd-whorl crown roots responded to soil water potential. Instead, it is likely due to the plastic responses of xylem number and diameter in the crown root tip under water deficit. The diameter of 1st whorl crown roots and 2nd whorl crown roots decreased from 64 to 58 μm and 96 to 92 μm , which is smaller in magnitude than the reductions observed in maize (cv. CML538) root tips, where diameter decreased from 150 to 30 μm reported by Jafarikouhini and Sincalir (2023). The xylem vessel diameter and their plasticity to water-deficit varied among maize genotypes, with the wide range of diameter from 50 – 150 μm among 44 genotypes (Yang et al. 2019), and only two out of four genotypes showed reduced metaxylem number and area under

water deficit (Hazman and Kabil et al. 2022). These findings suggest that less plastic genotypes may have the potential to maintain their N uptake under water deficit, which need the further investigation.

The decrease in root hydraulic conductance in dry soil may also be attributed to root shrinkage or reduced apoplastic water uptake. While mucilage and root hairs aid in maintaining cohesion between the root and surrounding soil, root hair shrinkage can occur at soil water potentials below -10 kPa, followed by cortex shrinkage, leading to air gaps at the root-soil interface (Ahmed et al. 2018a; Duddek et al. 2022; Jiang et al. 2022). Our results indicated potential shrinkage in crown roots – in wet soil, the cortex of crown roots was 43 – 65% thicker than primary roots and seminal roots; however, in dry soil, the cortex of 1st whorl crown roots decreased to a level similar to that of primary and seminal roots (Fig.S4. 7, Carminati et al. 2013). We did not observe any shrinkage at the V6 stage, probably because maize with higher-order crown roots could manage to absorb sufficient water for the growth. Moreover, water uptake may partially shift from apoplastic pathway to cell-to-cell pathway in dry soil as indicated by the decreased transpiration due to partial stomatal closure (Fig. S4. 8, Suslov et al. 2024). The thicker cortex layer of crown roots might slow down the radial water movement because cell-to-cell pathway is 17 times slower than apoplastic pathway (Steudle 2001). Therefore, future research should investigate root shrinkage and water transport pathways across different root types under water deficit conditions, as these factors significantly impact water and nutrient uptake.

Under the wet soil, crown roots exert greater hydraulic conductance than primary and seminal roots. On average, crown roots of V3 maize had hydraulic conductivity of $6 \times 10^{-11} \text{ m}^3 \text{ Mpa}^{-1} \text{ s}^{-1}$ and primary/seminal roots had on average $1.8 \times 10^{-11} \text{ m}^3 \text{ Mpa}^{-1} \text{ s}^{-1}$, both falling within the range of $0.6 \times 10^{-11} - 6 \times 10^{-11} \text{ m}^3 \text{ Mpa}^{-1} \text{ s}^{-1}$ reported by Knipfer and Fricke (2011) using the root exudation

method. Greater hydraulic conductance in crown roots is attributed to their larger, numerous xylem vessels than in primary and seminal roots because plants translocate water and NO_3^- in xylem. For instance, a single crown root produced 7 metaxylem vessels, whereas seminal roots only produced 4 metaxylem vessels. The number of xylem vessels in this study is smaller than the B73 maize inbred line, which contains 9–12 xylem vessels in the crown roots and 4–6 xylem vessels in the primary and seminal roots (Tai et al. 2016). However, the xylem diameter in crown roots of the B73 maize inbred line was 27–68% larger than in primary and seminal roots, aligning with our results (Tai et al. 2016). Thus, the larger xylem vessel in crown roots produce a greater tension that drive the NO_3^- mass flow to the root surface. A greater difference in measured root hydraulic conductance than the calculated axial hydraulic conductance among the root types indicates that crown roots also have radial hydraulic conductance than the embryonic roots, possibly due to the activity of aquaporins (Chaumont and Tyerman 2014). Furthermore, maize crown root tips exhibited superior NO_3^- uptake kinetics compared to seminal root tips, with a more than 20% greater maximum NO_3^- influx rate (York et al. 2016). Therefore, we conclude that crown roots dominate NO_3^- uptake because of their greater hydraulic conductance, and it might also because of their abundant and active NO_3^- transporters on the root surface, but this remains to be confirmed in the future.

Our results suggested no difference in soil nitrification among root types, contrary to our initial hypothesis. Nitrification, a biological process controlled by ammonium oxidizers and nitrifiers, is influenced by soil physio-chemical properties such as soil moisture and pH. In our study, the observed nitrification rates ranged from 18 – 33 $\text{mg NO}_3^- \text{ kg}^{-1} \text{ d}^{-1}$ in the wet soil and 12 – 20 $\text{mg NO}_3^- \text{ kg}^{-1} \text{ d}^{-1}$ in the dry soil, falling within the reported range of <1 – 50 $\text{mg NO}_3^- \text{ kg}^{-1} \text{ d}^{-1}$ (Lteif et al. 2010; Zhang et al. 2024). The higher nitrification rate around crown roots in the wet soil than

the dry soil aligned with the optimal soil moisture range for nitrification (-5 – -20 kPa, equivalent to 50 % – 80% of field capacity, Whalen and Sampedro 2010). Notably, embryonic roots exhibited higher pH than crown roots likely because crown roots exude more organic acids (Fig. S4. 9, Tiziani et al. 2022). Nevertheless, soil pH remained within the range of 5.8 – 7.0, which favors the nitrification of autotrophic nitrifiers and results in the uniform nitrification among the root types (Whalen and Sampedro 2010). Further investigation into how soil N transformation varies across diverse root types will contribute to a precise understanding of soil-plant interactions.

4.6 Conclusions

In summary, N uptake in maize depends on the development of crown roots, which have greater hydraulic conductance than embryonic roots. Under dry soil conditions, N uptake and crown root hydraulic conductance decreased at V3 and V6 stages. The embryonic roots can contribute to maize N uptake in early vegetative growth (up to V3 stage), but their water and NO_3^- absorbing functions disappear by the V6 stage as the larger, solute-extracting crown root system develops. Our results suggest that soil water management is important to ensure optimal N uptake, especially at the V6 stage and thereafter, since the embryonic root functions are negligible.

4.7 References

- Ahmed MA, Passioura J, Carminati A. 2018a.** Hydraulic processes in roots and the rhizosphere pertinent to increasing yield of water-limited grain crops: a critical review. *Journal of Experimental Botany*, 69: 3255-3265. <https://doi.org/10.1093/jxb/ery183>
- Ahmed MA, Zarebanadkouki M, Meunier F, Javaux M, Kaestner A, Carminati A. 2018b.** Root type matters: measurement of water uptake by seminal, crown and lateral roots in maize. *Journal of Experimental Botany* **69**: 1199–1206. doi:10.1093/jxb/erx439
- Barber SA. 1962.** A diffusion and mass-flow concept of soil nutrient availability. *Soil Science* **93**: 39–49. doi: 10.1097/00010694-196201000-00007
- Barraclough D. 1996.** ¹⁵N isotope dilution techniques to study soil nitrogen transformations and plant uptake. In *Nitrogen Economy in Tropical Soils: Proceedings of the International Symposium on Nitrogen Economy in Tropical Soils, held in Trinidad, WI, January 9–14, 1994* (pp. 185–192). Springer Netherlands.
- Brooks PD, Stark JM, McInteer BB, Preston T. 1989.** Diffusion method to prepare soil extracts for automated nitrogen-15 analysis. *Soil Science Society of America Journal* **53**: 1707–1711.
- Carminati A, Vetterlein D, Koebnick N, Blaser S, Welle U, Vogel HJ. 2013.** Do roots mind the gap?. *Plant and Soil* **367**: 651–661.
- Doussan C, Pagès L, Vercambre G. 1998.** Modelling of the hydraulic architecture of root systems: an integrated approach to water absorption—model description. *Annals of Botany* **81**: 213–223. doi: <https://doi.org/10.1006/anbo.1997.0540>

- Duddek P, Carminati A, Koebernick N, et al. 2022.** The impact of drought-induced root and root hair shrinkage on root–soil contact. *Plant Physiology* 189: 1232–1236. Doi: <https://doi.org/10.1093/plphys/kiac144>
- Flynn NE, Comas LH, Stewart CE, Fonte SJ. 2023.** High N availability decreases N uptake and yield under limited water availability in maize. *Scientific reports* **13**: 14269. doi: <https://doi.org/10.21203/rs.3.rs-2721193/v1>
- Hammad HM, Farhad W, Abbas F, Fahad S, Saeed S, Nasim W, Bakhat HF. 2017.** Maize plant nitrogen uptake dynamics at limited irrigation water and nitrogen. *Environmental Science and Pollution Research*, 24: 2549–2557. doi: <https://doi.org/10.1007/s11356-016-8031-0>
- Hazman MY, Kabil FF. 2022.** Maize root responses to drought stress depend on root class and axial position. *Journal of plant research* 1–16. doi: <https://doi.org/10.1007/s10265-021-01348-7>
- Henriksson N, Lim H, Marshall J, et al. 2021.** Tree water uptake enhances nitrogen acquisition in a fertilized boreal forest—but not under nitrogen-poor conditions. *New Phytologist* **232**: 113-122. doi:<https://doi.org/10.1111/nph.17578>
- Jafarikouhini N, Sinclair TR. 2023.** Hydraulic conductance and xylem vessel diameter of young maize roots subjected to sustained water-deficit. *Crop Science* **63**: 2458–2464. doi: <https://doi.org/10.1002/csc2.21023>
- Jiang Y, Hou L, Ding F, Whalen JK. 2022.** Root mucilage: Chemistry and functions in soil. *Encyclopedia of Soils in the Environment* (2nd edition).

- Knipfer T, Fricke W. 2011.** Water uptake by seminal and adventitious roots in relation to whole-plant water flow in barley (*Hordeum vulgare* L.). *Journal of experimental botany* **62**: 717–733. doi: <https://doi.org/10.1093/jxb/erq312>
- Lambers H, Atkin OK, Millenaar FF. 2002.** Respiratory patterns in roots in relation to their functioning. *In Plant roots: the hidden half* **3**: 521–552.
- McMurtrie RE, Näsholm T. 2018.** Quantifying the contribution of mass flow to nitrogen acquisition by an individual plant root. *New Phytologist* **218**: 119–130. doi: <https://doi.org/10.1111/nph.14927>
- Plett DC, Ranathunge K, Melino VJ, Kuya N, Uga Y, Kronzucker HJ. 2020.** The intersection of nitrogen nutrition and water use in plants: new paths toward improved crop productivity. *Journal of experimental botany* **71**: 4452–4468. <https://doi.org/10.1093/jxb/eraa049>
- Shane MW, McCully ME. 1999.** Root xylem embolisms: implications for water flow to the shoot in single-rooted maize plants. *Functional Plant Biology* **26**: 107–114. doi: <https://doi.org/10.1071/PP98060>
- Stedle, E. 2001.** The cohesion-tension mechanism and the acquisition of water by plant roots. *Annual Review of Plant Biology* **52**: 847–875. doi:10.1146/annurev.arplant.52.1.847
- Suslov M, Daminova A, Egorov J. 2024.** Real-Time Dynamics of Water Transport in the Roots of Intact Maize Plants in Response to Water Stress: The Role of Aquaporins and the Contribution of Different Water Transport Pathways. *Cells* **13**: 154. doi: <https://doi.org/10.3390/cells13020154>
- Tai H, Lu X, Opitz N, Marcon C, Paschold A, Lithio A, Nettleton D, Hocchholdinger F. 2016.** Transcriptomic and anatomical complexity of primary, seminal, and crown roots highlight

- root type-specific functional diversity in maize (*Zea mays* L.). *Journal of Experimental Botany* **67**: 1123–1135. doi:10.1093/jxb/erv513
- Wang Y, Mi G, Chen F, Zhang J, Zhang F. 2005.** Response of root morphology to nitrate supply and its contribution to nitrogen accumulation in maize. *Journal of Plant Nutrition* **27**: 2189–2202. doi: <https://doi.org/10.1081/PLN-200034683>
- Whalen JK, Bottomley PJ, Myrold DD. 2001.** Short-term nitrogen transformations in bulk and root-associated soils under ryegrass. *Soil Biology and Biochemistry* **33**: 1937–1945. doi: [https://doi.org/10.1016/S0038-0717\(01\)00121-3](https://doi.org/10.1016/S0038-0717(01)00121-3)
- Yang JT, Schneider HM, Brown KM, Lynch JP. 2019.** Genotypic variation and nitrogen stress effects on root anatomy in maize are node specific. *Journal of Experimental Botany* **70**: 5311–5325. doi: <https://doi.org/10.1093/jxb/erz293>
- York LM, Silberbush M, Lynch JP. 2016.** Spatiotemporal variation of nitrate uptake kinetics within the maize (*Zea mays* L.) root system is associated with greater nitrate uptake and interactions with architectural phenes. *Journal of Experimental Botany* **67**: 3763–3775. doi: <https://doi.org/10.1093/jxb/erw133>
- Zhan A, Lynch JP. 2015.** Reduced frequency of lateral root branching improves N capture from low-N soils in maize. *Journal of Experimental Botany* **66**: 2055–2065. doi: <https://doi.org/10.1093/jxb/erv007>

GENERAL DISCUSSION

The overarching goal of this thesis is to elucidate the plasticity of maize roots adapt to water-deficient and N-limited soil, focusing on N uptake from these challenging environments. Plasticity, defined as the ability of maize roots to modify their phenotype in response to environmental stimuli, reflects the interaction between genotype and environment (G×E). This thesis focused on morphological and anatomical plasticity in response to soil mineral N and soil water potential. Understanding how maize roots adjust to water and N deficits is crucial for enhancing agricultural productivity. This is because the water and N are recognized as the first two limiting factors for crop growth, according to Liebig's law. Notably, alterations in precipitation patterns due to climate change have been shown to reduce global maize production by 15–20%. Therefore, uncovering the plasticity of maize roots in response to water and N deficits contributes to knowledge on root development for maximizing N uptake.

In Chapter 2, we used perlites as a growth medium, which has some advantages and limitations for the experiment. Using perlites is different from most previous research that planted maize in hydroponic (Gao et al., 2015), aeroponic (Guadin et al., 2011) or in the soil system. The rationale behind selecting pure perlite as the growth medium is twofold. First, perlite, being an amorphous volcanic glass, contains minimal nutrients and limited biological process such as N mineralization. This allowed precise control over the NO_3^- concentration in the perlite medium by the addition of NO_3^- solution. In contrast, real soil typically contains mineral N and undergoes N mineralization processes. For example, the non-fertilized sandy loam soil contained about $0.1 \text{ mg kg}^{-1} \text{ NO}_3\text{-N}$ (equivalent to $0.04 \text{ mmol N L}^{-1}$), and the clay loam soil contained minimum $0.25 \text{ mg kg}^{-1} \text{ NO}_3\text{-N}$ (equivalent to $0.1 \text{ mmol N L}^{-1}$, Gurmessa et al., 2022). Thus, it is challenging to include

a control treatment with 0 mmol L⁻¹ NO₃⁻ concentration, even with non-fertilized soil. Second, maintaining NO₃⁻ concentrations in the perlite growth medium at nominal levels (0, 0.5, 1, 2, 4, 8 mmol L⁻¹) is feasible, allowing the NO₃⁻ concentration stayed within ±10% of the nominal NO₃⁻ concentration added to the pot. Although maize received fertilization every 2 days, negligible cations bound to exchange sites and accumulated in the growth medium because of perlite's low cation exchange capacity (about 0 cmol_c kg⁻¹). This characteristic facilitated a straightforward procedure to monitor NO₃⁻ concentration, as leachates could be collected from pot drainage after fertilization. However, questions remained that if perlites perfectly mimic the physical property of soil. Perlite growth medium may be more closely related to soil than traditional hydroponic or aeroponic system, because both perlites and field soil contained pore structures which break in the continuity of water flow. However, maize grown in perlites produced root length ranging from 590 – 950 cm root⁻¹, longer than maize grown in soil at the same stage (250 – 800 cm root⁻¹, Chapter 3). This might be because the lack of physical impendence in perlites due to its porous structure (bulk density = 0.11 g cm⁻³) than the typical field soil (bulk density = 1 – 1.4 g cm⁻³), consistent with the observation elsewhere (Guadin et al., 2011). Therefore, perlite offered a well-controlled environment for investigating the plastic responses of maize roots, but it could not completely reflect the soil condition.

Build on Chapter 2, I conducted a comprehensive investigation into the plasticity of maize roots concerning N fertilizer inputs in real soil, under the controlled growth chamber conditions and in the field. The controlled growth chamber provided an opportunity to investigate the interactive effects of N fertilizer inputs and soil water potential. Soil water potential can be maintained at two levels: -5 kPa and -15 kPa, through regularly weighing and watering. However, maintaining soil mineral N concentration was difficult. Although pots were received 85 or 170 kg

N ha⁻¹ treatments, they had the similar soil mineral N concentration ($p>0.05$) at the end due to plant N uptake and other biological processes. Destructive sampling of maize and soil at only one growth stage (V6) limits our ability to know the real exposure of soil mineral N concentration during the growing. Therefore, the experiment can be improved by destructive sampling at the multiple growth stage. Alternatively, the portable soil NO₃⁻ sensor utilized the electrochemical impedance spectroscopy provides a non-destructive solution to monitor the in situ real-time NO₃⁻ concentration in soil (Eldeed et al., 2023). In addition, pot-grown maize can only explore the limited soil volume restricted by the container (12.7 cm dia., 15 cm depth). This condition may not accurately reflect the field environment. Within the growth chamber, there was only <25 mg mineral N kg⁻¹ left in the relatively wet soil, indicating the depletion of mineral N at the V6 growth stage. Finally, the experiment design of 2 × 2 factorial with two levels of water (-5 kPa and -15 kPa) and two levels of N fertilization (85 or 170 kg N ha⁻¹) limits our predictive ability for root plastic responses. In future experiments, it would be beneficial to incorporate a wider range of soil moisture and N fertilizer levels to develop a predictive model of root responses to environmental factors using regression analysis.

The field experiment provides the opportunities to do multiple samplings of maize plants and soils, from V1 to V7 growth stages. In Chapter 3, the field experiment was conducted over two consecutive years to investigate how maize roots respond to variable soil NO₃⁻ concentration rates in the field environment. The 2021 field experiment revealed no difference in soil NO₃⁻ concentration, N uptake, and shoot biomass among plots receiving different N fertilizer rates (30, 40, and 50 kg N ha⁻¹). This is because of no limitation of soil mineral N in the field site, due to the plow down of clover forage and perennial grass previously planted from 2017 – 2020. To refine the experimental setup, the 2022 field experiment introduced control plots that received 0 kg N ha⁻¹

¹. Plots receiving 0, 30, 40, and 50 kg N ha⁻¹ had significant differences in soil mineral N concentration. From the V5 growth stage, maize receiving 0 kg N ha⁻¹ started to have about 25 – 50% N uptake than those receiving 30 – 50 kg N ha⁻¹, while maize in 30, 40, and 50 kg N ha⁻¹ treatments had similar N uptake levels. According to Bender et al., (2013), maize only absorbs 5% of the total N before V3 growth stage, with most of the N in maize seedling originating from embryonic resources. This suggests that maize seedlings before the V5 stage can absorb sufficient N from plots receiving only 0 kg N ha⁻¹, which contained only <10 mg N kg⁻¹. Consequently, these findings imply that the initial banded fertilizer rate for maize production in sandy loam soil in this region could be reduced by at least 40% (30 kg N ha⁻¹).

The results of Chapter 2 and Chapter 3 consistently demonstrated that higher NO₃⁻ concentration and greater N fertilizer inputs did not alter growth of axial roots and laterals of primary root, but laterals of crown root types were responsive. However, our observations were based on the observation on two maize genotypes (cv. PS2790 in the field experiment and cv. MZ3877 in the growth chamber experiment). The plasticity of phenotype, reflecting the interaction between genotype and environment (G×E), may vary depending on the genotype. For example, Dowd et al., (2020) observed that the first-order primary laterals of the FR697 genotype exhibited increased length under mild water deficit (-0.28 MPa, ~2.8 g g⁻¹ peat) than in well-watered condition (-0.1 MPa, ~6 g g⁻¹ peat) seven days after transplanting. In contrast, the length of laterals of transplanted B73 remained constant in both conditions, indicating the genotype-specific response of maize root to soil water availability. In the field experiment, the root length of V5 maize reported ranged from 500 – 1100 cm plant⁻¹, which falls within the reported range of 500 – 1200 cm plant⁻¹ for wide-range of genotypes at the same stage (Wang et al., 2005; Liu et al., 2008). However, it was lower than B73 genotypes and its inbred lines (800 – 2400 cm plant⁻¹, Cai et al.,

2021; Saengwilai et al., 2021). This highlights the necessity of comparing the phenotypic plasticity of variable maize genotypes, particularly those with different lateral root length, such as B73 genotypes.

Lateral root initiation requires auxin sensing of the concentration in soil solution, primarily signaled by the acropetal auxin transport in the roots (Casimiro et al. 2001). N-demanding shoots transmit auxin signals to the root tissues, which elongates the lateral roots in crown and seminal roots. It remains to be seen whether auxin levels change in maize exposed to variable water and N fertilizer levels, which could be done by measuring the auxin activity in shoot and root tissues. For example, [³H] indole-3-acetic solution can be used to trace the transport of auxin in both shoot and root tissues. By applying the labeled solution to the cut shoot or root tip of different root types, the direction of the ³H radioactivity transport can be detected. The lack of response in primary lateral roots indicated that lateral growth on primary roots might be controlled by genetic factors rather than the environment (NO₃⁻ concentration in soil solution). As the first root organ of maize life cycle, the primary root serves as the only root stock for the first 5 d, until the emergence of the seminal roots. Given that maize mainly relies on the embryonic resources in the endosperm during the first 14 d, the main function for primary roots should be anchorage and water. Ahmed et al., (2016) reported that the water uptake of seminal lateral roots was about 5 orders of magnitude higher than that of seminal and primary axial roots, indicating a higher pulling force for NO₃⁻ in seminal lateral roots. Therefore, the observed growth plasticity of seminal and crown lateral roots may signify their specialized function, as lateral roots tend to absorb more NO₃⁻ than structural root tissues (Lazof et al. 1992).

Root xylem area and number did not respond to N fertilizer inputs, as revealed by both growth chamber and field environment. This result indicates that xylem vessels did not show

plasticity to limited- N conditions. It is crucial to note that the measurements were specifically conducted on the 1st and 2nd whorl crown roots of maize, observed up to the V7 stage. However, it is important to acknowledge that the responses of root anatomy to N limitation are whorl specific, given that maize produce up to six whorls. Yang et al., (2019) pointed out that the 1st and 2nd whorl crown roots may not be representative of subsequent notes, as they emerge during early growth stages (before V6 stage). Higher-order crown roots, which emerge later, exhibit increased xylem area and number and demonstrate greater plasticity to N limitation compared to the 1st and 2nd whorls (Yang et al., 2019). Greater plasticity in higher- order crown roots is due to the increased demand for water and nutrients as maize continues to grow. To comprehensively understand root xylem plasticity, future research could extend the investigation to maize growth stages from V6 to R1 stage, during the complete development of the crown root system. This is particularly relevant as maize absorbs approximately 60% of its N during this period (Bender et al., 2013). Examining the plastic responses during these critical growth stages could provide deeper insights into the adaptive mechanisms of maize roots to varying N conditions.

The results showed that maize receiving 0 kg N ha⁻¹ produced 27 – 60 % fewer crown roots than those receiving 30 – 50 kg N ha⁻¹ before the V7 stage. This result is consistent with Guadin et al., (2011), who reported that 30-d old maize produced about 80 crown roots under 20 mmol L⁻¹, and about 50 crown roots under 8 mmol L⁻¹. The reduction in crown root number may contribute to development of a deeper root system, enabling maize to access water and mobile resources (NO₃⁻) from the deep soil layers. For example, Saengwilai et al., (2014) reported a 45% greater root depth in maize genotypes with fewer crown root number. However, in this research, the roots were sampled up to the top 25 cm of soil. While this sampling method is validated for assessing plasticity in lateral root morphology, anatomy, and root angles (Ordóñez et al., 2021), it does not

provide information on root depth. Therefore, the next step will be investigating whether maize, with a reduced number of crown roots, develops a deeper root system under limited N conditions to enhance N uptake from deeper soil layers. This can be achieved by extracting the intact maize root system using the root-core sampling system, comprising a sampling cylinder and a demountable lift module (Wu and Guo, 2014). In addition, the root-depth can be determined through the deep injection of ^{15}N stable isotope into the soil layer (up to 1.5 m) via a long polyvinyl chloride pipe, and measuring the ^{15}N enrichment in maize shoot biomass.

The observation that root hydraulic conductance is correlated with N uptake only under the wet soil indicates that N uptake is mainly through mass flow. However, in relatively dry soil, N uptake is not correlated with root hydraulic conductance. Additionally, N uptake by embryonic roots is not correlated with root hydraulic conductance. These observations suggest that when soil water is limited or when maize only has embryonic roots during the early growth stage, other processes, such as diffusion, may contribute to NO_3^- uptake as a supplement to mass flow. To validate this hypothesis, future studies will need to measure the relative importance of mass flow and diffusion process under various soil water potential. Several methods can be employed for these measurements. First, mass flow can be calculated by measuring transpiration over a period of time multiplied by the N concentration in the soil solution. The diffusion process can then be calculated by the difference between total plant N uptake and the mass flow process. Second, the diffusion process can be directly measured by microdialysis method, which induces diffusion of NO_3^- ions along the concentration gradient from the soil solution over a nonselective membrane into high-purity deionized water (Miro and Frenzel, 2004; Oyewole et al., 2014). The mass flow rate is proportional to the water potential difference between soil solution and the high-purity deionized water. Knowing the driving force of N uptake under various soil water potential will

provide valuable insights into soil N dynamics, and so, uncover the beneficial root traits related to N uptake.

It is worth noting that soil water potential in the field experiment was not manually controlled. The year 2021 was relatively dry, whereas 2022 was relatively wet, as indicated by soil water potential and simulated maize transpiration data from V1 to V7 stages over the two years. However, acknowledging that year-to-year comparisons may introduce bias due to differing factors such as temperature and seeding date, I suggest that future research explore maize root plasticity to N under varying soil water conditions through field experiments with controlled soil moisture. This can be achieved by employing an irrigation system under a rainout shelter design to regulate water supply and utilizing tools like time-domain reflectometry or tensiometers to monitor soil moisture. Additionally, the current N fertilizer rates of 120 kg N ha⁻¹, 96 kg N ha⁻¹, and 72 kg N ha⁻¹ did not impose any N limitation on maize growth or yield, as consistently observed over two years (Table S3. 7). We only observed decreased growth (N uptake, shoot biomass, and yield) of maize receiving 0 kg N ha⁻¹. Despite the highest N fertilization rates in the field experiment falling at the lower end of the recommended N fertilizer rates (120 – 170 kg N ha⁻¹), the grain yield was similar to the regional average of 9.94 Mg ha⁻¹ (CRAAQ, 2010; Institut de la statistique du Québec, 2023). Therefore, I recommend that future field experiments in this humid temperate region consider lowering the N fertilization levels, for example, to < 50 kg N ha⁻¹ for a maize growing season, particularly if the experimental setup aims to impose N stress treatments. Additionally, well-fertilized plots with 170 kg N ha⁻¹ as a reference to ensure maize reaches its maximum yield and growth potential could be included.

The plasticity observed in maize roots is closely linked to the distinct functions of different root types. Chapter 4 revealed that crown roots are the main location for N uptake from the wet

soil (-5 kPa) at V3 and V6 stages, due to their higher root hydraulic conductance. However, crown roots are more sensitive to soil water-deficit, with a 35% reduction ($p < 0.05$) in xylem diameter at the root tip and the possible shrinkage of crown roots under the dry soil, as shown by the decreased of cortex thickness. In contrast, primary and seminal roots maintained their xylem vessels and cortex thickness even under the water-deficit. I encourage future research to explore root shrinkage across different root types and among various maize genotypes. This is crucial because different maize genotypes possess varying root hair lengths and mucilage production, which influence the contact between the root surface and surrounding soil particles, thereby affecting the degree of shrinkage (Ahmed et al., 2018). For example, the root hair length of 169 recombinant inbred lines of B73×Mo17 ranged from 0.6 – 3.5 mm, with root hairs starting to shrink at a soil matric potential of -10 kPa, potentially affecting the degree of root cortex shrinkage thereafter (Zhu et al., 2005). Additionally, mucilage production around the maize root tip varied from 4 – 25 $\mu\text{g mm}^{-2}$ across maize genotypes (Jiang et al., 2022). The extent of root shrinkage can be quantified using X-ray micro-CT scanners (Carminati et al., 2013). Alternatively, it can also be determined through thin-sectioning of soil column contained roots, after the freeze-drying and impregnating with resin (Noordwijk et al., 1992).

My results indicated that embryonic roots may compensate for N and water uptake during the early growth stages of maize. In the dry soil, there is a significant reduction of 80% in crown root hydraulic conductance, while embryonic root hydraulic conductance remains consistent. Consequently, embryonic roots can potentially compensate for plant N uptake in dry soil during the early growth stages. Based on our study with one maize genotype, we found that embryonic roots contribute to less than 20% of N uptake at the V6 stage, even in dry soil, with some embryonic roots dying off by this stage. However, in certain maize genotypes (e.g., cv. Seneca Chief),

embryonic roots may persist until physiological maturity (Shane and McCully, 1999). Retaining extra root mass is considered inefficient, as root maintenance costs can exceed 50% of daily photosynthesis (Lambers et al., 2002). Therefore, it is possible that embryonic roots serve as a compensatory site for water and nutrient uptake during water-deficit period throughout maize's life span, although this hypothesis needs to be confirmed across various maize genotypes.

GENERAL CONCLUSIONS

This thesis documents the adaptable plasticity of root systems and the strategy employed by maize to absorb N from the water-deficient soil. It starts with a critical review of maize root responses to soil water and N limitations (Chapter 1). Then, it shows root-type specific plasticity in response to varying environmental NO_3^- concentration, highlighting the positive quadratic response of seminal and crown lateral roots across varying NO_3^- concentrations (Chapter 2). The thesis then reports the morphological responses of maize roots, such as decreased lateral root length and surface area, as well as reduced crown root number, to reduced N fertilization in relatively wet soil conditions, across growth chamber and field environments (Chapter 3). Building on this, Chapter 4 investigates the strategy of maize roots for N uptake from both wet and dry soils, revealing the reliance on crown roots for N uptake from the early growth stage, and the compensatory role of embryonic roots under water-deficient conditions up to the V3 stage. Overall, this thesis highlights the importance of soil water as a prerequisite for having an adaptable root system capable of optimizing N uptake, even in soils with reduced N fertilization.

This thesis advances our knowledge of how maize adapts to the water-deficient and N-limited soils. It reveals the importance of soil water in shaping the plasticity of maize roots in response to varying NO_3^- concentrations/N fertilizer inputs across different environments, emphasizing that maize growth is primarily constrained by water, and then by the NO_3^- supply. It suggests that farmers should prioritize irrigation systems to ensure optimal soil water content, which is crucial for efficient N uptake. The insights gained from this study have implications beyond maize and can be applied to other crops with fibrous root systems, such as sorghum, wheat,

and barley, to enhance N uptake efficiency and yield potential, especially in the context of anticipated climate change-induced water-deficient croplands.

REFERENCES

- Ahmed, M. A., Zarebanadkouki, M., Kaestner, A., Carminati, A. 2016. Measurements of water uptake of maize roots: the key function of lateral roots. *Plant and soil* 398: 59–77. doi: <https://doi.org/10.1007/s11104-015-2639-6>
- Ahmed, M. A., Passioura, J., Carminati, A. 2018. Hydraulic processes in roots and the rhizosphere pertinent to increasing yield of water-limited grain crops: a critical review. *Journal of Experimental Botany* 69: 3255-3265. <https://doi.org/10.1093/jxb/ery183>
- Anghinoni, I., and Barber, S. A. 1980. Phosphorus influx and growth characteristics of corn roots as influenced by phosphorus supply 1. *Agronomy Journal* 72: 685–688. doi: <https://doi.org/10.2134/agronj1980.00021962007200040028x>.
- Barber, S. A. 1962. A diffusion and mass-flow concept of soil nutrient availability. *Soil Science* 93: 39–49. doi: <https://doi.org/10.1097/00010694-196201000-00007>
- Barber, S. A., Walker J. M., and Vasey E. H. 1963. Mechanisms for movement of plant nutrients from soil and fertilizer to plant root. *Journal of Agricultural and Food Chemistry* 11: 204–207. doi: <https://doi.org/10.1021/jf60127a017>
- Bao, Y., Aggarwal, P., Robbins, N. E., Sturrock, C. J., and Dinneny, J. R. 2014. Plant roots use a patterning mechanism to position lateral root branches toward available water. *Pro. Natl. Acad. Sci.* 111: 9319–9324. doi: <https://doi.org/10.1073/pnas.1400966111>
- Bender, R. R., Haegele, J. W., Ruffo, M. L., et al. 2013. Nutrient uptake, partitioning, and remobilization in modern, transgenic insect-protected maize hybrids. *Agronomy Journal* 105: 161–170. doi: <https://doi.org/10.2134/agronj2012.0352>

- Burton, A. L., Brown, K. M., and Lynch, J. P. 2013. Phenotypic diversity of root anatomical and architectural traits in *Zea* species. *Crop Science* **53**: 1042–1055. doi:10.2135/cropsci2012.07.0440
- Cahn, M. D., Zobel, R. W., Bouldin, D. R. 1989. Relationship between root elongation rate and diameter and duration of growth of lateral roots of maize. *Plant and Soil* 119: 271–279. doi: <https://doi.org/10.1007/BF02370419>
- Cai, G., Carminati, A., Abdalla, M., Ahmed, M. A. 2021. Soil textures rather than root hairs dominate water uptake and soil–plant hydraulics under drought. *Plant Physiology* 187: 858–872. <https://doi.org/10.1093/plphys/kiab271>
- Cai, G., Ahmed, M. A., Abdalla, M., and Carminati, A. 2022a. Root hydraulic phenotypes impacting water uptake in drying soils. *Plant, Cell & Environment* 45: 650–663. doi: <https://doi.org/10.1111/pce.14259>
- Cai, G., König, M., Carminati, A., Abdalla, M., Javaux, M., Wankmüller, F., and Ahmed, M. A. 2022b. Transpiration response to soil drying and vapor pressure deficit is soil texture specific. *Plant and Soil* 1–17. doi:10.1007/s11104-022-05818-2
- Carminati, A., Vetterlein, D., Weller, U., Vogel, H. J., and Oswald, S. E. 2009. When roots lose contact. *Vadose Zone Journal* 8: 805–809. doi:10.2136/vzj2008.0147
- Carminati, A., Vetterlein, D., Koebernick, N., Blaser, S., Welle, U., Vogel, H. J. 2013. Do roots mind the gap?. *Plant and Soil* 367: 651–661. doi: <https://doi.org/10.1007/s11104-012-1496-9>
- Casimiro, I., Marchant, A., Bhalerao, R. P., Beeckma, T., Dhooge, S., Swarup, R. 2001. Auxin transport promotes *Arabidopsis* lateral root initiation. *The Plant Cell* 13: 843–852. doi: <https://doi.org/10.1105/tpc.13.4.843>

- Claassen, M. M., Shaw, R. H. 1970. Water deficit effects on corn. II. Grain components 1. *Agronomy journal* **62**: 652–655. doi: <https://doi.org/10.2134/agronj1970.00021962006200050032x>
- Chimungu, J. G., Brown, K. M., and Lynch, J. P. 2014. Reduced root cortical cell file number improves drought tolerance in maize. *Plant Physiology* **166**: 1943–1955. doi:10.1104/pp.114.249037
- Crawford, N. M., and Glass, A. D. M. 1998. Molecular and physiological aspects of nitrate uptake in plants. *Trends Plant Science* **3**: 389–395. doi: [https://doi.org/10.1016/S1360-1385\(98\)01311-9](https://doi.org/10.1016/S1360-1385(98)01311-9)
- CRAAQ. 2010. Guide de référence en fertilisation (In French). 2nd ed. Centre de référence en Agriculture et Agroalimentaire du Québec, Québec, Canada.
- Devi, M. J., and Reddy, V. R. 2020. Stomatal closure response to soil drying at different vapor pressure deficit conditions in maize. *Plant Physiology and Biochemistry* **154**: 714–722. doi: <https://doi.org/10.1016/j.plaphy.2020.07.023>
- Doğan, M., Alkan, M. 2014. Some physicochemical properties of perlite as an adsorbent. <https://hdl.handle.net/20.500.12462/7482>
- Doussan, C., Pagès, L., and Vercambre, G. 1998. Modelling of the hydraulic architecture of root systems: an integrated approach to water absorption—model description. *Annals of Botany* **81**: 213–223. doi: <https://doi.org/10.1006/anbo.1997.0540>
- Dowd, T. G., Braun, D. M., and Sharp, R. E. 2019. Maize lateral root developmental plasticity induced by mild water stress. I: Genotypic variation across a high-resolution series of water potentials. *Plant Cell Environment* **42**: 2259–2273. <https://doi.org/10.1111/pce.13399>

- Dowd, T. G., Braun, D. M., and Sharp, R. E. 2020. Maize lateral root developmental plasticity induced by mild water stress. II: Genotype-specific spatio-temporal effects on determinate development. *Plant Cell Environment* 43: 2409-2427. <https://doi.org/10.1111/pce.13840>
- Eldeeb, M. A., Dhamu, V. N., Paul, A., Muthukumar, S., Prasad, S. 2023. Electrochemical Soil Nitrate Sensor for In Situ Real-Time Monitoring. *Micromachines* 14:1314. <https://doi.org/10.3390/mi14071314>
- FAO 2022. Agricultural production statistics 2000 – 2021. Retrieved from <https://www.fao.org/3/cc3751en/cc3751en.pdf>
- Gao, K. U. N., Chen, F., Yuan, L., Zhang, F., Mi, G. 2015. A comprehensive analysis of root morphological changes and nitrogen allocation in maize in response to low nitrogen stress. *Plant, cell & environment* 38: 740–750. doi: <https://doi.org/10.1111/pce.12439>
- Garnett, T., Conn, V., Plett, D., Conn, S., Zanghellini, J., Mackenzie, N., Enju, A., Francis, K., Holtham, L., Roessner, U., Boughton, B., Bacic, A., Shirley, N., Rafalski, A., Dhugga, K., Tester, M., and Kaiser, B. N. 2013. The response of the maize nitrate transport system to nitrogen demand and supply across the lifecycle. *New Phytologist* 198: 82–94. doi:10.1111/nph.12166
- Gaudin, A. C., McClymont, S. A., Holmes, B. M., Lyons, E., & Raizada, M. N. 2011. Novel temporal, fine-scale and growth variation phenotypes in roots of adult-stage maize (*Zea mays L.*) in response to low nitrogen stress. *Plant, Cell & Environment* 34: 2122-2137. <https://doi.org/10.1111/j.1365-3040.2011.02409.x>
- Griffiths, M., Mellor, N., Sturrock, C. J., et al. 2022. X-ray CT reveals 4D root system development and lateral root responses to nitrate in soil. *The Plant Phenome Journal* 5: e20036. doi: <https://doi.org/10.1002/ppj2.20036>

- Guo, H., and York, L. M. 2019. Maize with fewer nodal roots allocates mass to more lateral and deep roots that improve nitrogen uptake and shoot growth. *Journal of Experimental Botany* 70: 5299-5309. [doi: 10.1093/jxb/erz258](https://doi.org/10.1093/jxb/erz258)
- Gurmesa, G. A., Hobbie, E. A., Zhang, S., et al. 2022. Natural ¹⁵N abundance of ammonium and nitrate in soil profiles: New insights into forest ecosystem nitrogen saturation. *Ecosphere* 13: e3998. doi: <https://doi.org/10.1002/ecs2.3998>
- Hachez, C., Veselov, D., Ye, Q., Reinhardt, H., Knipfer, T., Fricke, W., and Chaumont, F. 2012. Short-term control of maize cell and root water permeability through plasma membrane aquaporin isoforms. *Plant, Cell & Environment* 35: 185–198. doi:10.1111/j.1365-3040.2011.02429.x
- Hart, A. T., Merlin, M., Wiley, E., and Landhäusser, S. M. 2021. Splitting the difference: Heterogeneous soil moisture availability affects aboveground and belowground reserve and mass allocation in trembling aspen. *Frontiers in Plant Science* 12: 654159. doi:10.3389/fpls.2021.654159
- Hazman, M.Y., and Kabil, F.F. 2022. Maize root responses to drought stress depend on root class and axial position. *Journal of Plant Research* 1-16. <https://doi.org/10.1007/s10265-021-01348-7>
- Hetz, W., Hochholdinger, F., Schwall, M., and Feix, G. 1996. Isolation and characterization of *rtes*, a maize mutant deficient in the formation of nodal roots. *The Plant Journal* 10: 845-857. doi: 10.1046/j.1365-313X.1996.10050845.x
- Hey, S., Baldauf, J., Opitz, N., Lithio, A., Pasha, A., Provard, N., et al. 2017. Complexity and specificity of the maize (*Zea mays* L.) root hair transcriptome. *Journal of Experimental Botany* 68: 2175-2185. doi: 10.1093/jxb/erx104

- Hochholdinger F., and Feix, G. 1998. Early post-embryonic root formation is specifically affected in the maize mutant *lrt1*. *The Plant Journal* 16: 247–255. doi:10.1046/j.1365-313x.1998.00280.x
- Hochholdinger, F., Wen, T. J., Zimmermann, R., Chimot-Marolle, P., Da Costa e Silva, O., Bruce, W., Lamkey, K. R., Wienand, U., and Schnable, P. S. 2008. The maize (*Zea mays*, L) *roothairless3* gene encodes a putative GPI-anchored, monocot-specific, COBRA-like protein that significantly affects grain yield. *The Plant Journal* 54: 888–898. doi:10.1111/j.1365-313X.2008.03459.x
- Hund, A., Fracheboud, Y., Soldati, A., Frascaroli, E., Salvi, S., and Stamp, P. 2004. QTL controlling root and shoot traits of maize seedlings under cold stress. *Theoretical and Applied Genetics* 109: 618-629. doi:10.1007/s00122-004-1665-1
- Husakova, E., Hochholdinger, F., and Soukup, A. 2013. Lateral root development in the maize (*Zea mays*) *lateral rootless1* mutant. *Annals of Botany* 112: 417–428. doi:10.1093/aob/mct043
- Institute de la statistique du Quebec (2023). Area of field crops, yield per hectare and production, by combined administrative regions, Québec, 2007-2023. Gouvernement du Québec, Québec, Canada. Retrieved from https://statistique.quebec.ca/en/document/area-of-field-crops-yield-per-hectare-and-production-by-combined-administrative-regions/tableau/area-of-field-crops-yield-per-hectare-and-production-by-combined-administrative-regions#tri_cult=35
- Ishikawa, H., and Evans, M. L. 1995. Specialized zones of development in roots. *Plant Physiology* 109: 725. doi: 10.1104/pp.109.3.725

- Jafarikouhini, N., and Sinclair, T.R. 2023. Hydraulic conductance and xylem vessel diameter of young maize roots subjected to sustained water-deficit. *Crop Science* **63**: 2458-2464.
- Jia, Z., Giehl, R. F. H., and von Wirén, N. 2022. Nutrient–hormone relations: Driving root plasticity in plants. *Molecular Plant* **15**: 86–103. doi: 10.1016/j.molp.2021.12.004
- Jiang, Y., Hou, L., Ding, F., & Whalen, J. K. 2022. Root mucilage: Chemistry and functions in soil. *Encyclopedia of Soils in the Environment* (2nd edition).
- Jiang, Y., Hung, C. Y., and Whalen, J. K. 2023. Distinctive plasticity of maize (*Zea mays*) root types to variable nitrate concentration. *Canadian Journal of Plant Science* **103**:319–323. doi: <https://doi.org/10.1139/cjps-2022-0246>
- Kablan, L. A., Chabot, V., Mailloux, A., Bouchard, M. È., Fontaine, D., Bruulsema, T. 2017. Variability in corn yield response to nitrogen fertilizer in eastern Canada. *Agronomy Journal* **109**: 2231–2242. doi: <https://doi.org/10.2134/agronj2016.09.0511>
- Kreszies, T., Shellakkutti, N., Osthoff, A., Yu, P., Baldauf, J. A., Zeisler-Diehl, V. V., Ranathunge, K., Hochholdinger, F., and Schreiber, L. 2019. Osmotic stress enhances suberization of apoplastic barriers in barley seminal roots: analysis of chemical, transcriptomic and physiological responses. *New Phytologist* **221**: 180–194. doi:10.1111/nph.15351
- Kou, X., Han, W., and Kang, J. 2022. Responses of root system architecture to water stress at multiple levels: A meta-analysis of trials under controlled conditions. *Frontiers in Plant Science* **13**: 1085409. doi: <https://doi.org/10.3389/fpls.2022.1085409>
- Lambers H, Atkin O.K., Millenaar F.F. 2002. Respiratory patterns in roots in relation to their functioning. *Plant roots: the hidden half* **3**: 521–552.

- Lazof D.B., Rufty T.W. Jr., Redinbaugh M.G. 1992. Localization of nitrate absorption and translocation within morphological regions of the corn root. *Plant Physiology* 100: 1251–1258. doi: <https://doi.org/10.1104/pp.100.3.1251>
- Li, L., Hey, S., Liu, S., Liu, q., McNinch, C., Hu, H. C., Wen, T. J., Marcon, C., Paschold, A., Bruce, W., Schnable, P. S., and Hochholding, F. 2016. Characterization of maize roothairless6 which encodes a D-type cellulose synthase and controls the switch from bulge formation to tip growth. *Scientific Reports* 6: 34395. doi:10.1038/srep34395
- Li, Z., Phillip, D., Neuhäuser, B., Schulze, W. X., and Ludewig, U. 2015. Protein dynamics in young maize root hairs in response to macro-and micronutrient deprivation. *Journal of Proteome Research* 14: 3362–3371. doi: <https://doi.org/10.1021/acs.jproteome.5b00399>
- Liu, J., An, X., Cheng, L., Chen, F., Bao, J., Yuan, L., Zhang, F., and Mi, G. 2010. Auxin transport in maize roots in response to localized nitrate supply. *Annals of Botany* 106:1019–1026. doi: 10.1093/aob/mcq202
- Liu, Z., Giehl, R. F. H., Hartmann, A., Hajirezaei, M. R., Carpentier, S., von Wirén, N. 2020. Seminal and nodal roots of barley differ in anatomy, proteome and nitrate uptake capacity. *Plant and Cell Physiology* 61: 1297-1308. doi: <https://doi.org/10.1093/pcp/pcaa059>
- Liu, J., Li, J., Chen, F., Zhang, F., Ren, T., Zhuang, Z., Mi, G. 2008. Mapping QTLs for root traits under different nitrate levels at the seedling stage in maize (*Zea mays* L.). *Plant Soil* 305: 253–265. doi: <https://doi.org/10.1007/s11104-008-9562-z>
- Lobell, D. B., Schlenker, W., and Costa-Roberts, J. 2011. Climate trends and global crop production since 1980. *Science* 333: 616–620. doi:10.1126/science.1204531

- Lynch, J. P., Chimungu, J. G., and Brown, K. M. 2014. Root anatomical phenes associated with water acquisition from drying soil: targets for crop improvement. *Journal of Experimental Botany* 65: 6155–6166. doi:10.1093/jxb/eru162.
- Lynch, J. P., Strock, C. F., Schneider, H. M., et al. 2021. Root anatomy and soil resource capture. *Plant and Soil* 466: 21-63. doi: <https://doi.org/10.1007/s11104-021-05010-y>.
- Mallikarjuna, M. G., Thirunavukkarasu, N., Sharma, R., Shiriga, K., Hossain, F., Bhat, J., Mithra, A. C., Marla, S. S., Manjaiah, K. M., Rao, A. R., and Gupta, H. S. 2020. Comparative transcriptome analysis of iron and zinc deficiency in maize (*Zea mays* L.). *Plants* 9: 1812. doi:10.3390/plants9121812.
- Mano, Y., Omori, F., Takamizo, T., Kindiger, B., Bird, R. M., and Loaisiga, C. H. 2006. Variation for root aerenchyma formation in flooded and non-flooded maize and teosinte seedlings. *Plant and Soil* 281: 269–279. doi:10.1007/s11104-005-4268-y
- Miller, A. J., and Smith, S. J. 1996. Nitrate transport and compartmentation in cereal root cells. *Journal of Experimental Botany* 47: 843–854. doi:10.1093/jxb/47.7.843
- Miro, M., Frenzel, W. 2004. Implantable flow-through capillary-type microdialyzers for continuous in situ monitoring of environmentally relevant parameters. *Analytical Chemistry* 76: 5974–5981. doi: <https://doi.org/10.1021/ac049406a>
- Mollier, A., and Pellerin, S. 1999. Maize root system growth and development as influenced by phosphorus deficiency. *Journal of Experimental Botany* 50: 487–497. doi: <https://doi.org/10.1093/jxb/50.333.487>
- Moreno-Risueno, M. A., Van Norman, J. M., Moreno, A., Zhang, J., Ahnert, S. E., and Benfey, P. N. 2010. Oscillating gene expression determines competence for periodic Arabidopsis root branching. *Science* 329: 1306–1311. doi:10.1126/science.1191937

- Nájera, F., Tapia, Y., Baginsky, C., Figueroa, V., Cabeza, R., and Salazar, O. 2015. Evaluation of soil fertility and fertilisation practices for irrigated maize (*Zea mays* L.) under Mediterranean conditions in central Chile. *Journal of Soil Science and Plant Nutrition* 15: 84–97. doi:10.4067/S0718-95162015005000008
- Nestler, J., Liu, S., Wen, T. J., et al. 2014. Roothairless5, which functions in maize (*Zea mays* L.) root hair initiation and elongation encodes a monocot-specific NADPH oxidase. *The Plant Journal* 79: 729–740. doi: <https://doi.org/10.1111/tpj.12578>
- Niu, L., Wang, Z., Zhu, G., Yu, K., Li, G., and Long, H. 2022. Stable Soil Moisture Improves the Water Use Efficiency of Maize by Alleviating Short-Term Soil Water Stress. *Frontiers in Plant Science* 13: 833041. doi: <https://doi.org/10.3389/fpls.2022.833041>
- Niu, Y. F., Chai, R. S., Jin, G. L., Wang, H., Tang, C. X., and Zhang, Y. S. 2013. Responses of root architecture development to low phosphorus availability: a review. *Annals of Botany* 112: 391–408. doi:10.1093/aob/mcs285
- Ordóñez, R. A., Archontoulis, S. V., Martinez-Feria, R., Hatfield, J. L., Wright, E. E., Castellano, M. J. 2020. Root to shoot and carbon to nitrogen ratios of maize and soybean crops in the US Midwest. *European Journal of Agronomy* 120: 126130. doi: <https://doi.org/10.1016/j.eja.2020.126130>
- Ordóñez, R. A., Castellano, M. J., Danalatos, G. N., Wright, E. E., Hatfield, J. L., Burras, L., Archontoulis, S. V. 2021. Insufficient and excessive N fertilizer input reduces maize root mass across soil types. *Field Crops Research* 267: 108142. doi: <https://doi.org/10.1016/J.FCR.2021.108142>

- Orsel, M., Filleur, S., Fraissier, V., and Daniel-Vedele, F. 2002. Nitrate transport in plants: which gene and which control? *Journal of Experimental Botany* 53: 825–833. doi: <https://doi.org/10.1093/jexbot/53.370.825>
- Orosa-Puente, B., Leftley, N., Von Wangenheim, D., Banda, J., Srivastava, A. K., Hill, K., Truskina, J., Bhosale, R., Morris, E., Srivastava, M., Kumpers, B., Goh, T., Fukaki, H., Vermeer, J. E. M., Vernoux, T., Dinneny, J. R., French, A. P., Bishopp, A., Sadanandom, A., and Bennett, M. 2018. Root branching toward water involves posttranslational modification of transcription factor ARF7. *Science* 362: 1407–1410. doi:10.1126/science.aau3956
- Oyewole, O. A., Inselsbacher, E., Näsholm, T. 2014. Direct estimation of mass flow and diffusion of nitrogen compounds in solution and soil. *New Phytologist* 201: 1056–1064. doi: <https://doi.org/10.1111/nph.12553>
- Postma, J. A., Lynch, J. P. 2011. Root cortical aerenchyma enhances the growth of maize on soils with suboptimal availability of nitrogen, phosphorus, and potassium. *Plant physiology* 156: 1190–1201. doi: <https://doi.org/10.1104/pp.111.175489>
- Plett, D. C., Ranathunge, K., Melino, V. J., Kuya, N., Uga, Y., and Kronzucker, H. J. 2020. The intersection of nitrogen nutrition and water use in plants: new paths toward improved crop productivity. *Journal of Experimental Botany* 71: 4452–4468. <https://doi.org/10.1093/jxb/eraa049>
- Plett, D., Toubia, J., Garnett, T., Tester, M., Kaiser, B. N., and Baumann, U. 2010. Dichotomy in the NRT gene families of dicots and grass species. *PloS One* 5: e15289. doi: <https://doi.org/10.1371/journal.pone.0015289>

- Postma, J. A., and Lynch, J. P. 2011. Root cortical aerenchyma enhances the growth of maize on soils with suboptimal availability of nitrogen, phosphorus, and potassium. *Plant Physiology* 156: 1190–1201. doi:10.1104/pp.111.175489
- Rao, T. P., Ito, O., Matsunaga, R., and Yoneyama, T. 1997. Kinetics of ¹⁵N-labelled nitrate uptake by maize (*Zea mays* L.) root segments. *Soil Science and Plant Nutrition* 43: 491–498. doi:10.1080/00380768.1997.10414776
- Robbins, N. E., and Dinneny, J. R. 2018. Growth is required for perception of water availability to pattern root branches in plants. *Proceedings of National Academy of Sciences* 115: E822–E831. doi: <https://doi.org/10.1073/pnas.1710709115>
- Saengwilai, P., Nord, E. A., Chimungu, J. G., Brown, K. M., and Lynch, J. P. 2014. Root cortical aerenchyma enhances nitrogen acquisition from low-nitrogen soils in maize. *Plant Physiology* 166: 726–735. doi: <https://doi.org/10.1104/pp.114.241711>
- Saengwilai, P., Strock, C., Rangarajan, H., Chimungu, J., Salungyu, J., Lynch, J. P. 2021. Root hair phenotypes influence nitrogen acquisition in maize. *Annals of botany* 128: 849-858. doi: <https://doi.org/10.1093/aob/mcab104>
- Saengwilai, P., Tian, X., Lynch, J. P. 2014. Low crown root number enhances nitrogen acquisition from low-nitrogen soils in maize. *Plant physiology* 166: 581–589. doi: <https://doi.org/10.1104/pp.113.232603>
- Sánchez-Calderón, L., López-Bucio, J., Chacón-López, A., Gutiérrez-Ortega, A., Hernández-Abreu, E., and Herrera-Estrella, L. 2006. Characterization of low phosphorus insensitive mutants reveals a crosstalk between low phosphorus-induced determinate root development and the activation of genes involved in the adaptation of Arabidopsis to

- phosphorus deficiency. *Plant Physiology* 140: 879–889. doi:
<https://doi.org/10.1104/pp.105.073825>
- Sorgona, A., Lupini, A., Mercati, F., Di, D. L., Sunseri, F., and Abenavoli, M. R. 2011. Nitrate uptake along the maize primary root: an integrated physiological and molecular approach. *Plant, Cell & Environment* 34: 1127–1140. doi:10.1111/j.1365-3040.2011.02311.x
- Steudle, E., and Peterson, C. A. 1998. How does water get through roots? *Journal of Experimental Botany* 49: 775–788. doi: <https://doi.org/10.1093/jxb/49.322.775>
- Steudle, E. 2001. The cohesion-tension mechanism and the acquisition of water by plant roots. *Annual Reviews of Plant Biology* 52: 847–875. doi:10.1146/annurev.arplant.52.1.847
- Tai, H., Lu, X., Opitz, N., Marcon, C., Paschold, A., Lithio, A., Nettleton, D., Hocchholdinger, F. 2016. Transcriptomic and anatomical complexity of primary, seminal, and crown roots highlight root type-specific functional diversity in maize (*Zea mays* L.). *Journal of Experimental Botany* 67: 1123–1135. doi: <https://doi.org/10.1093/jxb/erv513>
- Trevisan, S., Borsa, P., Botton, A., Varotto, S., Malagoli, M., Ruperti, B., and Quaggiotti, S. 2008. Expression of two maize putative nitrate transporters in response to nitrate and sugar availability. *Plant Biology* 10: 462–475. doi:10.1111/j.1438-8677.2008.00041.x
- Tian, Q., Chen, F., Liu, J., Zhang, F., Mi, G. 2008. Inhibition of maize root growth by high nitrate supply is correlated with reduced IAA levels in roots. *Journal of Plant Physiology* 165: 942–951. <https://doi.org/10.1016/j.jplph.2007.02.011>
- Van Noordwijk, M., Kooistra, M. J., Boone, F. R., Veen, B. W., Schoonderbeek, D. 1992. Root-soil contact of maize, as measured by a thin-section technique: I. Validity of the method. *Plant and Soil* 139:109–118. doi: <https://doi.org/10.1007/BF00012848>

- von Behrens, I., Komatsu, M., Zhang, Y., Kenneth, W. B., Niu, X., Sakai, H., Taramino, G., and Hochholdinger, F. 2011. Rootless with undetectable meristem 1 encodes a monocot-specific AUX/IAA protein that controls embryonic seminal and post-embryonic lateral root initiation in maize. *The Plant Journal* 66: 341–353. doi:10.1111/j.1365-313X.2011.04495.x
- Wang, Y., Afeworki, Y., Geng, S., Kanchupati, P., Gu, M., Martins, C., Rude, B., Tefera, H., Kim, Y., Ge, X., Auger, D., Chen, S., Yang, P., Hu, T., Wu, Y. 2020. Hydrotropism in the primary roots of maize. *New Phytology* 226: 1796–1808. doi: <https://doi.org/10.1111/nph.16472>
- Wen, T. J., Hochholdinger, F., Sauer, M., Bruce, W., and Schnable, P. S. 2005. The roothairless1 gene of maize encodes a homolog of sec3, which is involved in polar exocytosis. *Plant Physiology* 138: 1637–1643. doi:10.1104/pp.105.062174
- Woll, K., Borsuk, L. A., Stransky, H., Nettleton, D., Schnable, P. S., and Hochholdinger, F. 2005. Isolation, characterization, and pericycle-specific transcriptome analyses of the novel maize lateral and seminal root initiation mutant rum1. *Plant Physiology* 139: 1255–1267. doi: <https://doi.org/10.1104/pp.105.067330>
- Wu, J., Guo, Y. 2014. An integrated method for quantifying root architecture of field-grown maize. *Annals of botany* 114: 841–851. doi: <https://doi.org/10.1093/aob/mcu009>.
- Xu, C., Tai, H., Saleem, M., Ludwig, Y., Majer, C., and Berendzen, K. W. 2015. Cooperative action of the paralogous maize lateral organ boundaries (LOB) domain proteins RTCS and RTCL in shoot-borne root formation. *New Phytologist* 207: 1123–1133. doi: <https://doi.org/10.1111/nph.13420>
- Yang, J.T., Schneider, H. M., Brown, K. M., Lynch, J. P. 2019. Genotypic variation and nitrogen stress effects on root anatomy in maize are node specific. *Journal of Experimental Botany* 70: 5311–5325. doi: <https://doi.org/10.1093/jxb/erz293>.

- York, L.M., Silberbush, M., and Lynch, J.P. 2016. Spatiotemporal variation of nitrate uptake kinetics within the maize (*Zea mays* L.) root system is associated with greater nitrate uptake and interactions with architectural phenes. *Journal of Experimental Botany* 67: 3763-3775. <https://doi.org/10.1093/jxb/erw133>
- Zarebanadkouki, M., Trtik, P., Hayat, F., Carminati, A., and Kaestner, A. 2019. Root water uptake and its pathways across the root: quantification at the cellular scale. *Scientific Reports* 9: 12979. doi:10.5194/EGUSPHERE-EGU2020-13520
- Zhan, A., Lynch, J.P. 2015. Reduced frequency of lateral root branching improves N capture from low-N soils in maize. *Journal of Experimental Botany* 66: 2055–2065. <https://doi.org/10.1093/jxb/erv007>
- Zhao, X., Yu, H., Jing, W., Wang, X., Qi, D., Jing, W., and Qiao, W. 2016. Response of root morphology, physiology and endogenous hormones in maize (*Zea mays* L.) to potassium deficiency. *Journal of Integrative Agriculture* 15: 785–794. doi:10.1016/S2095-3119(15)61246-1
- Zhu, J., Brown, K. M., and Lynch, J. P. 2010. Root cortical aerenchyma improves the drought tolerance of maize (*Zea mays* L.). *Plant, Cell & Environment* 33: 740–749. doi:10.1111/j.1365-3040.2009.02099.
- Zhu, J., Kaepler, S.M., Lynch, J.P. 2005. Mapping of QTL controlling root hair length in maize (*Zea mays* L.) under phosphorus deficiency. *Plant and Soil* 270: 229–310. doi: <https://doi.org/10.1007/s11104-004-1697-y>

Zimmermann, H. M., Hartmann, K., Schreiber, L., and Steudle, E. 2000. Chemical composition of apoplastic transport barriers in relation to radial hydraulic conductivity of corn roots (*Zea mays* L.). *Planta* 210: 302–311.

APPENDICES

Table S2. 3 Measured NO_3^- concentration in leachate, representing maize root exposure to NO_3^- in perlite-filled pots receiving modified Hoagland solution containing 0 to 8 mM NO_3^- , 15 to 29 d after planting maize seeds. The NO_3^- concentration extracted from perlite with 2 M KCl solution at maize harvest (30 d after seeding) is reported. LOD is the limit of detection. Data are the mean \pm standard error of the mean (n=15)

		Nominal NO_3^- concentration (mM)					
Time (d)		0	0.1	1	2	4	8
		-----mM-----					
Measured NO_3^- (mM)	15	<LOD	0.1 \pm 0	1.0 \pm 0	1.8 \pm 0.1	4.2 \pm 0.4	7.8 \pm 0.4
	17	<LOD	0.1 \pm 0	1.0 \pm 0	1.9 \pm 0.4	4.0 \pm 0.6	7.9 \pm 0.6
	19	<LOD	0.1 \pm 0	1.0 \pm 0	2.1 \pm 0.4	3.9 \pm 0	8.2 \pm 0.1
	21	<LOD	0.1 \pm 0	0.9 \pm 0	2 \pm 0.4	3.7 \pm 0.4	7.4 \pm 0.4
	23	<LOD	0.1 \pm 0	1.0 \pm 0	1.9 \pm 0.2	4.1 \pm 0.6	7.8 \pm 0.2
	25	<LOD	0.1 \pm 0	0.9 \pm 0	2.2 \pm 0.4	3.9 \pm 0.2	7.8 \pm 0.4
	27	<LOD	0.1 \pm 0	1.0 \pm 0	2 \pm 0.4	3.7 \pm 0.4	7.9 \pm 0.6
	29	<LOD	0.1 \pm 0	1.0 \pm 0	1.9 \pm 0.4	3.8 \pm 0.4	7.6 \pm 0.6
	30	<LOD	0.1 \pm 0	0.8 \pm 0.1	1.6 \pm 0.4	3.4 \pm 0.4	7.2 \pm 0.4

Data are the NO_3^- concentrations in leachates (15 to 29 d), except after 30 d when the perlite was extracted with 2M KCl solution for NO_3^- analysis.

Table S2. 4 Root dry mass, tips and number of roots of primary, seminal and crown roots, after maize roots were exposed to variable NO_3^- concentrations (mean value of measured NO_3^- concentration from 15 to 29 d) in perlite-filled pots for 30 d. Data are mean \pm standard error

		NO_3^- concentration (mM)					
		0	0.1	1	2	3.9	7.8
Primary root	Dry mass (mg)	35 \pm 3	37 \pm 2	46 \pm 3	51 \pm 4	47 \pm 2	43 \pm 5
	Tips	2470 \pm 210	3930 \pm 550	3480 \pm 690	2650 \pm 350	2550 \pm 220	2940 \pm 580
Seminal roots	Dry mass (mg)	51 \pm 5	50 \pm 5	61 \pm 5	67 \pm 3	70 \pm 6	59 \pm 5
	Tips	2320 \pm 320	2220 \pm 340	3690 \pm 430	3360 \pm 550	3050 \pm 300	2640 \pm 340
	Numbers of roots	3 \pm 0	2 \pm 0	3 \pm 0	3 \pm 0	3 \pm 0	3 \pm 0
Crown roots	Dry mass (mg)	39 \pm 6	36 \pm 3	45 \pm 3	49 \pm 4	44 \pm 3	40 \pm 5
	Tips	700 \pm 120	690 \pm 110	1230 \pm 230	1070 \pm 220	940 \pm 190	950 \pm 140
	Numbers of roots	3 \pm 0	3 \pm 0	4 \pm 0	4 \pm 0	4 \pm 0	4 \pm 0

Number of root tips was measured by WinRhizo software REG 2008b 32-bit software (Regent Instruments, Quebec, Canada).

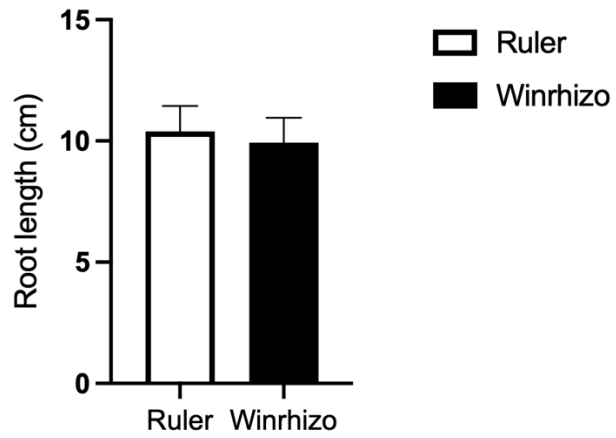


Fig. S2. 1 Comparison of the maize root length measured by ruler versus WinRhizo software (Regent Instruments, Quebec, Canada). The error bars are standard error (n = 10)

Table S3. 1 Goodness-of-fit statistics for shoot biomass of field-grown maize, estimated by the Root Zone Water Quality Model, in response to variable N fertilizer rates. The field experiment was in Sainte-Anne-de-Bellevue, Québec, Canada. Root mean square error (RMSE), relative root mean square error (RRMSE), and coefficient of determination (R^2) were calculated with equations S1 to S4, below. n = number of observations.

Year	N fertilizer rate (kg N ha ⁻¹)	RMSE	RRMSE (%)	Index of agreement	of R^2	n
2021	30	237.0	11.3	0.96	0.963	80
	40	286.3	13.6	0.95	0.948	80
	50	284.4	13.7	0.94	0.947	80
2022	0	1255.9	21.2	0.73	0.831	80
	30	1161.2	19.6	0.77	0.850	79
	40	1161.2	22.5	0.73	0.740	80
	50	1074.4	19.2	0.78	0.833	80

$$RMSE = \sqrt{\frac{\sum_{i=1}^n (simulated - observed)^2}{n}} \quad (S1)$$

$$RRMSE = \frac{RMSE}{\overline{Observed}} \quad (S2)$$

$$R^2 = \left(\frac{n * \sum_{i=1}^{i=n} (Sim_i * Obs_i) - \sum_{i=1}^{i=n} Sim_i * \sum_{i=1}^{i=n} Obs_i}{\sqrt{n * \sum_{i=1}^{i=n} Sim_i^2 - (\sum_{i=1}^{i=n} Sim_i)^2} * \sqrt{n * \sum_{i=1}^{i=n} Obs_i^2 - (\sum_{i=1}^{i=n} Obs_i)^2}} \right)^2 \quad (S3)$$

$$Index\ of\ agreement = 1 - \frac{\sum_{i=1}^{i=n} (Simulated_i - Observed_i)^2}{\sum_{i=1}^{i=n} (|Simulated_i - \overline{Observed}| + |Observed_i - \overline{Observed}|)^2} \quad (S4)$$

Table S3. 2 Biostimulant treatments had no effect ($p > 0.05$, n.s.: not significant) on the growth and nitrogen (N) uptake of maize (V6 stage), which varied according to the N fertilizer \times soil water treatments ($p < 0.001$, ***), but not the 3-way interaction ($p > 0.05$, n.s.) in a growth chamber environment. Values are the mean \pm standard error, n= 5.

Biostimulant treatment	Height (cm)	Shoot biomass (g)	Root biomass (g)	Root Length (cm)	N uptake (mg)
Control	40.4 \pm 6.4	13.7 \pm 6.2	1.5 \pm 0.3	1026 \pm 220	412 \pm 152
Seed soaking	41.6 \pm 5.8	14.5 \pm 4.3	1.5 \pm 0.4	955 \pm 200	397 \pm 142
Soil application	41.1 \pm 6.5	13.5 \pm 4.8	1.5 \pm 0.3	1029 \pm 207	386 \pm 154
Seed and soil	40.5 \pm 6.2	17.1 \pm 9.8	1.6 \pm 0.4	955 \pm 253	415 \pm 131
-----Analysis of variance-----					
Biostimulant	n.s	n.s.	n.s.	n.s.	n.s.
N fertilizer \times soil water	***	***	***	***	***
Biostimulant \times N \times soil water	n.s	n.s.	n.s.	n.s.	n.s.

Table S3. 3Xylem number and area, measured from three segments (tip: 0–20 mm from root tip, mid: 40–60 mm from root tip, base: 0–20 mm from the base of the stem) of a representative thin-sectioned axial root for each type (primary, seminal and crown, 1st and 2nd whorls) of maize (V6 stage) in a growth chamber environment. Maize was grown in pots with two levels of N fertilizer (equivalent to 85 and 170 kg N ha⁻¹) and watered to a constant soil water potential of -15 and -5 kPa. Values are the mean ± standard error, n= 4.

Axial root type		Root Segment	$\Psi_{\text{soil}} = -15 \text{ kPa}$		$\Psi_{\text{soil}} = -5 \text{ kPa}$	
			85 kg N ha ⁻¹	170 kg N ha ⁻¹	85 kg N ha ⁻¹	170 kg N ha ⁻¹
Xylem number	Primary	Tip	7 ± 0	6 ± 1	6 ± 0	7 ± 0
		Mid	6 ± 1	5 ± 0	7 ± 0	7 ± 0
		Base	8 ± 1	8 ± 1	7 ± 0	7 ± 0
	Seminal	Tip	5 ± 1	5 ± 0	4 ± 0	7 ± 0
		Mid	5 ± 0	6 ± 1	5 ± 0	5 ± 0
		Base	7 ± 1	7 ± 0	5 ± 1	7 ± 1
	Crown (1 st whorl)	Tip	9 ± 0	9 ± 1	8 ± 1	11 ± 1
		Mid	11.0 ± 0	10 ± 1	11 ± 1	11 ± 0
		Base	10 ± 1	11 ± 1	12 ± 2	13 ± 0
	Crown (2 nd whorl)	Tip	10 ± 1	9 ± 1	9 ± 0	9 ± 0
		Mid	10 ± 1	10 ± 1	9 ± 0	10 ± 0
		Base	10 ± 1	10 ± 1	13 ± 1	11 ± 0
Xylem area (μm^2) × 10 ⁴	Primary	Tip	1.76 ± 0.31	1.42 ± 0.25	0.96 ± 0.06	1.07 ± 0.11
		Mid	1.15 ± 0.18	1.20 ± 0.20	1.44 ± 0.31	1.84 ± 0.06

	Base	1.71 ± 0.16	1.61 ± 0.16	3.37 ± 0.86	2.17 ± 0.20
Seminal	Tip	0.70 ± 0.16	0.70 ± 0.16	0.68 ± 0.04	0.73 ± 0
	Mid	1.09 ± 0.13	0.86 ± 0.09	0.88 ± 0.15	1.18 ± 0.25
	Base	0.88 ± 0.08	0.87 ± 0.14	0.73 ± 0.08	1.10 ± 0.17
Crown (1 st whorl)	Tip	4.13 ± 0.69	3.64 ± 1.11	6.09 ± 1.47	4.52 ± 0.43
	Mid	7.12 ± 0.27	6.83 ± 0.55	6.30 ± 1.11	8.58 ± 0.30
	Base	6.67 ± 0.57	6.70 ± 0.56	7.94 ± 1.00	9.28 ± 1.28
Crown (2 nd whorl)	Tip	6.09 ± 1.6	5.17 ± 1.70	4.19 ± 0.97	5.77 ± 0.91
	Mid	6.30 ± 0.56	6.22 ± 0.61	8.50 ± 2.00	7.32 ± 0.62
	Base	5.75 ± 0.65	5.10 ± 0.51	10.87 ± 1.14	8.68 ± 0.44

Table S3. 4 Root hydraulic conductance, estimated for segments (tip: 0–20 mm from root tip, mid: 40–60 mm from root tip, base: 0–20 mm from the base of the stem) of a representative thin-sectioned axial root for each type (primary, seminal and crown, 1st and 2nd whorls) of maize (V6 stage) in a growth chamber environment. Maize was grown in pots with two levels of N fertilizer (equivalent to 85 and 170 kg N ha⁻¹) and watered to a constant soil water potential of -15 and -5 kPa. Values are the mean ± standard error, n= 4.

Axial root type	Root Segment	$\Psi_{\text{soil}} = -15 \text{ kPa}$		$\Psi_{\text{soil}} = -5 \text{ kPa}$	
		85 kg N ha ⁻¹	170 kg N ha ⁻¹	85 kg N ha ⁻¹	170 kg N ha ⁻¹
-----Root hydraulic conductance (kg m MPa ⁻¹ s ⁻¹) × 10 ⁻⁶ -----					
Primary	Tip	1.82 ± 0.53	1.44 ± 0.38	0.67 ± 0.13	0.77 ± 0.17
	Mid	1.02 ± 0.31	1.23 ± 0.37	1.48 ± 0.56	2.02 ± 0.08
	Base	1.55 ± 0.25	1.40 ± 0.22	7.70 ± 0.47	2.72 ± 0.41
Seminal	Tip	0.49 ± 0.19	0.48 ± 0.19	0.51 ± 0.03	0.31 ± 0.02
	Mid	0.96 ± 0.23	0.56 ± 0.15	0.72 ± 0.33	1.28 ± 0.42
	Base	0.49 ± 0.08	0.47 ± 0.14	0.46 ± 0.14	0.85 ± 0.26
Crown (1 st whorl)	Tip	7.8 ± 2.7	6.12 ± 0.2	15.0 ± 7.2	7.41 ± 0.72
	Mid	18.4 ± 1.4	18.4 ± 2.0	26.1 ± 6.2	26.7 ± 1.9
	Base	17.0 ± 2.0	16.5 ± 0.2	22.3 ± 3.2	26.8 ± 5.0
Crown (2 nd whorl)	Tip	15.5 ± 6.0	16.4 ± 0.7	5.62 ± 3.31	17.5 ± 4.1
	Mid	15.9 ± 1.6	15.4 ± 1.7	32.0 ± 2.3	22.3 ± 2.9
	Base	18.2 ± 2.5	16.5 ± 7.4	36.1 ± 5.7	27.7 ± 2.7

Table S3. 5 Xylem area measured from three segments (tip: 0–20 mm from root tip, mid: 40–60 mm from root tip, base: 0–20 mm from the base of the stem) of a representative thin-sectioned axial root for each type (primary, seminal and crown, 1st and 2nd whorls) of maize (V1 to V7 stage) in a simulated-field condition. Maize was grown in pots with two levels of N fertilizer (equivalent to 0 and 50 kg N ha⁻¹) before seeding and moistened to the average soil water content from the 2021 and 2022 field seasons. Pots received 50 kg N ha⁻¹ treatment before seeding, with additional N fertilizer applied at a rate of 70 kg N ha⁻¹ at the V6 stage. Some data was missing because roots did not produce enough root length for anatomical measurements. Values are the mean ± standard error, n= 4.

Axial root type	Root Segment	2021	2022		
		50 kg N ha ⁻¹	0 kg N ha ⁻¹	50 kg N ha ⁻¹	
----- Xylem area (µm ²) × 10 ⁴ -----					
V1	Primary	Tip	2.72 ± 0.43	1.56 ± 1.03	3.01 ± 0.43
		Mid	2.77 ± 0.16	2.73 ± 0.09	1.57 ± 0.19
		Base	2.50 ± 0.2	2.54 ± 0.24	2.71 ± 0.11
	Seminal	Tip	1.83 ± 0.80	0.81 ± 0	1.03 ± 0.20
		Mid	0.88 ± 0.13	1.15 ± 0.09	0.90 ± 0
		Base	1.05 ± 0	1.56 ± 0.32	1.61 ± 0.20
	Crown (1 st whorl)	Tip	0.18 ± 0	.	0.77 ± 0.01
		Mid	0.50 ± 0.04	.	0.50 ± 0.04
		Base	1.62 ± 0	0.50 ± 0	0.77 ± 0.01
V3	Primary	Tip	1.00 ± 0	1.42 ± 0.10	1.40 ± 0
		Mid	1.28 ± 0	1.73 ± 0.20	1.72 ± 0.41

		Base	3.08 ± 0.15	2.91 ± 0.08	2.10 ± 0.02
	Seminal	Tip	0.93 ± 0.18	0.61 ± 0.09	0.71 ± 0.09
		Mid	1.15 ± 0.12	0.87 ± 0.14	0.77 ± 0.14
		Base	1.18 ± 0.06	1.15 ± 0.07	1.18 ± 0.09
	Crown (1 st whorl)	Tip	2.39 ± 0.52	0.69 ± 0.04	1.20 ± 0
		Mid	2.70 ± 0.20	0.72 ± 0.07	3.11 ± 0.60
		Base	3.35 ± 0.36	0.67 ± 0.10	4.51 ± 1.05
V5	Primary	Tip	4.33 ± 0	1.60 ± 0.08	1.79 ± 1.78
		Mid	4.32 ± 1.430	2.27 ± 0.11	3.78 ± 1.74
		Base	2.16 ± 0.42	2.84 ± 0.13	2.73 ± 1.71
	Seminal	Tip	0.88 ± 0.10	0.77 ± 0.12	0.98 ± 0.10
		Mid	0.87 ± 0.11	0.60 ± 1.73	1.33 ± 0.25
		Base	1.46 ± 0.15	1.01 ± 1.41	0.68 ± 0.04
	Crown (1 st whorl)	Tip	1.90 ± 0	5.02 ± 0.83	4.34 ± 0
		Mid	3.85 ± 0.48	4.50 ± 1.26	5.80 ± 0.85
		Base	3.97 ± 0.49	4.91 ± 0.44	4.78 ± 0.49
	Crown (2 nd whorl)	Tip	5.90 ± 0.95	0.49 ± 0	3.66 ± 0.75
		Mid	5.81 ± 0.65	0.72 ± 0.04	6.38 ± 0.56
		Base	7.88 ± 1.77	0.59 ± 0.04	7.54 ± 1.02
V7	Primary	Tip	0.95 ± 0.18	1.34 ± 0.16	0.65 ± 0.18
		Mid	1.18 ± 0.31	2.01 ± 0.21	1.65 ± 0.12
		Base	1.60 ± 0.52	2.41 ± 0.26	1.93 ± 0.18

Seminal	Tip	0.50 ± 0	0.71 ± 0.17	0.95 ± 0.16
	Mid	0.92 ± 0.38	1.17 ± 0.08	0.99 ± 0.20
	Base	1.21 ± 0.19	0.82 ± 0.13	0.87 ± 0.12
Crown (1 st whorl)	Tip	4.29 ± 0.95	6.44 ± 1.55	6.44 ± 1.55
	Mid	4.90 ± 0.48	5.44 ± 0.34	5.44 ± 0.34
	Base	3.85 ± 0.55	5.80 ± 0.58	5.80 ± 0.58
Crown (2 nd whorl)	Tip	6.59 ± 0.15	2.75 ± 0.49	2.75 ± 0.49
	Mid	6.84 ± 0.75	6.30 ± 0.77	6.30 ± 0.77
	Base	7.65 ± 0.62	8.55 ± 1.66	8.55 ± 1.66

Table S3. 6 Root hydraulic conductance, estimated for segments (tip: 0–20 mm from root tip, mid: 40–60 mm from root tip, base: 0–20 mm from the base of the stem) of a representative thin-sectioned axial root for each type (primary, seminal and crown, 1st and 2nd whorls) of maize (V6 stage) in a simulated-field condition. Maize was grown in pots with two levels of N fertilizer (equivalent to 0 and 50 kg N ha⁻¹) before seeding and moistened to the average soil water content from the 2021 and 2022 field seasons. Pots received 50 kg N ha⁻¹ treatment before seeding, with additional N fertilizer applied at a rate of 70 kg N ha⁻¹ at the V6 stage. The pots received 50 kg N ha⁻¹ treatment before seeding were supplied with N fertilizer at the rate of 70 kg N ha⁻¹ at V6 stage. Some data was missing because roots did not produce enough root length for anatomical measurements. Values are the mean ± standard error, n= 4.

Axial root type		Root Segment	2021	2022	
			50 kg N ha ⁻¹	0 kg N ha ⁻¹	50 kg N ha ⁻¹
----- Root hydraulic conductance (kg m MPa ⁻¹ s ⁻¹) × 10 ⁻⁶ -----					
V1	Primary	Tip	3.9 ± 1.3	2.1 ± 1.7	5.5 ± 1.3
		Mid	5.4 ± 4.0	5.1 ± 0.2	1.8 ± 0.3
		Base	4.0 ± 2.4	3.8 ± 0.7	4.5 ± 0.4
	Seminal	Tip	0.19 ± 0.12	0.6 ± 0	1.2 ± 0.1
		Mid	0.56 ± 0.011	1.3 ± 0.1	0.8 ± 0
		Base	0.10 ± 0.01	2.8 ± 1.0	2.4 ± 0.5
	Crown (1 st whorl)	Tip	0.4 ± 0	.	0.3 ± 0
		Mid	3.4 ± 0	.	0.2 ± 0

V3	Primary	Base	5.4 ± 0	0.8 ± 0	0.1 ± 0	
		Tip	1.0 ± 0	1.5 ± 0.35	1.7 ± 0.35	
		Mid	0.82 ± 0	2.1 ± 0.26	2.4 ± 0.83	
	Seminal	Base	6.9 ± 0.40	5.6 ± 0.31	2.5 ± 0.06	
		Tip	0.92 ± 0.29	0.81 ± 0.30	0.70 ± 0.17	
		Mid	1.3 ± 0.27	0.74 ± 0.20	0.64 ± 0.19	
	Crown (1 st whorl)	Base	1.4 ± 0.15	1.8 ± 0.21	1.5 ± 0.26	
		Tip	5.0 ± 1.5	0.21 ± 0.03	1.1 ± 0	
		Mid	4.6 ± 1.08	0.21 ± 0.65	7.8 ± 2.8	
V5	Primary	Base	7.2 ± 2.1	0.22 ± 0.07	11.8 ± 4.2	
		Tip	0.75 ± 0	1.9 ± 0.16	2.5 ± 1.2	
		Mid	1.4 ± 0.7	3.2 ± 0.42	8.2 ± 2.4	
	Seminal	Base	3.3 ± 1.1	5.1 ± 0.34	4.3 ± 0.2	
		Tip	0.73 ± 0.11	0.81 ± 0.13	0.91 ± 0.30	
		Mid	0.77 ± 0.18	0.51 ± 0.21	0.21 ± 0.48	
	Crown (1 st whorl)	Base	2.2 ± 0.4	1.2 ± 0.2	0.53 ± 0.05	
		Tip	2.9 ± 0	15.5 ± 3.9	15.0 ± 0	
		Mid	7.7 ± 1.2	10.3 ± 2.00	17.6 ± 3.3	
	Crown (2 nd whorl)	Base	9.2 ± 1.4	13.5 ± 1.8	13.9 ± 2.3	
		Tip	13.2 ± 2.9	0.10 ± 0	8.1 ± 2.8	
		Mid	13.4 ± 2.1	0.22 ± 0.03	17.4 ± 2.2	
			Base	22.9 ± 9.5	0.11 ± 0.01	23.2 ± 6.2

V7	Primary	Tip	0.27 ± 0.11	0.37 ± 0.14	0.37 ± 0.14
		Mid	1.6 ± 0.7	1.7 ± 0.3	1.6 ± 0.3
		Base	1.7 ± 0.9	2.3 ± 0.3	2.3 ± 0.3
	Seminal	Tip	0.17 ± 0	0.51 ± 0.22	0.87 ± 0.22
		Mid	0.92 ± 0.05	1.8 ± 0.3	1.2 ± 0.4
		Base	0.11 ± 0.03	0.78 ± 0.2	0.69 ± 0.1
	Crown (1 st whorl)	Tip	10.8 ± 2.2	17.5 ± 3.5	23.5 ± 9.0
		Mid	13.6 ± 1.9	14.7 ± 1.9	15.5 ± 1.7
		Base	38.5 ± 1.6	6.7 ± 2.0	15.9 ± 2.8
	Crown (2 nd whorl)	Tip	14.4 ± 0.7	11.5 ± 4.7	3.8 ± 1.1
		Mid	16.7 ± 2.8	18.0 ± 1.0	17.2 ± 3.1
		Base	19.0 ± 2.6	15.4 ± 3.3	28.8 ± 10.3

Table S3. 7 Maize grain yield of two field growing seasons at Sainte-Anne-de-Bellevue, Québec, Canada. Data was collected at the V1 to V7 stages of maize growth in 2021 and 2022. The fertilizer treatment delivered about 40% of the target N rate banded as ammonium sulfate at planting (0, 32, 40 or 50 kg N ha⁻¹) and the remaining 60% side-dressed as calcium ammonium nitrate at the V6 stage, supplying 0, 72, 96 or 120 kg N ha⁻¹ during the growing season.

N fertilizer rates	Growing season	
	2021	2022
	-----Mg ha ⁻¹ -----	
0 kg N ha ⁻¹	-	7.0 ± 0.5 ^b
72 kg N ha ⁻¹	10.5 ± 0.4	8.9 ± 0.5 ^a
96 kg N ha ⁻¹	10.8 ± 0.3	9.8 ± 0.5 ^a
120 kg N ha ⁻¹	10.9 ± 0.3	10.2 ± 0.5 ^a

Data is the mean ± standard error (n = 16). Values followed by a different letter are significantly different among the N fertilizer rates ($p < 0.05$).

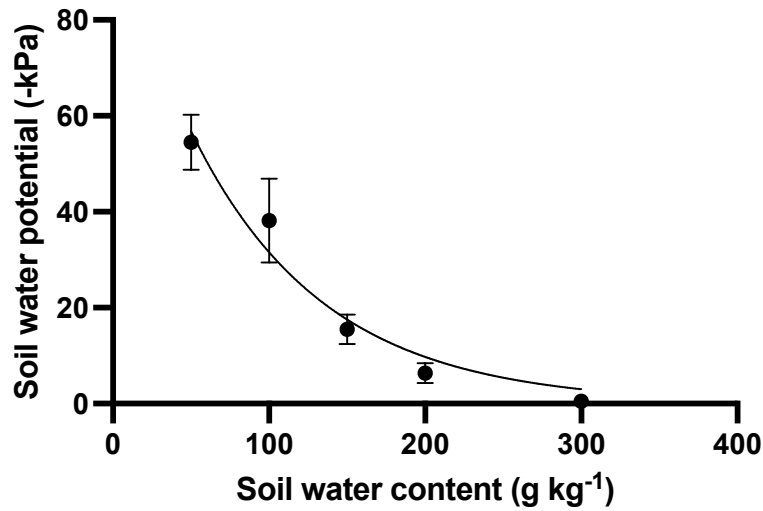


Fig. S3. 1 Water retention curve of the soil used in the growth and field experiment. Soil was collected from the maize growing field in Sainte-Anne-de-Bellevue, Québec, Canada. Soil at this location is a sandy-loam Humic Gleysol of the St. Amable series containing 620 g sand kg⁻¹, 60 g clay kg⁻¹, and 48 g organic C kg⁻¹, with pH 6.3, field capacity of 23% and an average bulk density of 1110 kg m⁻³. Data points are the mean with standard error bars, n= 3.

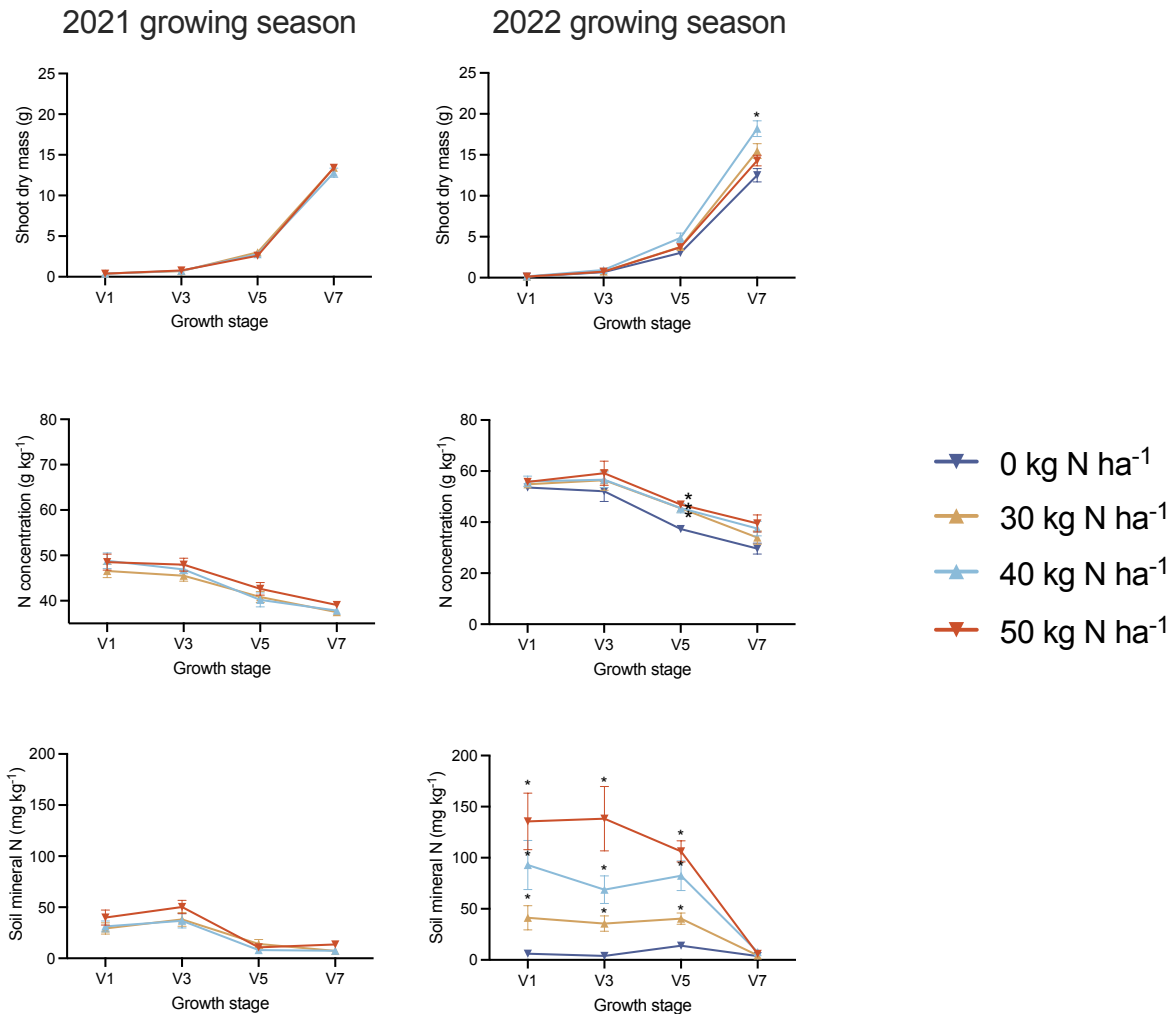


Fig. S3. 2 Maize shoot biomass and N concentration (V1 to V7 stage) and soil mineral N concentration in plots receiving variable N fertilizer rates located in Sainte-Anne-de-Bellevue, Québec, Canada. Maize plants and root-associated soil were collected at V1, V3, V5, and V7 stages in 2021 and 2022. The control plot received 0 kg ha⁻¹ (2022 only) while fertilized plots had about 40% of the target N rate (30, 40 and 50 kg N ha⁻¹) banded as ammonium sulfate at planting and the remaining 60% side-dressed as calcium ammonium nitrate at the V6 stage, supplying 72, 96 and 120 kg N ha⁻¹ during the growing period. Data points are the mean with standard error bars, n= 16. Asterisk (*) indicates significant difference ($p < 0.05$) compared to control plot received 0 kg ha⁻¹.

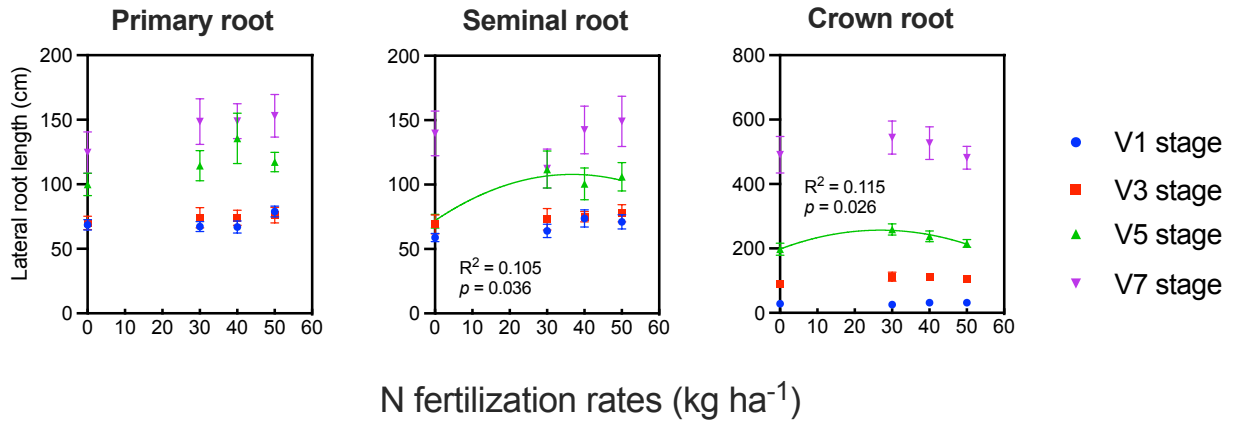
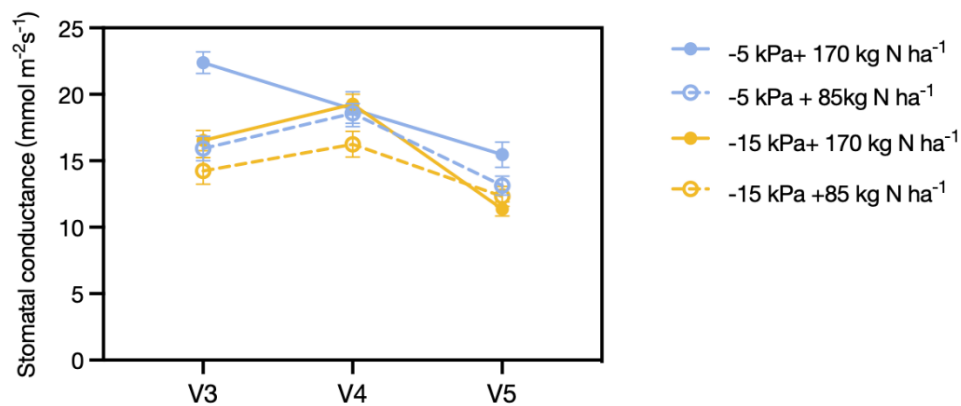


Fig. S3. 3 Lateral root plasticity of three types – primary, seminal and crown – from maize (V1 to V7 stage) collected in 2022 from plots receiving variable N fertilizer rates located in Sainte-Anne-de-Bellevue, Québec, Canada. The control plot received 0 kg ha⁻¹ while fertilized plots had about 40% of the target N rate (30, 40 and 50 kg N ha⁻¹) banded as ammonium sulfate at planting and the remaining 60% side-dressed as calcium ammonium nitrate at the V6 stage, supplying 72, 96 and 120 kg N ha⁻¹ during the growing period. Data points are the mean with standard error bars, n= 16.



	Growing stage		
	V3	V4	V5
Soil water potential	***	NS	**
N fertilization levels	***	NS	NS
Water * N	*	NS	*

Fig. S3. 4 Stomatal conductance of maize (V3 to V5 stage) in a growth chamber environment. Maize was grown in pots with two levels of N fertilizer (equivalent to 85 and 170 kg N ha⁻¹) and watered to a constant soil water potential of -15 and -5 kPa. Error bars represent standard error of means, n = 20.

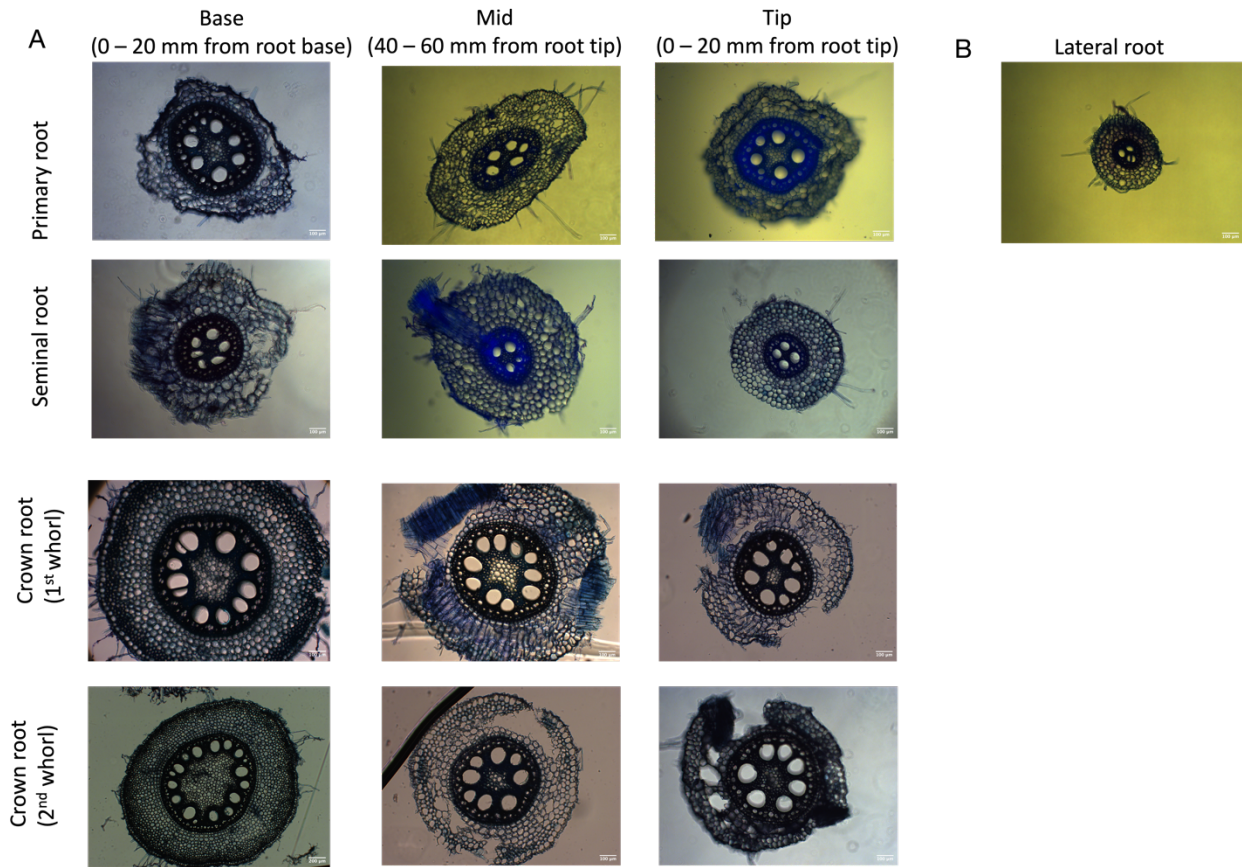


Fig. S3. 5 Anatomical structure of (A) axial root types – primary, seminal, crown (1st whorl), crown (2nd whorl) – of field-grown maize roots and (B) lateral roots. The scale bar = 100 μm , except for the base of second whorl crown root with a scale bar = 200 μm .

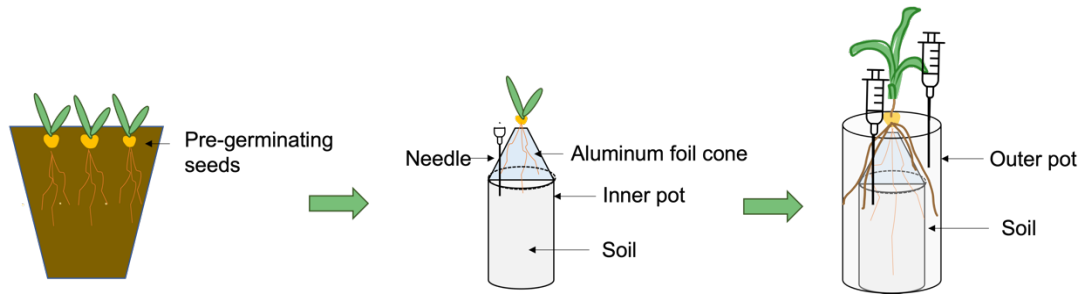


Fig. S4. 1 Schematic illustration of the split-root system. Maize seeds were pre-germinated for about 10 d before transplanting to the split-root pots designed to segregate the embryonic root system (primary and seminal roots) from the crown roots. An inner chamber (PVC pipe with 5 cm diameter, 25 cm height) was placed in the middle of the outer chamber (PVC pipe with 10 cm diameter, 30 cm height). The bottom of split-root pots was covered with the aluminum foil to prevent water and soluble nutrient losses.

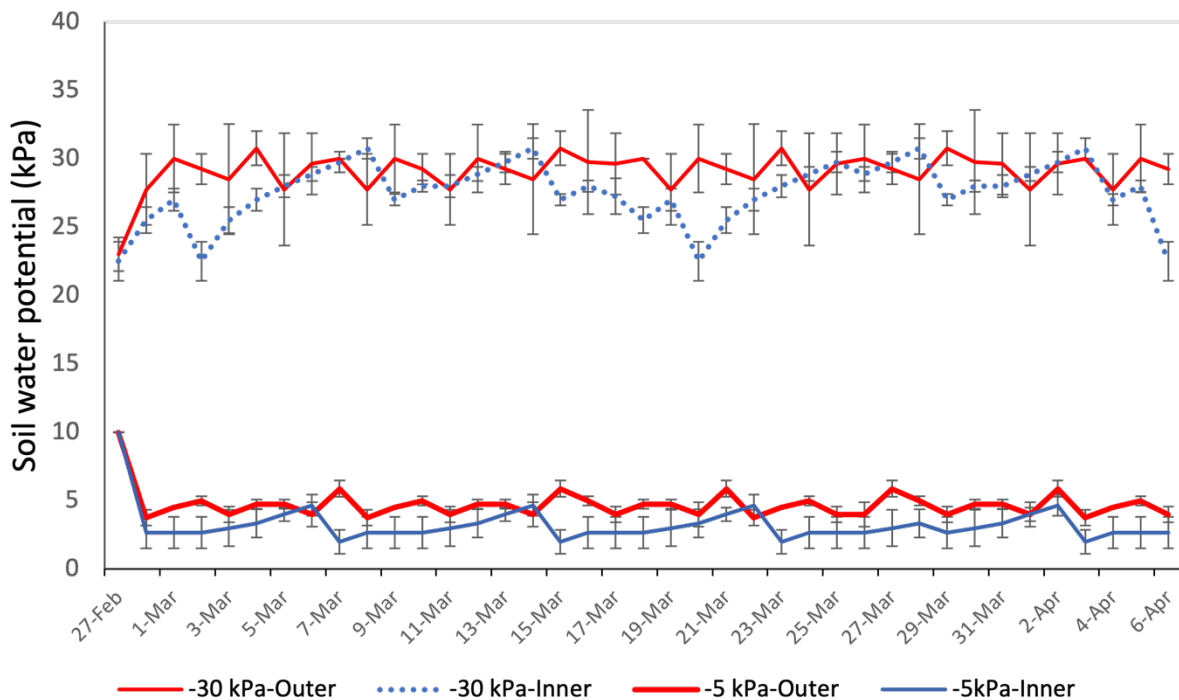


Fig. S4. 2 Soil water potential in the inner and outer pots of the split-root system. Tensiometers were inserted into the inner and outer chambers to monitor the soil water potential of the pots. The plants were watered to achieve the target soil water potential (-5kPa or -30kPa) every 2 days, from the first day after transplanting the maize seedling to the split-root system until the V6 stage. Data represents the mean and standard error, n = 4.

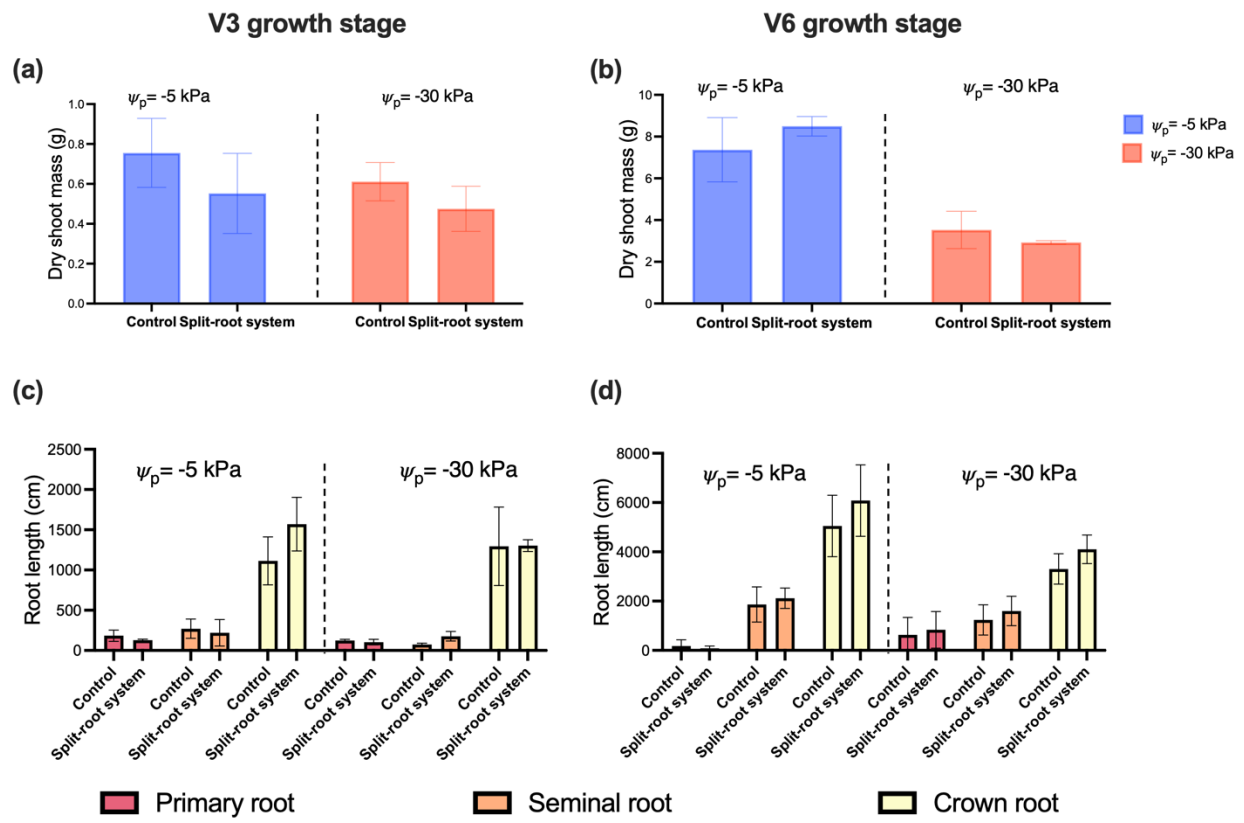


Fig. S4. 3 Shoot biomass (a, b) and root length (c, d) were the same for maize planted in split-root pots and control pots (PVC pipe with 10 cm diameter, 30 cm height, without an inner chamber). Maize was grown in pots watered to a constant water potential (-5kPa or -30kPa) and was destructively sampled at the V3 and V6 stages. Values are the mean \pm standard error, n = 4.

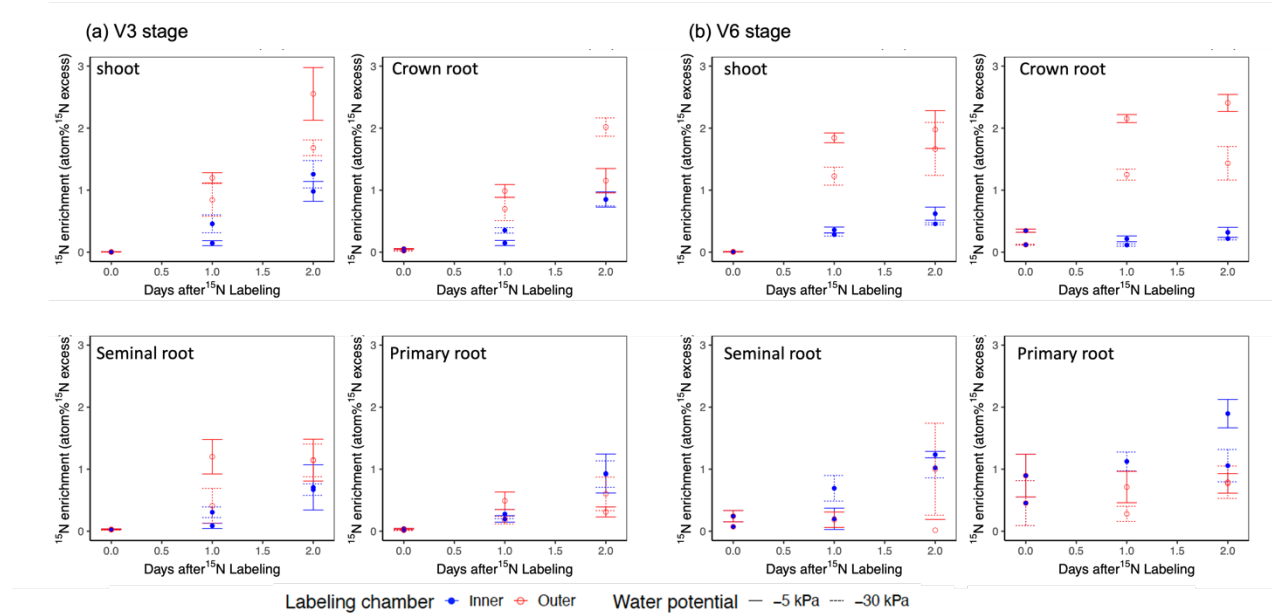


Fig. S4. 4 The ^{15}N enrichment (atom% excess) of maize shoot, crown root, seminal root, and primary root after 0, 24 and 48 h of exposure to ^{15}N enrichment in the split-root system, and the V3 and V6 stages. Maize was grown in pots kept at a constant water potential (-5kPa or -30kPa). At V3 and V6 stages, one of the chambers, either the inner or outer, received an injection of ^{15}N - KNO_3 solution (18.4% atom ^{15}N excess), while the other chamber received ^{14}N - KNO_3 solution, ensuring exposure of only one root type (either embryonic or crown roots) to ^{15}N - KNO_3 solution. Points with error bars represent the mean and standard error, connected with the best-fit line, $n = 4$. Some data points and lines are missing due to the death of primary and seminal roots by the V6 stage.

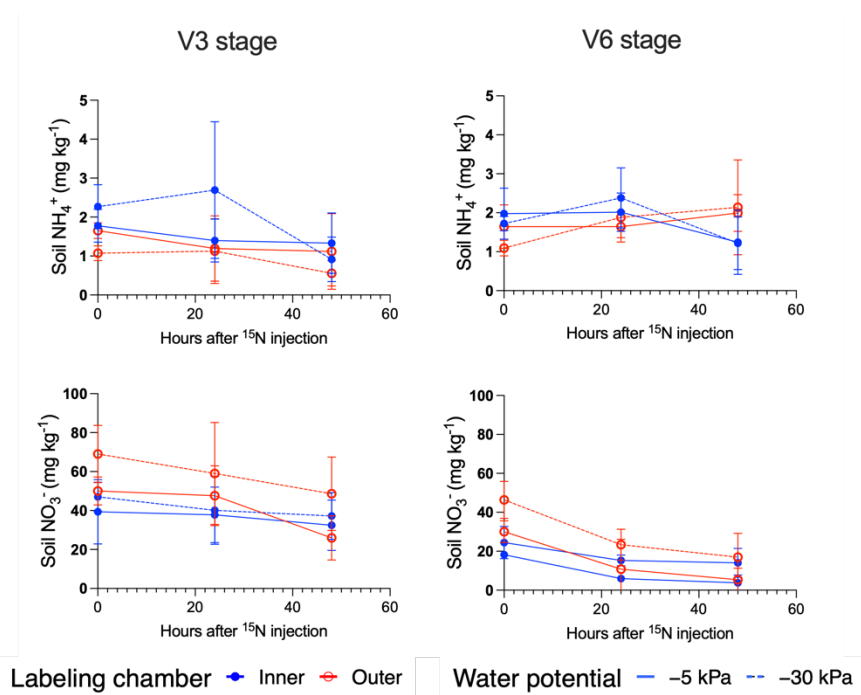


Fig. S4. 5 Soil mineral N (NO_3^- and NH_4^+) in the inner chamber and outer chamber of the split-root system after 0, 24 and 48 h exposure to ^{15}N enrichment at the V3 and V6 stages. The inner and outer chambers were kept at a constant water potential (-5kPa or -30kPa). At V3 and V6 stages, one of the chambers, either the inner or outer, received an injection of ^{15}N - KNO_3 solution (18.4% atom ^{15}N excess), while the other chamber received ^{14}N - KNO_3 solution, ensuring exposure of only one root type (either embryonic or crown roots) to ^{15}N - KNO_3 solution. Data was pooled among each chamber type (inner or outer) with the same water potential, regardless of received KNO_3 solution type (^{14}N - KNO_3 or ^{15}N - KNO_3). Data points represent the mean and standard error, $n = 12$.

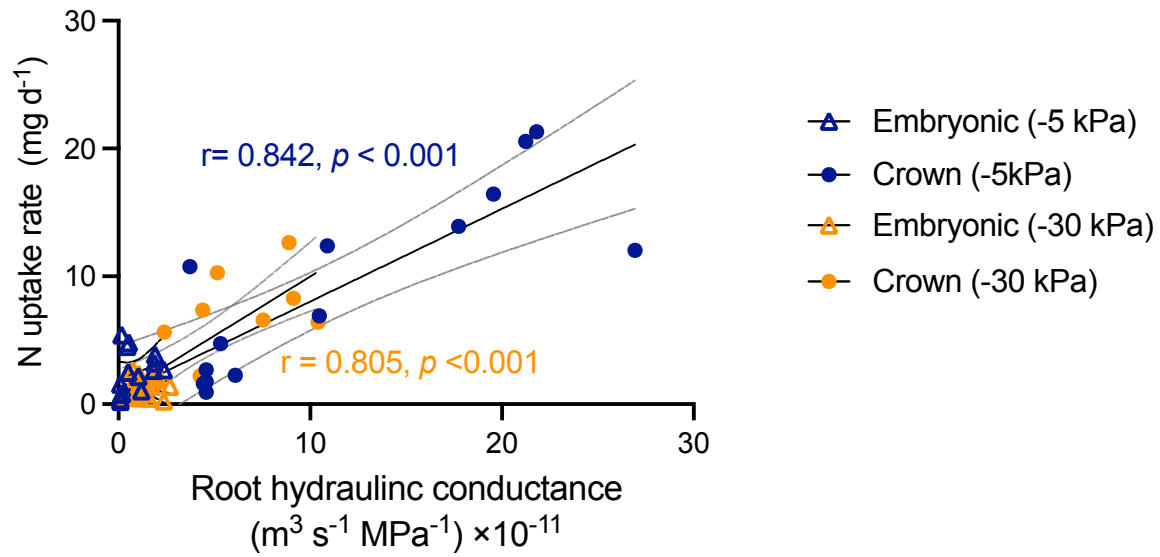


Fig. S4. 6 The relationship between maize N uptake rate and root hydraulic conductance of embryonic and crown roots. The relationship was described with best-fit lines (with 95% confidence intervals) when r , the Pearson correlation coefficient, was significant ($p < 0.05$). Maize was grown in pots kept at a constant water potential (-5kPa or -30kPa). Data collected from V3 and V6 growth stage were pooled, $n = 16$ for each root type.

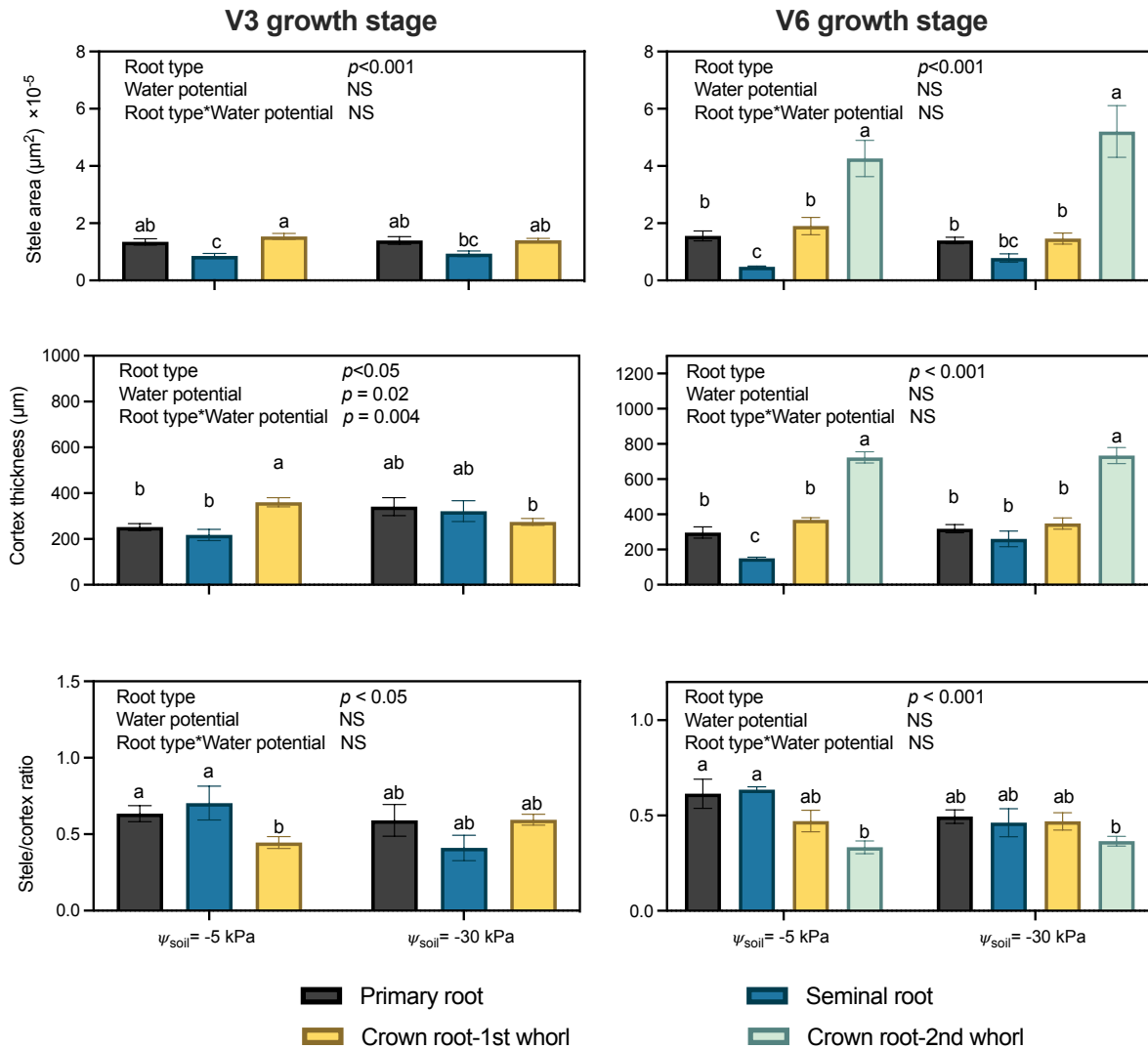


Fig. S4. 7 Stele area, cortex thickness, stele/cortex ratio of maize grown in the split-root system until V3 and V6 stages. Maize was grown in pots watered to a constant water potential (-5kPa or -30kPa). One primary, seminal, 1st whorl crown root, and 2nd whorl crown root collected from each of the 4 individual plants (n = 4). Error bars represent standard error of means. Different letters over the bars represent significantly different ($p < 0.05$, Tukey's honestly significant test). NS, not significant ($p > 0.05$).

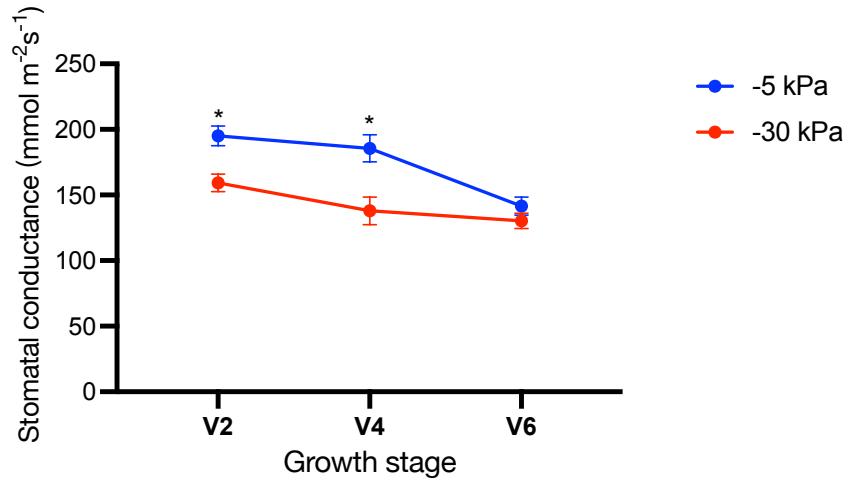


Fig. S4. 8 Stomatal conductance of maize grown in the split-root system V6 stages. Maize was grown in pots watered to a constant water potential (-5kPa or -30kPa). The stomatal conductance was measured at the mid-blade of the newest fully formed leaf when maize reached V2, V4, and V6 stages. Error bars represent standard error of means (n = 12). Asterisks (*) indicate the significant difference between the water potential treatments ($p < 0.05$).

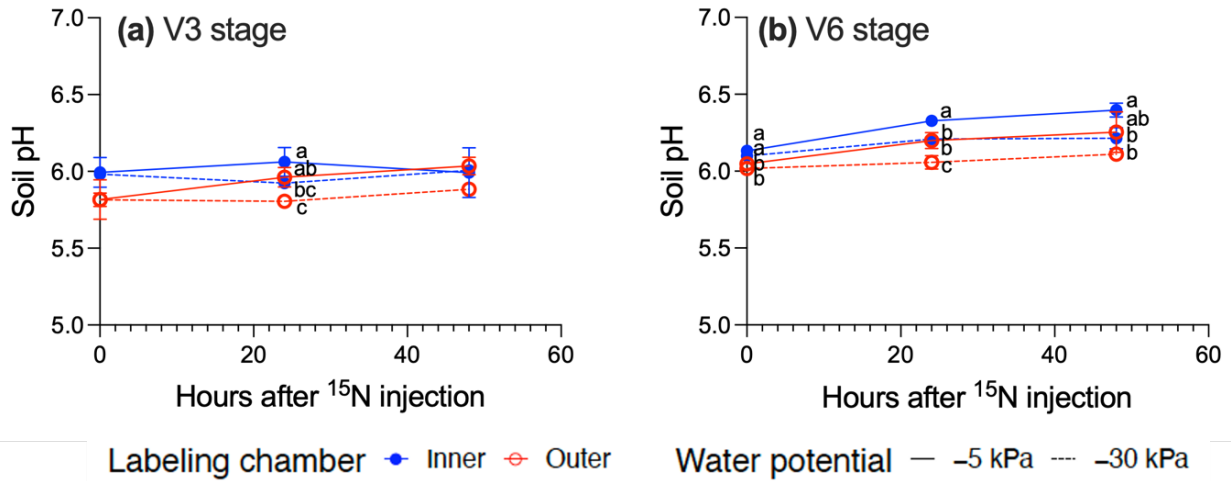


Fig. S4. 9 Soil pH in the inner chamber and outer chamber of the split-root system after 0, 24 and 48 h exposure to ¹⁵N enrichment at the (a) V3 and (b) V6 stages. The inner and outer chambers were kept at a constant water potential (-5kPa or -30kPa). At V3 and V6 stages, one of the chambers, either the inner or outer, received an injection of ¹⁵N-KNO₃ solution (18.4% atom ¹⁵N excess), while the other chamber received ¹⁴N-KNO₃ solution, ensuring exposure of only one root type (either embryonic or crown roots) to ¹⁵N-KNO₃ solution. Data points represent the mean and standard error, n = 4. Different letters represent significantly different (p < 0.05, Tukey's honestly significant test).

Copyright transfer agreement for Chapter 2 publication in Canadian Journal of Plant Science

Canadian Science Publishing license to publish agreement

Date of agreement: 13-Jan-2023

Article: "Distinctive plasticity of maize (*Zea mays*) root types to variable nitrate concentration"
(10.1139/CJPS-2022-0246)

Authors: Jiang, Yutong; Hung, Chih-Yu; Whalen, Joann K.

Journal: Canadian Journal of Plant Science

To allow the Article in the Journal to be distributed as widely as possible, the copyright holder (the Owner) grants Canadian Science Publishing (the Publisher) a licence to publish the above Article. The Article is deemed to include all material submitted for publication, including, but not limited to, title, abstract, text, figures, tables, supplementary material, and author-supplied promotional material. Unless otherwise specified, the Article is deemed to include the Submitted Article, the Accepted Article, and the Article Version of Record.

Definitions for different versions of the Article

Submitted Article = the version of the Article submitted to the Journal for peer review

Accepted Article = the version of the Article revised by authors to incorporate suggestions by peer reviewers and subsequently accepted for publication in the Journal

Article Version of Record = the official version of the Article that has been prepared by the Publisher and published on the Journal website

What license is being granted

Please select which license the copyright holder (Owner) is granting to the Publisher. License Terms and conditions are described under the signatures area. Authors who plan to pay for open access publication of the Article must select CC BY.

(1) Standard license to publish: terms and conditions 1.1–1.10 apply

Who is the copyright holder

Please identify the Owner of your copyright interests in the Article by selecting from options A–D.

(A) I am an Author whose employer does not hold copyright. I am an Owner and hold all or some of the copyright.

Signature for:

Ms. Yutong Jiang

21111 Chem. Lakeshore Sainte-Anne-de-Bellevue Quebec Canada H9X3V9

If you selected option A above, sign here

Author signature:

Type your name at right Yutong Jiang

If you selected option B, C, or D, complete the section below Owner name and address:

Name and address of government institution or company

Name and title of signing officer:

The signing officer is a representative of the Owner with

the authority to sign legal documents on its behalf

Signature of signing officer:

Email signature to cjps@cdnsiencepub.com. If you have the authority to sign legal documents on behalf of your employer, type your own name at right. Otherwise, you may:

- use a print-out of this online form, OR
- use our PDF standard or OA form, OR
- forward an email from your signing officer declaring their agreement to publication of the Article in Canadian Journal of Plant Science under the terms of the CSP license to publish agreement.

Names of Author(s) who are employed by the Owner:

The Publisher requires only one copy of the form on behalf of Authors listed at right Owner's copyright statement to be published with the article:

Provide only if Owner requires specific text in the copyright statement

By checking the box and clicking the SUBMIT button below the License terms, the Owner confirms that they have read and agree to the terms and conditions of this license agreement.

License terms

1. Standard license to publish

Publisher rights

1.1. In consideration of the Publisher publishing the Article, the Owner grants to the Publisher for the full term of copyright and any extensions thereto an irrevocable, royalty-free, exclusive licence

to edit, publish, reproduce, distribute, transmit, display, store, translate, adapt, create derivative works from, and use the Article in any language and in any form, manner, format, or medium now known or hereafter developed, throughout the world; to license others to do any or all of the above; and to assign this license.

1.2. In consideration of the Publisher publishing the Article, the Owner also grants to the Publisher for the full term of copyright and any extensions thereto all the same rights provided for in clause 1.1, for any supplementary material and author-supplied promotional material submitted with the Article, but on a non-exclusive basis.

1.3. The Owner authorizes the Publisher to take such steps as it considers necessary, at its own discretion and expense, in the Author(s)' name and on their behalf, if it believes that a third party is infringing or is likely to infringe copyright in the Article, including but not limited to taking legal proceedings.

Author and Owner rights

1.4. The Author(s) retain their moral rights to attribution, association, and integrity of their work in the Article.

1.5. Ownership of the copyright in all versions of the Article remains with the Owner. The Owner retains the following non-exclusive rights:

(a) To post an electronic copy of the Submitted Article (pre-print) and/or the Accepted Article (post-print) on their own website, an institutional repository, or their funding body's designated archive, provided that posted versions of the Accepted Article include a hyperlink to the Article Version of Record.

(b) Subject to the Owner’s permission, the Author(s) and any academic institution where they work at the time may reproduce the Article for the purpose of teaching.

(c) To reuse all or part of any version of the Article in other works created by the Author(s), provided the Article Version of Record is acknowledged with a note or citation that includes author, year of publication, article title, journal title, digital object identifier (DOI), and a hyperlink to the Article Version of Record on the Journal website.

Warranties

1.6. Publisher and Journal branding, and Article identifiers – including but not limited to copyright notices, unique digital object identifiers (DOIs), Publisher and Journal logos, references, hyperlinks, and any other notices that are included in the Article or that are provided by the Publisher with instructions that such must accompany display of the Article – shall not be removed or tampered with in any way.

1.7. The Owner(s) warrant and represent that:

(a) The Author(s) qualify for authorship and are the only contributors who qualify for authorship of the Article.

(b) The Article represents original work, is not under consideration for publication elsewhere, and has not been previously published in any way, except as listed below:

an un-refereed, preliminary version of the Article may be posted to a preprint server, institutional repository, Author website, or funder archive;

the work underpinning the Article may be presented at a conference as an abstract, poster, lecture, or paper; and

the Article may comprise the Author’s thesis or dissertation (in full or in part).

(c) The Article accepted for publication by the Publisher, or its equivalent, will not be submitted for publication elsewhere.

(d) All of the facts contained in the Article are true and accurate.

(e) Nothing in the Article is obscene, defamatory, libellous, violates any right of privacy, or infringes any intellectual property rights or human rights.

(f) Nothing in the Article infringes any duty of confidentiality that any of the Author(s) may owe to anyone else or violates any contract, express or implied, of any of the Author(s), and all the institutions in which work recorded in the Article was carried out have authorized publication of the Article.

(g) If the Article includes material from other copyrighted work, the Author(s) have obtained permission from the copyright owners of such materials to enable the Authors to grant the rights contained herein. Any copyrighted material has been appropriately acknowledged in the Article. Copies of all such permissions have been sent to the Publisher.

(h) The Owner(s) have communicated the terms and conditions of this license with the Authors, and the Authors hereby acknowledge and agree to abide by said terms and conditions.

General

1.8. If after acceptance the Article is withdrawn, rejected, or not published within 2 years, the license is revoked.

1.9. The terms and conditions of this license may not be modified without the express written consent of both parties.

1.10. This Agreement shall endure to the benefit of and be binding on the Publisher and the Owner, and their respective heirs, legal representatives, successors, and assigns.

2. Open access license (CC BY)

Open access: Publisher responsibilities

2.1. The Publisher will enable unrestricted access to the Article on the Journal website under the terms of the Creative Commons Attribution 4.0 International license (CC BY 4.0), <https://creativecommons.org/licenses/by/4.0/>. This license allows others to share (copy, distribute, and transmit the work), remix (to adapt the work), and to make commercial use of the work under the condition that they acknowledged the original publication with a credit line that includes author, year of publication, article title, journal title, and digital object identifier (DOI).

Open access: non-exclusive license

2.2. License terms and conditions 1.1–1.10 apply with the following modifications:

(a) Replace Clause 1.1 with 2.2(a). In consideration of the Publisher publishing the Article, the Owner grants to the Publisher for the full term of copyright and any extensions thereto an irrevocable, royaltyfree, non-exclusive license to edit, publish, reproduce, distribute, transmit, display, store, translate, adapt, create derivative works from and use the Article in any language and in any form, manner, format, or medium now known or hereafter developed, throughout the world; to license others to do any or all of the above; and to assign this license.

(b) Replace Clause 1.5(a) with 2.2(b). To post any version of the Article on their own website, an institutional repository, or their funding body's designated archive, provided they include a hyperlink to the Article Version of Record on the Journal website.